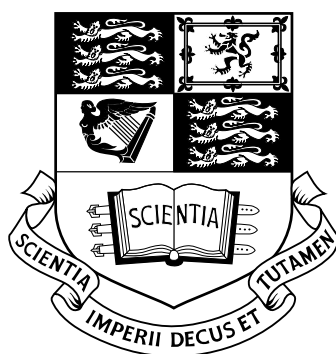


# THE POTENTIAL OF NMR SPECTROSCOPY FOR THE CHEMICAL CHARACTERISATION OF ALKYD RESINS IN MODERN FINE ART

*Thesis towards the award of Master of Science (M.Sci.)  
Chemistry with Conservation Science: F RCD2*



*Matthew John Parkinson*

*Imperial College of Science, Technology and Medicine  
Victoria & Albert Museum  
Royal College of Art  
London, UK*

# Abstract

The emergence of a new paint media in the first half of this century has led to a number of historically important paintings undergoing degradation not previously encountered. Through understanding the method of production and synthesis, and analysis of commercial and model materials the structure of oil modified alkyd resins has been postulated. Through exposure to high intensity light artificial aging has been achieved and changes in structure have been deduced. This has led to a better understanding of the curing process and how this relates to the degradation of the polymeric material. A method of identification of the polyol used has also been established.

# Preface

This thesis is based on the research undertaken by Matthew John Parkinson, under the supervision of Dr. Robert Vernon Law in the Department of Chemistry, Imperial College, London, UK between October 1999 and July 2000.

M.J.PARKINSON 2000 AD

# Contents

|          |                                                         |           |
|----------|---------------------------------------------------------|-----------|
| <b>1</b> | <b>Introduction</b>                                     | <b>12</b> |
| 1.1      | The advent of synthetic paint media . . . . .           | 12        |
| 1.2      | Impact of alkyd resins on art . . . . .                 | 12        |
| 1.3      | Conservation of alkyd based paintings . . . . .         | 15        |
| 1.4      | Problems with alkyds . . . . .                          | 15        |
| 1.5      | Other reasons to study alkyds . . . . .                 | 16        |
| <b>2</b> | <b>Alkyd Resins</b>                                     | <b>17</b> |
| 2.1      | Alkyds . . . . .                                        | 19        |
| 2.1.1    | Oil modified alkyd resins . . . . .                     | 20        |
| 2.1.2    | Industrial manufacture . . . . .                        | 21        |
| 2.2      | Previous research . . . . .                             | 22        |
| 2.2.1    | Crosslinking mechanism . . . . .                        | 22        |
| 2.2.2    | Arial oxidation . . . . .                               | 23        |
| 2.2.3    | NMR spectroscopy . . . . .                              | 23        |
| 2.2.4    | X-ray diffraction techniques . . . . .                  | 24        |
| 2.2.5    | Currently research . . . . .                            | 24        |
| <b>3</b> | <b>Artificial Ageing &amp; NMR</b>                      | <b>25</b> |
| 3.1      | Artificial ageing . . . . .                             | 25        |
| 3.2      | Nuclear magnetic resonance (NMR) spectroscopy . . . . . | 26        |
| 3.2.1    | Pulse techniques in NMR . . . . .                       | 27        |
| 3.2.2    | Solid state NMR . . . . .                               | 28        |
| 3.2.3    | Magic angle spinning (MAS) . . . . .                    | 29        |
| <b>4</b> | <b>Experimental</b>                                     | <b>32</b> |

---

|          |                                                                |           |
|----------|----------------------------------------------------------------|-----------|
| 4.1      | Commercial resins analysed . . . . .                           | 32        |
| 4.2      | Analytical equipment and practice . . . . .                    | 33        |
| 4.3      | Analysis of neat resin . . . . .                               | 34        |
| 4.3.1    | Resin film preparation . . . . .                               | 34        |
| 4.3.2    | Artificial aging . . . . .                                     | 34        |
| 4.3.3    | UV irradiation of resin . . . . .                              | 34        |
| 4.4      | Model alkyd resins . . . . .                                   | 35        |
| 4.4.1    | Glyptalic resin preparation . . . . .                          | 35        |
| 4.4.2    | Control resin preparation . . . . .                            | 37        |
| <b>5</b> | <b>Results</b>                                                 | <b>39</b> |
| 5.1      | Spectral analysis of neat resin . . . . .                      | 39        |
| 5.1.1    | 2D NMR analysis of 826-00 . . . . .                            | 44        |
| 5.2      | Solid state spectral analysis of cured resin . . . . .         | 45        |
| 5.3      | Solid state spectral analysis of aged resin . . . . .          | 47        |
| 5.4      | Solid state spectral analysis of UV irradiated resin . . . . . | 48        |
| 5.5      | Solid state spectral analysis of glyptalic resin . . . . .     | 50        |
| 5.6      | Spectral analysis of control resin . . . . .                   | 52        |
| 5.7      | Solid state spectral analysis of control resin. . . . .        | 54        |
| 5.8      | Solid state proton spectral analysis . . . . .                 | 55        |
| 5.9      | Calorimetric analysis of resin . . . . .                       | 56        |
| <b>6</b> | <b>Discussion</b>                                              | <b>60</b> |
| 6.1      | Model resin synthesis . . . . .                                | 60        |
| 6.2      | Alkyd structural assignment . . . . .                          | 61        |
| 6.2.1    | Solution-state NMR . . . . .                                   | 61        |
| 6.2.2    | Solid-state NMR . . . . .                                      | 62        |
| 6.3      | Thermal Analysis . . . . .                                     | 66        |
| 6.4      | Polymerisation and cross-linking . . . . .                     | 66        |
| 6.4.1    | Cross-linking . . . . .                                        | 67        |
| 6.5      | Implication for conservation . . . . .                         | 68        |
| 6.5.1    | Aging of alkyd resins . . . . .                                | 68        |
| 6.5.2    | Neat resin composition . . . . .                               | 69        |

---

|          |                                                                      |           |
|----------|----------------------------------------------------------------------|-----------|
| 6.5.3    | Structural deterioration of alkyds . . . . .                         | 69        |
| 6.5.4    | Yellowing . . . . .                                                  | 70        |
| 6.5.5    | Alkyd identification . . . . .                                       | 70        |
| 6.5.6    | Future use of NMR in conservation . . . . .                          | 70        |
| <b>7</b> | <b>Conclusions</b>                                                   | <b>72</b> |
| 7.1      | Main conclusions . . . . .                                           | 72        |
| 7.2      | Other conclusions . . . . .                                          | 72        |
| <b>A</b> | <b>Research proposal</b>                                             | <b>73</b> |
| A.1      | Aim & Background . . . . .                                           | 73        |
| A.1.1    | Natural to Synthetic Media . . . . .                                 | 73        |
| A.1.2    | NMR Spectroscopy . . . . .                                           | 74        |
| A.1.3    | Alkyd Resins . . . . .                                               | 74        |
| A.1.4    | Present Work in this Field . . . . .                                 | 75        |
| A.2      | Program and Methodology . . . . .                                    | 76        |
| A.2.1    | Training . . . . .                                                   | 76        |
| A.2.2    | Neat Analysis . . . . .                                              | 76        |
| A.2.3    | Film Preparation . . . . .                                           | 76        |
| A.2.4    | Artificial Aging . . . . .                                           | 76        |
| A.2.5    | Solid State NMR Analysis . . . . .                                   | 77        |
| A.2.6    | Solid State DSC Analysis . . . . .                                   | 77        |
| A.2.7    | Solid State Swelling . . . . .                                       | 77        |
| A.2.8    | Polymer Digestion . . . . .                                          | 77        |
| A.2.9    | Interpretation . . . . .                                             | 78        |
| A.3      | Relevance to Beneficiaries . . . . .                                 | 79        |
| A.3.1    | Potential Impact of Proposed Work . . . . .                          | 79        |
| A.3.2    | Beneficiaries . . . . .                                              | 79        |
| A.3.3    | Collaboration . . . . .                                              | 79        |
| A.4      | Dissemination and Exploitation . . . . .                             | 80        |
| A.4.1    | Transfer of Knowledge to Beneficiaries . . . . .                     | 80        |
| A.4.2    | Communication of Findings . . . . .                                  | 80        |
| <b>B</b> | <b>Data gathered from commercial resin manufacturers data sheets</b> | <b>81</b> |

**C Abbreviations** **82**

**Acknowledgements** **86**

# List of Figures

|     |                                                                     |    |
|-----|---------------------------------------------------------------------|----|
| 1.1 | Guernica, Pablo Picasso (1939)                                      | 13 |
| 1.2 | Whamm!, Roy Lichtenstien (1963)                                     | 13 |
| 1.3 | Convergence: Number 10, Jackson Pollock (1952)                      | 14 |
| 1.4 | Grand Cairo, Frank Stella (1962)                                    | 14 |
| 2.1 | The structure of triglycerides                                      | 17 |
| 2.2 | Fatty acids in linseed oil.                                         | 18 |
| 2.3 | Cross linking in linseed oil: glycerol unit (G) and fatty acid (F). | 18 |
| 2.4 | Examples of anhydrides and bifunctional acids used in alkyd resins. | 19 |
| 2.5 | Polyfunctional alcohols used in alkyd resins.                       | 19 |
| 2.6 | Simple model for alkyd structure.                                   | 20 |
| 3.1 | Formation of Zeeman levels by application of $B_0$ .                | 26 |
| 3.2 | Fourier transform of the time domain to the frequency domain.       | 28 |
| 3.3 | Resolution and line broadening in solid state NMR spectra.          | 28 |
| 3.4 | Static powder pattern due to chemical shift anisotropy              | 29 |
| 3.5 | Magic angle spinning                                                | 30 |
| 4.1 | Emission spectrum of the mercury discharge tube.                    | 35 |
| 4.2 | Stage one: Transesterification of linseed oil with glycerol.        | 37 |
| 4.3 | Stage two: Condensation with phthalic anhydride to form alkyd.      | 37 |
| 5.1 | IR spectrum of neat resin 826-00.                                   | 39 |
| 5.2 | $^1\text{H}$ NMR spectra of neat resin 826-00                       | 41 |

|      |                                                                                   |    |
|------|-----------------------------------------------------------------------------------|----|
| 5.3  | Typical $^{13}\text{C}$ NMR spectrum of the neat resin 826-00. . . . .            | 42 |
| 5.4  | Typical $^{13}\text{C}$ DEPT 135 NMR spectrum of the neat resin 826-00. . . . .   | 42 |
| 5.5  | $^1\text{H}$ - $^1\text{H}$ COSY NMR spectra of 826-00. . . . .                   | 44 |
| 5.6  | $^1\text{H}$ - $^{13}\text{C}$ HMQC NMR spectra of 826-00. . . . .                | 45 |
| 5.7  | Typical CPMAS NMR spectra of the cured resin 826-00. . . . .                      | 46 |
| 5.8  | CPMAS spectra of 270-00 to 270-10. . . . .                                        | 47 |
| 5.9  | CPMAS spectra of 444-00 to 444-10. . . . .                                        | 48 |
| 5.10 | CPMAS spectra of 826-00 to 826-10. . . . .                                        | 48 |
| 5.11 | CPMAS spectra of 270-00, 270-10 and 270-UV. . . . .                               | 49 |
| 5.12 | CPMAS spectra of 444-00, 444-10 and 444-UV. . . . .                               | 50 |
| 5.13 | CPMAS spectra of 826-00, 826-10 and 826-UV. . . . .                               | 50 |
| 5.14 | CPMAS spectra of TG-21D. . . . .                                                  | 51 |
| 5.15 | CPMAS spectra of TP-21D. . . . .                                                  | 52 |
| 5.16 | IR spectra of neat ALK-00. . . . .                                                | 53 |
| 5.17 | $^1\text{H}$ NMR spectra of neat ALK-00. . . . .                                  | 53 |
| 5.18 | CPMAS spectra of ALK-00 and ALK-UV. . . . .                                       | 54 |
| 5.19 | $^1\text{H}$ SPE Static spectra of 826-00 and 826-UV. . . . .                     | 55 |
| 5.20 | $^1\text{H}$ SPE MAS spectra of 826-00 and 826-UV. . . . .                        | 56 |
| 5.21 | DSC trace of 826-00, 826-10 and 826-UV. . . . .                                   | 57 |
| 5.22 | DSC traces of ALK-00 and ALK-UV. . . . .                                          | 58 |
| 5.23 | DSC traces of TG-21D and TP-21D. . . . .                                          | 58 |
| 5.24 | Repeat DSC traces of TG-21D and TP-21D. . . . .                                   | 59 |
| 6.1  | Structural assignment of glyptalic backbone of alkyd resins. . . . .              | 62 |
| 6.2  | Structural assignment of the four main fatty acids . . . . .                      | 62 |
| 6.3  | Structural assignment of cured oil modified alkyd resin . . . . .                 | 62 |
| 6.4  | Polyether with unusually high methylene chemical shift. . . . .                   | 63 |
| 6.5  | Possible peroxy crosslink between fatty acid side chains. . . . .                 | 64 |
| 6.6  | Assignment solution state $^{13}\text{C}$ NMR of pure phthalic anhydride. . . . . | 65 |
| 6.7  | Alkyd resin phthalate backbone. . . . .                                           | 66 |

---

|      |                                                                  |    |
|------|------------------------------------------------------------------|----|
| 6.8  | Possible glycerides competing for phthalic anhydride. . . . .    | 67 |
| 6.9  | The ene reaction . . . . .                                       | 68 |
| 6.10 | Radical and crosslink formation. . . . .                         | 68 |
| 6.11 | Action of cobalt salt driers on hydroperoxides. . . . .          | 68 |
| A.1  | The formation of glyptal, an alkyd resin [Chatfield 62]. . . . . | 74 |
| A.2  | Other common alkyd resin constituents [Chatfield 62]. . . . .    | 75 |

# List of Tables

|      |                                                                                               |    |
|------|-----------------------------------------------------------------------------------------------|----|
| 4.1  | The alkyd resin samples provided by the Tate Gallery, London. . . . .                         | 32 |
| 4.2  | Glyptalic resins synthesised . . . . .                                                        | 36 |
| 5.1  | Assignment of IR spectra of neat resins. . . . .                                              | 40 |
| 5.2  | Assignment of $^1\text{H}$ NMR spectra of neat resins. . . . .                                | 41 |
| 5.3  | Assignment of $^{13}\text{C}$ and DEPT 135 NMR spectra of neat resins. . . . .                | 43 |
| 5.4  | Assignment of $^1\text{H}$ - $^1\text{H}$ COSY NMR spectra of 826-00 (Figure 5.5). . . . .    | 45 |
| 5.5  | Assignment of $^1\text{H}$ - $^{13}\text{C}$ HMQC NMR spectra of 826-00 (Figure 5.6). . . . . | 46 |
| 5.6  | Assignment of CPMAS NMR spectra of cured resins. . . . .                                      | 47 |
| 5.7  | Assignment and change of 270-XX CPMAS spectra. . . . .                                        | 49 |
| 5.8  | Assignment and change of 444-XX CPMAS spectra. . . . .                                        | 49 |
| 5.9  | Assignment and change of 826-XX CPMAS spectra. . . . .                                        | 51 |
| 5.10 | Assignment of CPMAS spectra of neat glyptalic resins. . . . .                                 | 51 |
| 5.11 | Assignment of IR spectra of neat ALK-00. . . . .                                              | 52 |
| 5.12 | Assignment of $^1\text{H}$ NMR spectra of neat ALK-00. . . . .                                | 54 |
| 5.13 | Assignment of CPMAS spectra of ALK-00 and ALK-UV. . . . .                                     | 55 |
| 5.14 | Spin-lattice relaxation times of 826-00, 826-UV and ALK-00. . . . .                           | 56 |
| 5.15 | Assignment of DSC analysis. . . . .                                                           | 57 |
| B.1  | Manufacturers data for supplied resins. . . . .                                               | 81 |

# Chapter 1

## Introduction

### 1.1 The advent of synthetic paint media

At the beginning of the 20th century synthetic polymers started to be mass produced and widely used in many areas [Paul 85, Stevens 99, Rauve 95, Chatfield 62, Horie 88, Chapman 83, Seymour 97, Turner 86, Rodriguez 96, Morgans 90]. One such area was house paints based on synthetic polymers, as these had desirable properties not achievable with the linseed oil based paints of the time. Of particular interest were polyester resins made from polyfunctional alcohols and acids called alkyd resins, these were commonly modified with vegetable oils to create oil modified alkyd resins. These had the desirable properties of strong film formation and accelerated curing time when compared to the vegetable oil based paints of the time.

### 1.2 Impact of alkyd resins on art

Also during the period of development of the alkyd house paint, artists were beginning to want to express themselves in new ways not previously explored, thus spawning many new artistic movements. An important part of these new movements, as in the emergence of any new movement, was the use of new and interesting media to create a feel not yet encountered. In the 1930s artists started to use alkyd resin based house paints in their paintings. Many renowned artists of this period are known to have used commercial available house paints. One of the earliest and more well known to have done this was Pablo Picasso. An example of his work can be seen in Figure 1.1.

As the decades passed and commercial oil based house paint started to fade out and be replaced by alkyd based paint, and many more artists started to embrace

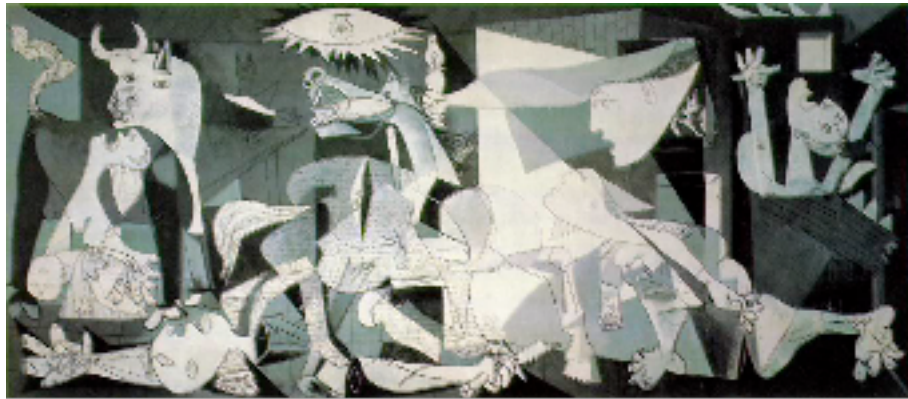


*Figure 1.1: Guernica, Pablo Picasso (1939)*

the new media. These include the likes of Roy Lichtenstien, Jackson Pollock, Frank Stella and many others. Example of their work can be seen in Figure 1.2, Figure 1.3 and Figure 1.4.



*Figure 1.2: Whamm!, Roy Lichtenstien (1963)*

Consultation with famous living artists by art historians and conservators has enabled direct questioning into why alkyds were used and what new effects could be achieved, not previously possible with the more traditional linseed oil based paint. The most common reason given for embracement of alkyds has been their more desirable physical properties like speed of drying, colour, finish, toughness and ability to flow, particularly important for Jackson Pollock. Also as common house paint these materials were cheap and freely available, again making them popular.



*Figure 1.3: Convergence: Number 10, Jackson Pollock (1952)*

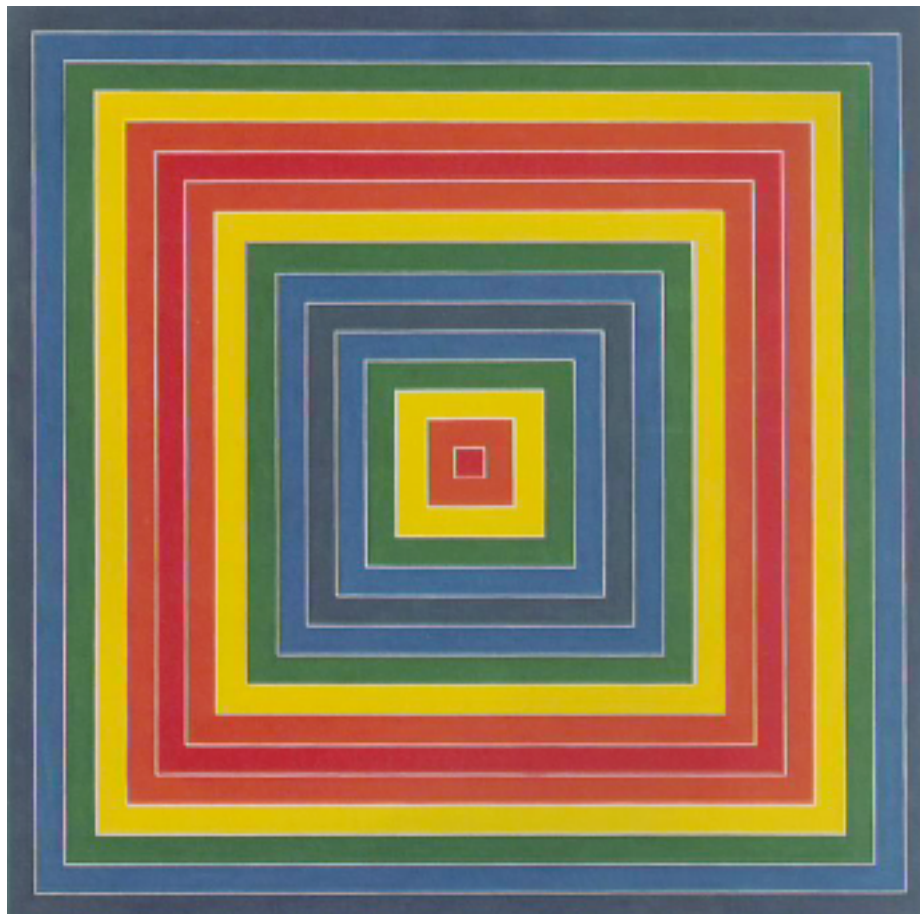


*Figure 1.4: Grand Cairo, Frank Stella (1962)*

### 1.3 Conservation of alkyd based paintings

The major concern of the modern conservator concerning alkyd resins is the unknown aspect of their aging [Chatfield 62]. Before their emergence as a common paint medium, the use of linseed oil based paint had been prevalent for at least 400 years. During this time many paintings were produced using this medium, affording the modern conservator many opportunities to experiment on oil paintings and an opportunity to build on previous knowledge. Alkyds on the other hand have only been around for at most 90 years so little knowledge of their aging properties are known. It is only now that important pieces of modern art are becoming under threat of damage from their deterioration.

### 1.4 Problems with alkyds

Alkyds were initially formulated and optimised for use on solid supports, walls and wood for example. When they are used on flexible supports, such as canvas, their properties when cured, such as a hard finishes, can become a disadvantage as this may, for example, encourage cracking [Stevens 99, Chapman 83, Seymour 97, Turner 86, Rodriguez 96, Morgans 90, Muizebelt 94]. Thus the use of preventive conservation plays an increasingly important role in the conservation of modern art. For example, control of temperature and humidity allows control over the expansion and contraction of materials which might lead to cracking or lifting of the media from the support.

Another important change in practice was in the application of varnish to finished works. In traditional oil paintings the pigmented surface is protected from the external environment by a layer of varnish. This enables the conservator to remove the varnish layer, along with all the dirt accumulated over the years, with gentle solvent cleaning. This exposes the original paint or pigment layer, which has been protected by the varnish, and does not contain accumulated dirt. The application of a new layer of varnish can then be used to, once again, protect the painting for the future. As most modern art is not varnished the dirt builds up on the actual original pigment layer over time. The implication of this is that prevention of dirt reaching the possibly sensitive surface becomes highly important. The use of a separate protective layer, like a sheet of glass, is often used although impairing the viewing pleasure. Of more importance than the accumulation of dirt is the direct exposure of the alkyd to light, heat, humidity and other possible damaging substances. All these may change the properties of the surface and thus the integrity of the piece. In order to understand what reactions occur when alkyd resins age an understanding of their structure is needed.

## 1.5 Other reasons to study alkyds

The gaining of knowledge about the aging of alkyd resins is not the only reason why it is important to study them. It is just as important to be able to characterise them and identify them to provide provenance, and an understanding of the working methods of the artist. It is in the aspect of alkyd identification, that NMR has a real possibility of being of use to the conservator.

## Chapter 2

# Alkyd Resins

As oil modified alkyd resins have a high oil content, the structure of the more traditional vegetable oil based paints like linseed oil are a logical place to start [Paul 85, Stevens 99, Rauve 95, Chatfield 62, Horie 88, Chapman 83, Seymour 97, Turner 86, Rodriguez 96, Morgans 90, Muizebelt 94]. Vegetable oils are triglycerides containing a glycerol backbone and three fatty acids side chains. The fatty acids are long chain carboxylic acids of lengths from C<sub>4</sub> to over C<sub>28</sub> with a varying degree of unsaturation (Figure 2.1).

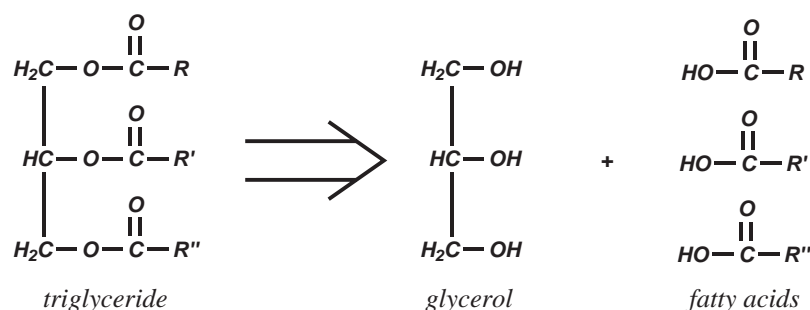


Figure 2.1: The structure of triglycerides

Each particular vegetable oil has a characteristic percentage of each fatty acid, for example linseed oil contains 52% linolenic acid, 22% oleic acid, 16% linoleic acid, 6% palmitic acid, 4% stearic acid and traces of palmitoleic, arachidic, and gadoleic acid (Figure 2.2).

The fatty acid compositions of vegetable oils have been determined by breaking down the triglycerides and chromatographic separation of components. The process by which this media 'dries, or more correctly cures, is by the formation of cross links between the triglyceride molecules, thus forming a hard, translucent three dimensional polymer network. This can be empirically explained by considering the chemical structure of vegetable oils. Reaction of a carbon-carbon double bonds on

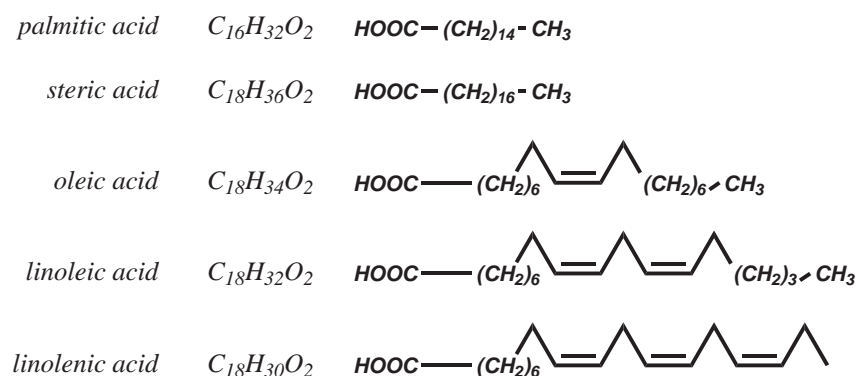


Figure 2.2: Fatty acids in linseed oil.

one fatty acid side chain with another fatty acid on a different molecule will lead to intermolecular bonds, and so cross linking the two triglycerides. This can be seen more clearly in Figure 2.3.

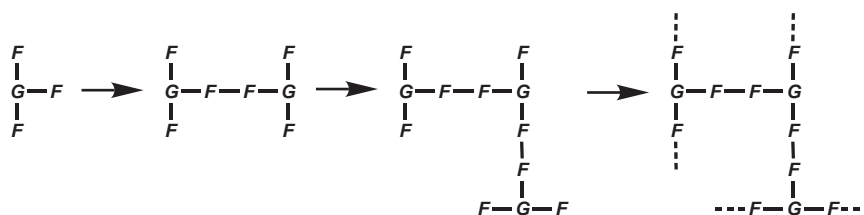


Figure 2.3: Cross linking in linseed oil: glycerol unit (G) and fatty acid (F).

Vegetable oils are classified as being oxidising or non-oxidising depending on whether they contain mainly unsaturated or saturated fatty acids respectively. Soya and linseed are oxidising oils where palm and Chinese cotton are non-oxidising oils. The degree of unsaturation of the fatty acids in the triglycerides determines the curing properties of the oil. Unsaturated fatty acids are liable to oxidation and thus yellow and harden quickly. Saturated fatty acids impart resistance to oxidation and thus good colour and gloss retention, but due to the lack of unsaturation cross linking, and thus hardening, does not occur readily. Sometimes a hardening agent has to be added to make these oils cure. Traditional oil paint medium is an oxidising vegetable oil medium, such as linseed oil, containing a suspension of finely ground pigment particles imparting colour to the translucent media.

## 2.1 Alkyds

Alkyds are the product of reaction between polyfunctional carboxylates with polyfunctional alcohols to form a three dimensional polymer networks, or resin [Paul 85, Stevens 99, Rauve 95, Chatfield 62, Horie 88, Chapman 83, Seymour 97, Turner 86, Rodriguez 96, Morgans 90, Muizebelt 94]. Linear polymers are obtained with bifunctional anhydrides and alcohols, but if the alcohol functionality is greater than two a three dimensional structure can be formed. The most common carboxylate used phthalic anhydride, by far. The resin properties can be changed by adding a mixture of carboxylates, other common carboxylates used include succinic anhydride, maleic anhydride, adipic acid, sebacic acid, fumaric acid and isophthalic acid (Figure 2.4).

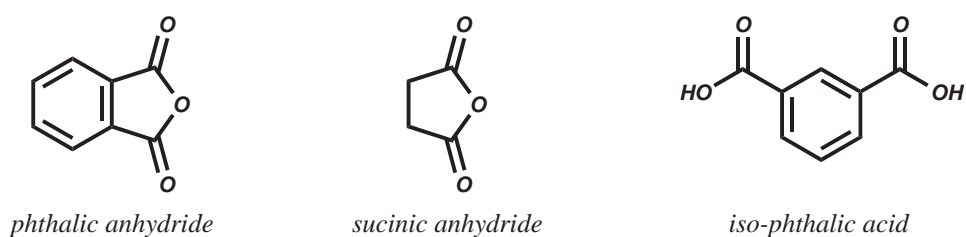


Figure 2.4: Examples of anhydrides and bifunctional acids used in alkyd resins.

There is less variety in the polyfunctional alcohol used, and this tends to be glycerol, but again this can be modified by the addition of other polyols such as, pentaerythritol, or sorbitol (Figure 2.5).

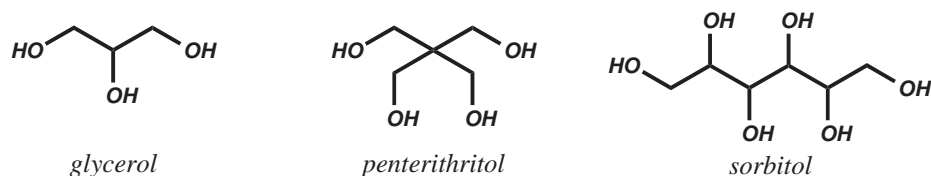


Figure 2.5: Polyfunctional alcohols used in alkyd resins.

Industrially the different combination of anhydrides, dicarboxylic acids and alcohols are formulated to give resins with different bulk properties. The formulation process is of key importance to the manufacture as this allows different bulk properties to be tuned. However this makes the analysis of such resins difficult as they are a mixtures of so many different chemical species.

### 2.1.1 Oil modified alkyd resins

Alkyd resins are commonly modified with triglyceride vegetable oils, or more historically correct, triglyceride vegetable oils were modified with alkyds, to produce resins with more desirable properties. Most oil modified alkyd resins are glyptalic resins, that is polyesters formed from phthalic anhydride and glycerol. Modification can take place with either oxidising or non-oxidising oils. The structure of the polymer network is thus going to be based on the three constituents, the diacid, the polyol and the triglyceride. When first produced in the 30s the most wide spread oil was linseed, but as time passed the use of less oxidisable oils, like soya, became more common due to the high degree of yellowing encountered with linseed. Typically oil modified alkyd resins are around 60% vegetable oil and 40% alkyd resin. As time passed oil modified alkyd resins became more important than unmodified alkyd resins and the oil modified prefix was often dropped. From here on the unmodified alkyd resins will be known as glyptalic resins and the oil modified alkyd resins as just alkyd resins [Paul 85, Stevens 99, Rauve 95, Chatfield 62, Horie 88, Chapman 83, Seymour 97, Turner 86, Rodriguez 96, Morgans 90, Muizebelt 94].

To gain insight into the reactions occurring within alkyd resins an understanding of their molecular structure is needed. The common approach to this in the past has been based on the linear copolymer of phthalic anhydride and glycerol, via the two primary hydroxyl groups, and the fatty acid bound via the secondary hydroxyl group on glycerol (Figure 2.6).

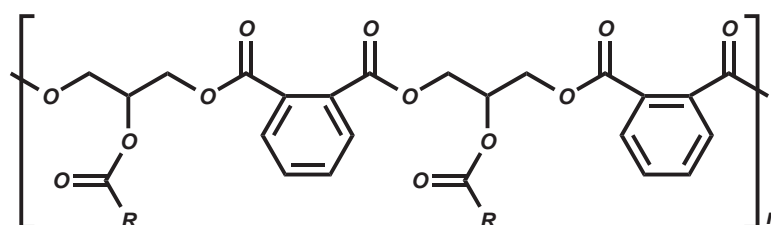


Figure 2.6: Simple model for alkyd structure.

It is thought that this is a highly simplified model that explains the similar curing process with linseed oil but in order to understand the structure further the methods of industrial manufacture of alkyds are needed.

## 2.1.2 Industrial manufacture

Industrially, during manufacture, the alkyd resins are polymerised and cross linked to such a degree that they are still soluble in a given solvent [Paul 85]. The resins are then applied in said solvent and left to cure. The curing process involves both further esterification and fatty acid crosslink formation. There are four main methods of alkyd synthesis:

1. The fatty acid process
2. The monoglyceride process
3. The acidolysis process
4. The fatty acid/oil process

The fatty acid process involves the simultaneous reaction of polyol, diacid and fatty acid. This is heated to 220–260°C until the required degree of polymerisation is reached.

The monoglyceride process involves two stages. Firstly one equivalent of triglyceride is reacted with two equivalents of glycerol and heated to 225–250°C, producing the monoglyceride. Secondly, diacid is added to the monoglyceride along with any additional polyol required. This is again heated until the required degree of polymerisation is reached.

The acidolysis method involves the direct reaction of triglyceride with diacid on heating free fatty acid is produced. To this is added polyol and again heated until the required degree of polymerisation is reached.

The fatty acid/oil process involves the direct reaction of triglyceride, fatty acid, diacid and polyol. Again, the mixture is heated until the required degree of polymerisation is reached.

Each process has advantages and disadvantages over the others regarding the final properties of alkyd resin produced. All the method can be carried out either with solvent, the solvent method, or neat, the fusion method. The addition of solvent allows azeotroping of the water off, and so speeding up the reaction.

## 2.2 Previous research

Much work has been carried out in the field of alkyd resins due to their important commercial application as durable, hardwearing paint. The research has concentrated on the curing process and the mechanism of cross linking, this is of importance as quick drying resins are commercially desirable. In order to investigate the curing process of alkyds model unsaturated systems have been used mimicking the unsaturated fatty acids of the oil.

### 2.2.1 Crosslinking mechanism

The catalysed oligomerisation of ethyl esters of fatty acids has been carried out, probing the crosslinking mechanism involved in alkyd curing [Muizebelt 94]. The ethyl ester oligomers were characterised using  $^{13}\text{C}$  nuclear magnetic resonance (NMR) spectroscopy, solid state NMR spectroscopy, infrared (IR) and Raman spectroscopy, chemical ionisation mass spectrometry (CI-MS), fast atom bombardment mass spectrometry (FAB-MS), secondary ion mass spectrometry (SIMS), size exclusion chromatography (SEC), thermomechanical analysis (TMA) and differential scanning calorimetry (DSC). The research concludes that fatty acid double bonds convert into ether cross links however the stability of alkyd systems was not reproduced. Implying the solid matrix of alkyds is not reproduced.

A more precise mechanistic understanding of the cross link formation was seen in the follow up paper where the use of (Z,Z)- and (E,E)-3,6-nonadiene was used as the model compound [Hubert 97a]. Here inter molecular reaction was catalysed using standard dryers and the large number of reaction products separated using high performance liquid chromatography (HPLC), and preparative SEC. Each separate fraction was then identified using  $^1\text{H}$  and  $^{13}\text{C}$  NMR. The identified compounds comprised of  $\text{C}_9$  hydroperoxides, endoperoxides, epoxides, aldehydes and ketones, along with some other minor oxidation products. The structure of products produced implied three types of oxidation processes taking place. Besides the main radical auto oxidation reaction, evidence was also found for photosensitised oxidation involving singlet oxygen. Thirdly, epoxidation occurs via reaction with peracid or hydroperoxide intermediates. The isolation of products was difficult due to the high degree of structural similarity. Nevertheless two dimers were separated and characterised. Their structures indicate cross linking to occur by recombination of radicals as a termination reaction. It was also found by MS that cross linking occurred by addition of radicals to double bonds.

### 2.2.2 Aerial oxidation

The role of singlet oxygen in the cross linking and curing process was further investigated with nonadienes [Hubert 97b]. Of particular importance was the promotion of the ene reaction, the conversion of a unsaturated systems into hydroperoxides. This was achieved by addition of a photo chemical sensitiser, such as rose Bengal or methylene blue, and found to accelerate the resin curing process.

Other research has been carried out in this area, more specifically on the auto oxidation of soya bean oil [Falla 92]. The significant uptake of oxygen and the evolution of similar amounts of volatile degradation products are modelled using methylanolates. Analysis of products was carried out using IR spectroscopy, liquid chromatography mass spectrometry (LCMS) and SEC. In conclusion it is hypothesised that the fatty acids undergoing scission to leave a C<sub>9</sub> residue remaining attached to a polyester backbone, in place of the C<sub>18</sub> moiety, releasing a small plasticising component in the system. This conclusion, although interesting, is not well substantiated by the data provided, or by any other parties research, in particular the claim of a well characterised repeat unit.

However, it has been shown that hexanal is one of the major volatile byproducts of fatty acid auto oxidation with aerial oxygen [Chang 98]. Indeed it is hexanal, and other aldehyde by products, that gives alkyd resins their characteristic smell. The kinetics of the auto oxidation reaction were investigated by monitoring the lag between oxygen uptake and aldehyde emission implying a series of first order reactions.

Artificial aging or alkyd resins has been carried out using high intensity ultraviolet (UV) light probing the kinetic of the curing via using differential scanning calorimetry and thermogravimetric analysis [Delahay 95]. Glass transition phenomena are observed at  $\approx 5^{\circ}\text{C}$  but are only observed by a small change in base line indicating a large dispersion of molecular weights. It is proposed that the two features observed are, the reaction of previously unreacted starting material, and resin degradation. Thermogravimetric analysis confirm the latter with characteristic decrease in mass at approximately the same point.

### 2.2.3 NMR spectroscopy

Analysis of cured drying oils has also been undertaken due to their importance in alkyd structure [Marshal 86]. Before this little examination had previously been undertaken except minor analysis by IR and Raman spectroscopy. The oils were catalytically cured and analysed in the swollen gel state using <sup>13</sup>C NMR. Comparison was made between these and the unreacted starting material using standard <sup>13</sup>C NMR. Assignment has been made although characterisation is mostly made by fingerprinting.

Further work by the same group into catalysed and uncatalysed curing of alkyds by gel state  $^{13}\text{C}$  NMR has also been carried out [Marshall 85b]. The spectra collected show generally little difference between catalysed and uncatalysed curing, although some peak changes are observed. Investigation into various alkyd modifiers were also investigated showing characteristic peaks where expected. The inclusion of titanium dioxide pigment in the resin was also not found to influence the quality of the spectra significantly [Marshall 85a]. The polyol base of the resin was also characterisable with specific peaks for glycerol and pentaerythritol. The  $^{13}\text{C}$  NMR analysis of fatty acid esters of polyols, such as pentaerythritol tertastearate has also been carried out. Thus aiding alkyd characterisation.

Solid state NMR analysis of cured linseed oil, glycerol and pentaerythritol based alkyd have been carried out to a limited degree [Marshall 87]. Spin lattice relaxation values  $T_1$  have been measured at between 0.1–0.2 s. The  $T_1\rho$  values show two distinct relaxation pathways providing possible information on the resin morphology.

#### 2.2.4 X-ray diffraction techniques

Analysis of cured alkyd resins has also been undertaken using X-ray diffraction techniques and has unsurprisingly shown that they are amorphous materials with no unit cell present [Swarup 92].

#### 2.2.5 Currently research

Currently research is being carried out at the Tate Gallery, London, into alkyd analysis by pyrolysis gas chromatography mass spectroscopy (GCMS). This research has shown significant amounts of phthalic anhydride being released from the resins on heating. Characterisation of polyol has also been achieved using a chemical work up followed by pyrolysis GCMS.

## Chapter 3

# Artificial Ageing & NMR

### 3.1 Artificial ageing

Artificial ageing can take a number of forms, controlled exposure to heat, humidity, light, or a combination of all these are common. For the purposes of this investigation light aging was chosen due to its ease and suitability in promotion of crosslinking, thought to occur by a photo chemical pathway. In order to calculate how many years in the museum environment artificial aging in a light box is equivalent to, the strength of light emitted from the light box is required. Two light boxes were considered, the light box at the Tate Gallery gave 15,000 lux and the light box at the National Gallery gave 22,000 lux. The National Galleries light box was chosen due to the higher intensity and the availability of more space for a longer period of time. Artificial aging calculations are based on the rule of reciprocity, implying that ten hours exposure at 200 lux is equivalent to one hour at 2000 lux [Learner 99]. In order to calculate the amount of aging carried out a few assumptions were made. These included, the museum lighting being held at a strength of 200 lux, the artifacts being exposed to this for 8 h a day, and the museum being open all year. Simple multiplication shows that in the museum environment artifacts are exposed for 2922 h per year at 200 lux. This is equivalent to 584,400 lux hours per year. In the National Galleries light box, one days aging is equivalent to 528,000 lux hours, which is approximately equivalent to one year. As samples are removed every two weeks they would have been exposed to 7,392,000 lux hours, this is approximately equivalent to 14 years in the museum environment.

## 3.2 Nuclear magnetic resonance (NMR) spectroscopy

Nuclear magnetic resonance, or more commonly NMR, spectroscopy probes the energy gap between nuclear spin states in the same way that infrared spectroscopy probes the energy gap between vibrational states [Bovey 96, Schmidt-Rohr 94, Ibbett 93]. Nuclear energy levels are formed as each nuclei has the quantum property of spin. This can either be spin up ( $\uparrow$ ) or spin down ( $\downarrow$ ). In the absence of a magnetic field, both these states have the same energy and so there is no energy gap. However by application of a large external magnetic field,  $B_0$ , one state will be lowered in energy and the other raised, relative to each other. This is due to higher energy states spin opposing the magnetic field, and so requiring more energy. This thus produces two energy levels between which transitions can occur. This is known as the Zeeman effect and the levels produced are called the Zeeman levels (Figure 3.1)

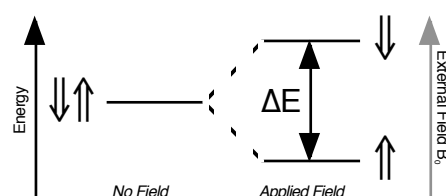


Figure 3.1: Formation of Zeeman levels by application of  $B_0$ .

Excitation between states is achieved by irradiation with electromagnetic radiation, of frequency  $\nu$ , this is proportional to the magnitude of the energy gap,  $\Delta E$ , by Planck's constant,  $h$ :

$$\Delta E = h\nu \quad (3.1)$$

The magnitude of  $\Delta E$  for NMR means that  $\nu$  is in the radio frequency (RF) part of the electromagnetic spectrum. The frequency of RF radiation needed to cause transitions between nuclear energy levels is specific to a particular nuclear nucleus and is called the Larmor frequency. As the Larmor frequency is proportional to the energy gap and this in turn is proportional to the magnetic field strength, spectrometers are characterised by their  $^1\text{H}$  Larmor frequency. For example by using a 1.4 T magnet the Larmor frequency is 60 MHz, but if a 14 T magnet is used the Larmor frequency is 600 MHz. To achieve frequencies above 100 MHz superconducting magnets are required utilising, liquid helium to produce the very low temperatures required for superconductivity.

The important structural information that NMR is so famed for arise from the phenomena of chemical shift. This is a perturbation in the Larmor frequency, due to very small perturbations in the Zeeman levels, caused by the nucleus particular environment. These perturbations are very small and in the magnitude of parts per mil-

lion (ppm). Chemical shift is measured as a relative scale to an internationally recognised set of standards, for  $^1\text{H}$  and  $^{13}\text{C}$  work this is tetramethylsilane (TMS),  $\text{Si}(\text{CH}_3)_4$ , which has a chemical shift of 0 ppm. The perturbation of Larmor frequency from TMS can be measured, for example aromatic protons appear at  $\approx 6$  ppm and methyl protons at  $\approx 1$  ppm. A normal NMR spectra correlates chemical shift and intensity showing what types of environments are present and how abundant they are. Due to the reference system correlation tables can be produced showing chemical shift ranges and structural moiety. Spin coupling can occur again providing more information on the nuclei environment. This is a perturbation in chemical shift due to the electrons in the intervening bonds.

In order for a nucleus to be NMR active it need to have a spin number,  $I > 0$ . If  $I = \frac{1}{2}$  the nucleus is said to be spin half, and the majority NMR experiment are cried out on spin half nuclei. If  $I > \frac{1}{2}$  the nucleus has a quadrapole and more than two Zeeman levels are produced on application of an external magnetic field complicating matters. This is not to say that quadrapole NMR experiments are not possible, or do not provide valuable information. Protons,  $^1\text{H}$ , are spin half and are 100% isotopically abundant and so are easy to observe. Carbon on the other hand has two main isotopes,  $^{12}\text{C}$  (99% abundant) and  $^{13}\text{C}$  (1% abundant). As  $^{12}\text{C}$  is spin inactive, i.e.  $I = 0$ , it isotopically dilutes the less abundant  $^{13}\text{C}$ . As only  $^{13}\text{C}$  is NMR active carbon spectra generally take much longer to acquire and are of lower resolution. This is improved by use of pulse techniques and Fourier transform NMR.

### 3.2.1 Pulse techniques in NMR

When first introduced NMR spectrometers swept a range of frequencies recording when resonance occurred, thus producing a spectrum. This was know as the continuous wave method. In the last 20 years the emergence of pulse techniques and Fourier transformations have revolutionised the world of spectroscopy. The basis of this is that a short pulsed of radiation can excite all the frequencies at once. This is analogous to striking a bell with a hammer producing all modes of vibration at once instead of sweeping all the frequencies and waiting for resonance. If the decay of the signal is recorded in the time domain a free induction decay (FID) is produced. The frequency information can be 'decoded' by applying a mathematical function called a Fourier transform (FT) to produce a the frequency domain of spectrum (Figure 3.2) This in itself does not produce higher resolution spectra but by repeating the pulse and adding together all the FIDs a higher signal to noise ratio can be achieved. Now when a FT is applied to the combined FID a dramatic improvement in resolution is gained, coupled with high field superconducting magnets this can produce high resolution  $^1\text{H}$  spectra from 16 scans in less than a minute. Due to isotopic dilution  $^{13}\text{C}$  spectra often need hundreds of scans thus taking longer.

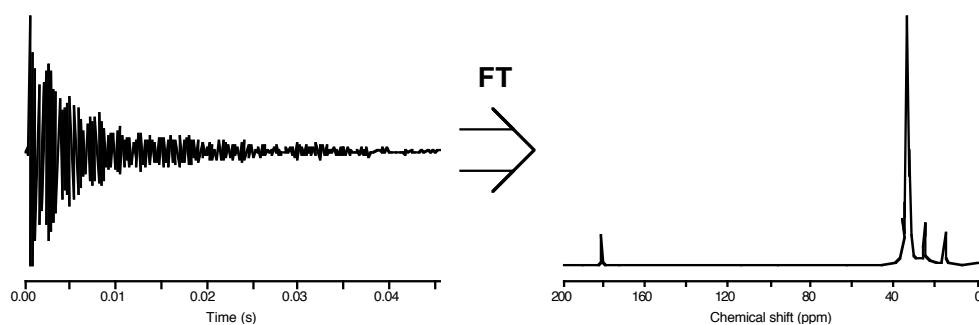


Figure 3.2: Fourier transform of the time domain to the frequency domain.

### 3.2.2 Solid state NMR

This particular area of NMR although around from the early 60s has only really taken off in the last 25 years due to the advances in stable superconducting magnets and amplifier design. The main difficulty with application of NMR to solids is the low resolution, this is characteristic solids (Figure 3.3). There are however good reasons for overcoming these difficulties [Bovey 96, Schmidt-Rohr 94, Ibbett 93, Holmberg 87, Atkins 95]. These include analysis of species that are unstable in solution, or those that are completely insoluble. More importantly some species are intrinsically important as solids and so it is important to determine their structure and dynamics in the solid state. Synthetic polymers are particularly interesting in this regard, and information can be gained about the arrangement of molecules, their conformation, and the motion of different parts of the chain. This information is important in the interpretation of bulk properties in terms of molecular characteristics.

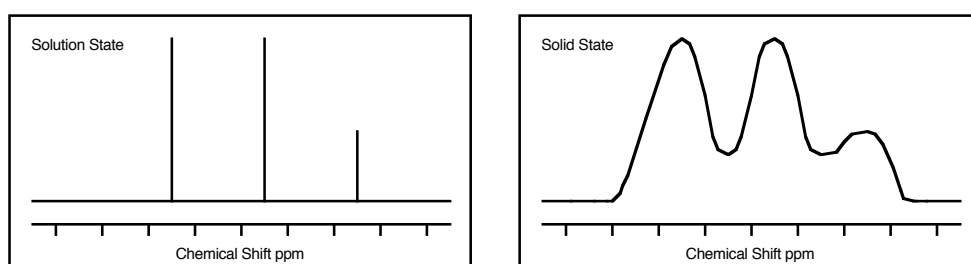


Figure 3.3: Resolution and line broadening in solid state NMR spectra.

Problems of resolution and line width are not the only features that cause problems in NMR studies of solids. Because molecular rotation has almost ceased, spin lattice relaxation times ( $T_1$ ) are very long, but spin-spin relaxation times ( $T_2$ ) are very short. Hence, in pulse experiment, there need to be long delays of several seconds between successive pulses to allow the spin system to revert to its equilibrium state. This means that gathering the low resolution information may be a lengthy process. The exceptions are plastic crystals, such as adamantane, here molecular rotation still occurs, but molecules are confined to the lattice sites. Another important difference

is that, because the lines are so broad, high power radio frequency radiation may be required to achieve saturation. Whereas solution state pulse NMR spectrometers uses amplifiers of a few tens or hundreds of watts, solid state spectrometers require amplifiers rated at kilowatts.

There are two main contributions to the line widths of solids. One is the direct magnetic dipolar interaction between nuclear spins. As each nuclear magnetic moment acts like a small magnet it will give rise to a local magnetic field. Many nuclei may contribute to the total field experienced by a nucleus of interest and thus nuclei in a sample may experience a wide range of fields. Typical dipole dipole fields are in the order of  $10^{-3}$  T, which correspond to line widths in the order of 104 Hz. In solution, this local field is averaged to zero by molecular tumbling. The second main source of line width is anisotropy of the chemical shift. As the chemical shift arises from the ability of an applied field to generate electron currents in the molecule, the orientation of the molecule relative to the field will be proportional to the chemical shift. In solution, only the average value of the chemical shift is relevant due to molecular tumbling. However, for stationary molecules in a solid, the anisotropy is not averaged to zero and molecules in different orientations have resonances at different frequencies leading to a static powder pattern being produced (Figure 3.4).

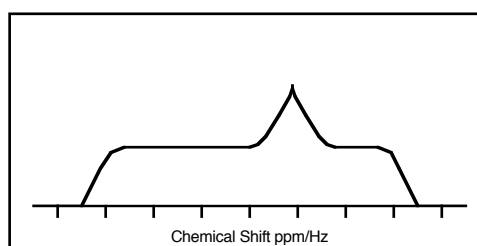


Figure 3.4: Static powder pattern due to chemical shift anisotropy

### 3.2.3 Magic angle spinning (MAS)

The dipole-dipole interaction and the chemical shift anisotropy vary with the angle between the applied field and the principle axis of the molecule as  $1 - \cos^2 \theta$ . This has been exploited by the technique of magic-angle spinning (MAS). The magic-angle is the angle which  $1 - 3 \cos^2 \theta = 0$ , and corresponds to  $54.74^\circ$ . An experiment using MAS involves the sample being spun at high speed at the magic angle to the applied field (Figure 3.5). By doing this all the dipolar anisotropies average to the value they would have at the magic angle, zero. The difficulty with MAS is that the spinning frequency must not be less than the frequency of the interaction trying to be removed, which is of the order of kilohertz. Advances in technology have enabled gas driven sample spinners that can spin at up to 15 kHz being routinely available.

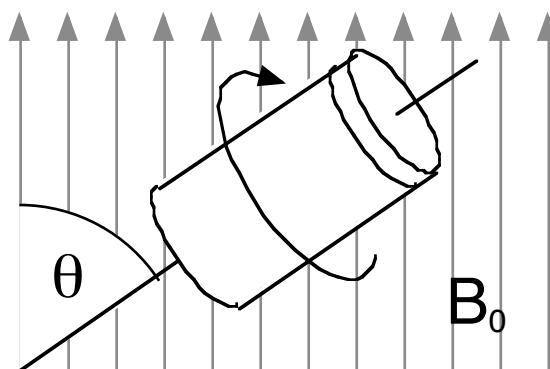


Figure 3.5: Magic angle spinning

Elaborate pulse sequences have also been devised to reduce line width. These work by twisting the magnetisation vector through an elaborate series of contortions producing average interactions thus reducing line width. One such example is the WAHUA sequence devised by Waugh, Huber, and Haeberlen:

$$\left[ \tau - 90_x^\circ - \tau - 90_{-y}^\circ - 2\tau - 90_y^\circ - \tau - 90_{-x}^\circ - \tau \right]_n \quad (3.2)$$

The FID acquisition takes place during one of the  $2\tau$  sections.

### Protons in solid

One of the main differences between solution and solid state NMR is the observation of proton. As they are 100% abundant they are very easy to observe at high resolution in solution. This is not true in the solid state [Ibbett 93]. As one of the major broadening factors in solids, the dipole-dipole interaction, is proportional to the magnetic moment of the nuclei. Protons have the largest magnetic moment of all nuclei except tritium ( $^3\text{H}$ ), and so experience extremely large dipolar broadening. As the frequency of this interaction is higher than 20 kHz this cannot be 'spun-out' by MAS. For this reason protons tend not to be observed as little or no information can be gained from them. As technology advances high field solid state NMR spectrometers are becoming available which can achieve spinning speeds greater than 35 kHz, and so will allow proton work in solids. As mentioned previously elaborate pulse sequences have been devised to produce average interactions, commonly they are termed combined rotational and multi pulse spectroscopy (CRAMPS). This is a complex pulse sequence which puts severe hardware strain on the spectrometer and so is aptly named.

### Cross-polarisation magic angle spinning

Due to the isotopic dilution of  $^{13}\text{C}$ , and the broad nature of solid state NMR, cross-polarisation (CP) is used to enhance the  $^{13}\text{C}$  signal. This works by causing polarisation in the protons and then transferring this polarisation to  $^{13}\text{C}$ . As protons are 100% abundant a dramatic improvement in  $^{13}\text{C}$  polarisation, and thus  $^{13}\text{C}$  signal, is achieved. The polarisation transfer is achieved by satisfying the Hartman-Hahn match condition, which is where both the proton and carbon Zeeman level are split by the same amount, and so  $\Delta E_C = \Delta E_H$ . This is achieved by application of a secondary magnetic field,  $B_1$ , that only affects the protons. When combined with magic angle spinning CPMAS becomes a quick easy method of acquiring  $^{13}\text{C}$  spectra and is the standard experiment in solid state NMR.

## Chapter 4

# Experimental

### 4.1 Commercial resins analysed

A small collection of 12 modern commercial resins had been gathered together by the Tate Gallery, London, as part of their research using pyrolysis GCMS. They kindly agreed to allow small samples to be taken and used for this project. The resins provided can be seen in Table 4.1. The coding system established here will be used throughout the project. The resins were analysed in both their neat liquid state and the cured solid state, a selection of the cured resins was then artificially aged and analysed with respect to aging.

*Table 4.1: The alkyd resin samples provided by the Tate Gallery, London.*

| Supplier     | Description             | Code   |
|--------------|-------------------------|--------|
| Attiva       | Smalto Brillante Bianco | SBB-00 |
| Cray Valley  | Synolac 28w             | S28-00 |
|              | Synolac 60w             | S60-00 |
| Croda Resins | Crodakys a2/1028        | CA2-00 |
|              | Crodakyd 444w           | 444-00 |
|              | Crodakyd 826w           | 826-00 |
|              | Crodakyd 850w           | 850-00 |
| Kalon        | Long Oil Alkyd          | LOA-00 |
|              | Thixotropic Alkyd       | THX-00 |
| Scott Bader  | Sobral 1241 ML 70       | 124-00 |
| Vil          | Vilkyd 211              | 211-00 |
|              | Vilkyd 270w65           | 270-00 |

## 4.2 Analytical equipment and practice

Infrared spectroscopy was carried out using a Perkin-Elmer RX FTIR spectrometer. Each spectra was obtained using sixteen scans producing spectra in the range of 4000–400  $\text{cm}^{-1}$ . Analysis of the neat resins and liquid samples were carried out using sodium chloride plates, for solid samples potassium bromide disks were made.

Solution state  $^1\text{H}$  and  $^{13}\text{C}$  NMR spectroscopy was under taken using a Jeol 270 MHz FT-NMR spectrometer for quick experiments, such as standard  $^1\text{H}$  and some  $^{13}\text{C}$  spectra. A Bruker 400 MHz FT-NMR spectrometer was used for the more complex time consuming experiments, such as  $^{13}\text{C}$  spectra,  $^{13}\text{C}$  DEPT 135 (distortionless enhancement by polarisation transfer),  $^1\text{H}$ - $^1\text{H}$  COSY (correlation spectroscopy) and  $^1\text{H}$ - $^{13}\text{C}$  HMQC (heteronuclear multiple quantum coherence). All spectra were recorded over the standard ranges of -1–12 ppm and -10–220 ppm, for  $^1\text{H}$  and  $^{13}\text{C}$  respectively, and referenced to TMS. Precision NMR tubes were made up with an approximate concentration of 50 mg/ml and 200 mg/ml for  $^1\text{H}$  and  $^{13}\text{C}$  work respectively with deuterated solvent. Common deuterated solvents used included deuteriochloroform ( $\text{CDCl}_3$ ),  $d_6$ -dimethylsulphoxide ( $(\text{CD}_3)_2\text{SO}_2$ ), deuterium oxide ( $\text{D}_2\text{O}$ ) and  $d_6$ -acetone ( $(\text{CD}_3)_2\text{C}=\text{O}$ ).

Solid state  $^1\text{H}$  and  $^{13}\text{C}$  NMR spectroscopy was under taken using a Bruker 200 MHz FT-NMR spectrometer. Samples were packed into 4 and 7 mm ceramic set zirconia ( $\text{ZrO}_2$ ) rotors and spun at a maximum speed of 15 kHz and 7 kHz respectively. A 4 mm rotors required approximately 70 mg of sample whereas a 7 mm rotor required approximately 200 mg. Most of the spectra obtained were taken using a 7 mm rotor as the larger amount of sample allowed for quicker spectra acquisition, typically around 1.5 hours for 2000 scans. Experiments undertaken included  $^{13}\text{C}$  CPMAS (cross polarisation magic angle spinning),  $^{13}\text{C}$  CPMAS NQS (non quaternary suppression), NOEMAS (nuclear Overhauser enhancement MAS),  $^1\text{H}$  SPE MAS (single pulse excitement), static  $^1\text{H}$  SPE and  $^1\text{H}$   $T_1$  spin-lattice relaxation experiments.

Differential scanning calorimetry was carried out on a TA Instruments DSC 2910 Differential Scanning Calorimeter using nonhemetic aluminium pans. Samples were equilibrated at  $-30^\circ\text{C}$ , using dry ice to allow sub ambient analysis, and then ramped at  $10^\circ\text{C min}^{-1}$  to  $300^\circ\text{C}$ . The samples were then allowed to cool and analysis was repeated to investigate components driven off.

### 4.3 Analysis of neat resin

The neat commercial resins obtained were analysed using standard chemical techniques. These included  $^1\text{H}$ ,  $^{13}\text{C}$  and DEPT-135 solution state NMR spectroscopy, and IR spectroscopy. The linseed based alkyd, 826-00, was also subjected to 2D solution state NMR in the form of homonuclear  $^1\text{H}$ - $^1\text{H}$  correlation, COSY, and heteronuclear  $^1\text{H}$ - $^{13}\text{C}$  correlation, HMQC, spectroscopy.

#### 4.3.1 Resin film preparation

Approximately 15 ml of each resin was spread out on a  $30 \times 50$  cm colourless polypropylene tray in thin even layers and allowed to cure until they became touch dry in a fume hood. The time taken to cure varied from between 5–15 days for the different resins. Due to the high spinning speeds of MAS NMR an even sample distribution was required to balance the rotor, cutting of the resin films into  $1 \times 1$  mm square was found to be sufficient, but time consuming, so the practice of freezing in liquid nitrogen and grinding in a pestle and mortar was employed. Comparison spectra were run to see if the freezing and thawing process had changed the structure significantly, this was not found to be the case.

#### 4.3.2 Artificial aging

Due to space limitations in the light box at the National Gallery three of the twelve resins were artificially aged. The selection of which resins would be used was carried out on merit of relevance of composition, speed of curing, and ease of spectral analysis. The three chosen resins were 270-00, 444-00 and 826-00, this allowed comparison between pentaerythritol (270) and glycerol (444) resins, based on soya oil, and a linseed resin (826). The linseed based resin is of most importance as the alkyd resins relevant to modern art were linseed based. The neat resin was spread in sections over a  $30 \times 50$  cm polypropylene tray and allowed to dry for approximately 10 days. The samples were then placed in the 22,000 lux light box at the National Gallery at approximately 1 pm on Monday 14th January 2000. For the next 5 months  $2 \times 10$  cm strips of each resin were cut and peeled from the tray every two weeks. The tray was also turned every time a collection was made to ensure even exposure.

#### 4.3.3 UV irradiation of resin

By exposure to high intensity UV radiation it was hoped to exaggerate any possible changes observed in the light box aged samples. Films of approximately  $2 \times 5$  cm of the commercial resin, 270-00, 444-00, 826-00, and the synthetic alkyd, ALK-00, were exposed to high intensity ultra-violet light. A 400 W medium pressure mercury

discharge tube was placed in a water cooled quartz immersion well with the four samples strapped to the outside using fine copper wire. The samples were irradiated for 3 hours in a specially blacked out fume hood, paying particular attention to the important safety issues involved with high intensity UV light. These included protective clothing, gloves and UV eye shields. Most of the radiation produced from the discharge tube was at 366 nm, but a significant amount of high intensity visible light was also produced, this can be seen in the emission spectrum of the tube (Figure 4.1). In this configuration the discharge produced  $> 5 \times 10^{19}$  photons per second.

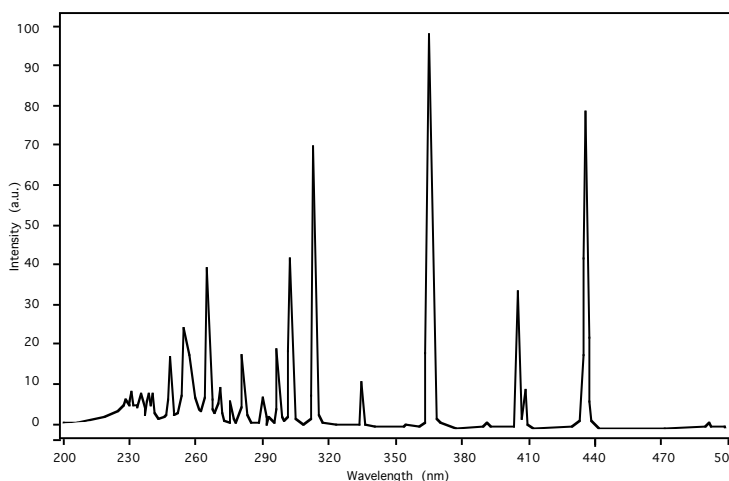


Figure 4.1: Emission spectrum of the mercury discharge tube.

## 4.4 Model alkyd resins

When dealing with complex systems the application of models allows gradual understanding by use of approximation. A number of model resins were synthesised in order to understand the main bonding motifs of the constituent materials. These were then analysed using the same techniques producing spectra helping alkyd assignment. This is of particularly important with alkyds due to their commercial nature and batch formulation manufacture. Determining resin composition is further complicated by manufacturers reluctance to release detailed information about their manufacturing processes. Thus making it very difficult to find out exactly what reagents and method of manufacture has used.

### 4.4.1 Glyptalic resin preparation

The current model of alkyd resins is that the fatty acids modify the polyol, phthalic anhydride polyester backbone. To investigate this a number of simple resins were synthesised and analysed. The components used included phthalic anhydride (T), maleic anhydride (M), glycerol (G), pentaerythritol (P) and sorbitol (S). A 1% catalyst of calcium hydroxide was used to facilitate the reaction. The linear polymer of phthalic anhydride and ethylene glycol (E) was also synthesised to aid characterisation. The comprehensive list of all compounds synthesised can be seen in Table 4.2.

*Table 4.2: Glyptalic resins synthesised*

| Resin  | Synthesised | Characterised |
|--------|-------------|---------------|
| TG-11  | Yes         | No            |
| TP-11  | Yes         | No            |
| TG-21D | Yes         | Yes           |
| TP-21D | Yes         | Yes           |
| MG-11  | Yes         | Yes           |
| MP-11  | Yes         | No            |
| MG-21D | Yes         | No            |
| MP-21D | Yes         | No            |
| TE-11  | Yes         | Yes           |
| TS-21D | Yes         | No            |

The method of resin synthesis was similar for all compounds produced. The correct molar ratio of reagents required to make 5 g of resin was placed in a small beaker and heated to 250°C on a hot plate with stirring. After a period of approximately 5 min, the liquid became more viscous and difficult to stir. The beaker was removed from the hot plate and allowed to cool to room temperature with continued stirring. When cool the resin was chipped out of the beaker and crushed. The resins were then swollen in chloroform and packed into a Soxhlet thimble and hot solvent extracted for 10 h with 100 ml of chloroform to remove unreacted reagents. After this period the swollen gel was removed from the thimble and dried under vacuum for 24 h until a solid powder was obtained.

Again the method of linear polymer synthesis was similar for all compounds produced. The correct molar ratio of reagents was placed in a small beaker and heated to 250°C on a hot plate with mechanical stirring, after a period of time,  $\approx 5$  min, the liquid became more viscous. The beaker was removed from the hot plate and allowed to cool to room temperature. When cool the product was removed from the beaker.

#### 4.4.2 Control resin preparation

To understand the curing process and the composition of the neat resin a control resin was synthesised with known reagents under standard conditions. Characterisation of this has enabled better assignment of spectra and provided insight in the neat resin composition. The commercial method of monoglyceride alcoholysis was chosen as this had the most scope for modification in further investigations. As linseed based alkyds are of more historical importance than soya alkyds synthesis of these was concentrated on. Stage one was transesterification of the linseed oil triglyceride with glycerol to produce a distribution of non, mono, bi and triglycerides (Figure 4.2).

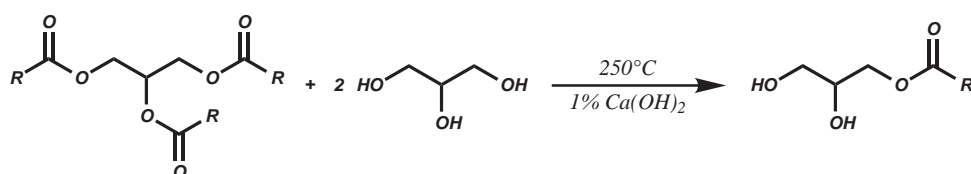


Figure 4.2: Stage one: Transesterification of linseed oil with glycerol.

Approximation of the molecular weight of linseed oil was made by averaging the known distribution of fatty acids in the triglyceride. The difference between minimal trilinolenic and maximum tristearate was not within experimental measurable values of the balances used. Assuming the molecular weight of linseed oil was 890 amu 25.5 g of linseed oil was mixed with 5.3 g of glycerol and 0.1 g  $\text{Ca}(\text{OH})_2$ , as a catalyst, in a 250 ml three necked flask. This was fitted with a thermometer, reflux condenser and mechanical stirrer. This mixture was heated to 250°C in an oil bath and agitated. The extent of reaction was monitored by miscibility with methanol, as tri and diglycerides are not miscible with methanol at room temperature. At 10 min intervals approximately 2 drops were removed and dissolved in 1 ml of methanol and agitated. The reaction usually took between 40–60 mins to reach the desired level of completion. Stage two was the condensation of monoglyceride, produced in stage one, with phthalic anhydride to produce the alkyd (Figure 4.3)

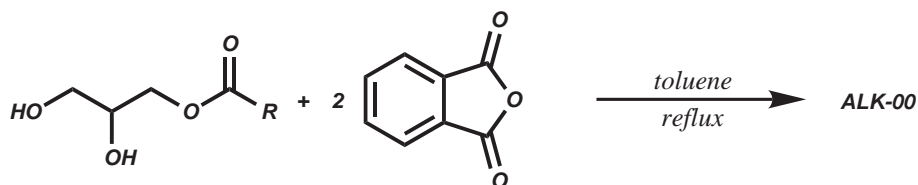


Figure 4.3: Stage two: Condensation with phthalic anhydride to form alkyd.

To the monoglyceride of stage one was added 19.2 g of phthalic anhydride a Dean-Stark trap was added to the flask. The flask was then again heated to 250°C and toluene added by syringe slowly into the vessel. The toluene-water azeotrope boiled

off and separated in the Dean-Stark trap and toluene flowed back into the vessel. Refluxing toluene also washed the sublimed phthalic anhydride back into the reaction vessel. The extent of reaction was measured using the same process used in industry, that is measurement of the acid number. This is the number of mg of KOH required to neutralise 1 g of resin. This was achieved by producing a 0.1 molar standard solution of alcoholic KOH and titrating it against the resin dissolved in  $\approx 2$  ml of toluene. The end point was indicated using phenothialene which undergoes a colour change at pH 7. Samples were taken at 10 min intervals and the acid number calculated. The end point of the reaction is defined as an acid number of 10, this is before the gel point of the resin allowing easy manipulation and storage. Reactivity was quenched by addition of excess toluene, this was later evaporated on a rotary evaporator before curing.

As a high percent of the final alkyd product is oil, pure linseed oil was also studied both in its natural liquid state and after bodying into a resin. Approximately 100 ml of linseed oil was placed into a round bottomed flash and a reflux condenser fitted. The oil was heated to 250°C until fuming occurred and heated for a further 3 h. On cooling a more viscous appearance and a more pungent odour noted. The material was then spread onto a polypropylene tray into a thin layer and left to cure. After approximately 2 weeks a film had formed allowing separation and removal of non solid content. CPMAS analysis was carried out.

## Chapter 5

# Results

### 5.1 Spectral analysis of neat resin

The neat commercial resins were analysed using IR,  $^1\text{H}$ ,  $^{13}\text{C}$  and  $^{13}\text{C}$  DEPT 135 solution state NMR. Group assignment has been carried out due to the high degree of similarity between spectra (Table 5.1). A typical IR spectrum for reference is shown in Figure 5.1. A comprehensive set of spectra can be seen in the appendix.

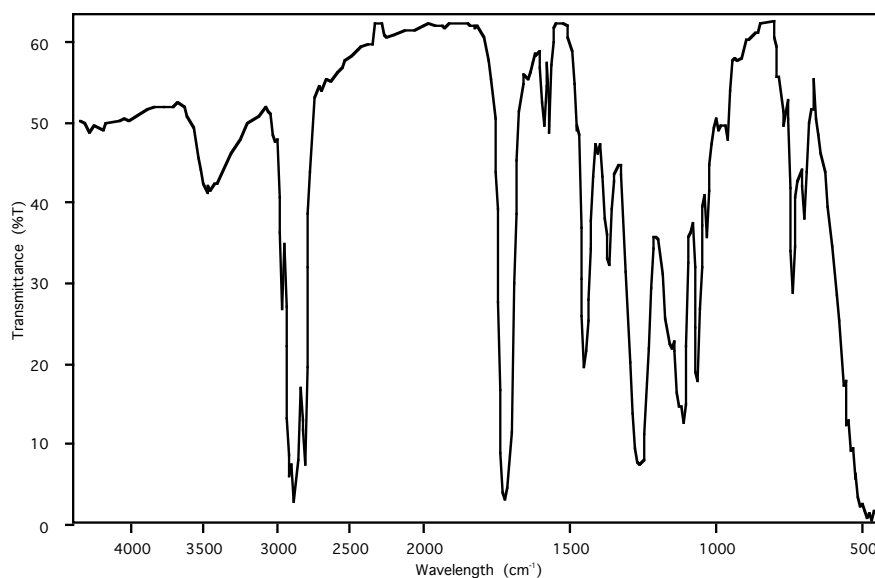


Figure 5.1: IR spectrum of neat resin 826-00.

The IR spectra show the presence of aliphatic chains and carbon-carbon double bonds, indicative of the fatty acid side chains. Carbonyl stretches are also present due to the phthalate ester, fatty acid ester and phthalic anhydride. Some free hydroxyl groups are also present.

Table 5.1: Assignment of IR spectra of neat resins.

| SBB-00 | S28-00 | S60-00 | CA2-00 | 444-00 | 826-00 | 850-00 | LOA-00 | THX-00 | ML7-00 | 211-00 | 270-00 | Assignment  |
|--------|--------|--------|--------|--------|--------|--------|--------|--------|--------|--------|--------|-------------|
| -      | -      | -      | 4329.4 | 4329.8 | -      | 4329.6 | -      | -      | 4332.7 | -      | -      | O-H Stretch |
| 3848.5 | -      | -      | -      | -      | -      | -      | -      | 3848.2 | -      | -      | 3848.8 | O-H Stretch |
| -      | -      | -      | -      | -      | 3538.4 | -      | -      | -      | -      | -      | -      | O-H Stretch |
| -      | 3521.5 | 3522.3 | -      | 3512.9 | -      | 3519.9 | -      | -      | 3521.5 | 3521.8 | -      | O-H Stretch |
| 3512.8 | -      | -      | 3512.3 | -      | -      | -      | -      | 3512.6 | -      | -      | 3512.4 | O-H Stretch |
| -      | -      | -      | -      | -      | -      | -      | 3467   | -      | -      | -      | -      | O-H Stretch |
| 3007.6 | 3007.8 | 3007.8 | 3009.7 | 3008.2 | 3009.8 | 3007.9 | 3007.3 | 3007.3 | 3007.4 | 3007.6 | 3007.4 | C-H stretch |
| 2923.1 | 2924.8 | 2922.7 | 2923.3 | 2921.7 | 2923.5 | 2924.2 | 2923.8 | 2923.8 | 2924.1 | 2924.1 | 2923.8 | C-H stretch |
| 2853.2 | 2854.1 | 2853.2 | 2853.3 | 2854.1 | 2853.7 | 2853.8 | 2853.6 | 2853.5 | 2853.5 | 2853.4 | 2854.1 | C-H stretch |
| -      | -      | -      | -      | 2348   | -      | -      | -      | 2348.3 | -      | -      | -      | C-H stretch |
| -      | -      | -      | 2282.4 | -      | 2284.4 | -      | -      | -      | -      | -      | 2285.7 | C-H stretch |
| 1738   | 1739.6 | 1737.3 | 1731.1 | 1731.3 | 1738.2 | 1738   | 1738.4 | 1736.9 | 1731.2 | 1738.1 | 1736.7 | C=O Stretch |
| -      | -      | -      | -      | -      | -      | -      | -      | 1640.1 | -      | -      | 1649.8 | Aromatic    |
| 1599.6 | 1599.4 | 1599.3 | 1599.3 | 1599.4 | 1599.6 | 1599.4 | 1599.3 | 1599.3 | 1599.3 | 1599.3 | 1599.4 | Aromatic    |
| 1580.2 | 1580   | 1580   | 1580   | 1580.1 | 1580   | 1580   | 1580   | 1579.9 | 1580   | 1580   | 1579.9 | Aromatic    |
| -      | -      | -      | 1489.1 | 1489.2 | -      | -      | -      | -      | -      | -      | -      | Aromatic    |
| 1463   | 1465.2 | 1465.1 | 1462   | 1462.5 | 1463.8 | 1465.4 | 1465.3 | 1464   | 1462.7 | 1465.4 | 1463.9 | C-O Stretch |
| 1378.1 | 1378.1 | 1378.1 | 1377.8 | 1377.8 | 1378.1 | 1378.3 | 1378.2 | 1377.9 | 1378.1 | 1378.2 | 1377.9 | C-O Stretch |
| -      | -      | -      | 1282.2 | 1282.9 | -      | -      | -      | -      | -      | -      | -      | C-O Stretch |
| 1274.3 | 1278.8 | 1276.5 | -      | -      | 1272.8 | 1272.3 | -      | 1277.8 | 1275.7 | 1273.5 | 1278   | C-O Stretch |
| -      | -      | -      | -      | -      | -      | -      | 1269   | -      | -      | -      | -      | C-O Stretch |
| 1122   | 1122.2 | 1122.4 | 1123.7 | 1123   | 1122.2 | 1122   | 1122.1 | 1122.5 | 1122.2 | 1122   | 1122.9 | C-O Stretch |
| 1072.7 | 1072.5 | 1072.5 | 1071.3 | 1071.3 | 1072.3 | 1072.6 | 1072.5 | 1073.1 | 1073.5 | 1072.7 | 1073.6 | C-H Stretch |
| 1040.7 | 1040.6 | 1040.6 | 1041   | 1041.1 | 1040.6 | 1040.7 | 1040.5 | 1040.5 | 741.3  | 1040.5 | 1040.5 | C-H Stretch |
| -      | -      | -      | 988.1  | 987.4  | -      | -      | -      | -      | -      | -      | -      | C-H Stretch |
| -      | -      | -      | -      | -      | 968.4  | -      | -      | -      | -      | -      | -      | C-H Stretch |
| -      | 794.7  | -      | -      | -      | -      | -      | -      | -      | -      | -      | -      | Aromatic    |
| -      | 767.9  | -      | -      | 760    | 769.3  | 768    | -      | -      | -      | -      | 767.3  | Aromatic    |
| -      | 741.7  | 741.4  | 742.3  | 742.6  | 741.5  | 741.4  | 741.2  | 741.1  | -      | 741.4  | 741    | Aromatic    |
| -      | 704.3  | 704.5  | 704.9  | 705.1  | 705.6  | 704.4  | 704.8  | 704.1  | 704.4  | 704.9  | 703.9  | Aromatic    |
| -      | -      | 666.3  | -      | 665.9  | -      | -      | -      | 669.8  | -      | -      | -      | C-H Stretch |
| -      | -      | -      | 455.9  | -      | -      | -      | -      | -      | -      | -      | -      | C-H Stretch |
| -      | -      | -      | -      | -      | -      | -      | -      | 434.5  | -      | -      | 426.3  | C-H Stretch |
| -      | -      | -      | -      | -      | -      | -      | -      | 358.8  | -      | -      | -      | C-H Stretch |
| -      | -      | -      | -      | -      | -      | -      | -      | 329.7  | -      | -      | 326.9  | C-H Stretch |
| -      | -      | -      | -      | -      | -      | -      | -      | 316.2  | -      | -      | -      | C-H Stretch |

The same high degree of similarity, as expected from the IR, was seen for the  $^1\text{H}$  NMR spectra, and again group assignment was used Table 5.2. The proton spectrum of 826-00 has been shown for reference (Figure 5.2). A comprehensive set of all spectra can be seen in the appendix.

The presence of aliphatic chains in the fatty acid are indicated in the high field part of the spectra with implication of methylene groups adjacent to oxygen. Non conjugated carbon-carbon double bonds are also seen as expected with natural fatty acids. Aromatic protons are present with varying shifts due to proximity to the phthalate esters or anhydrides. The presents of aldehydes is also implicated by the low field area of the spectra. Although the samples were extracted and the protonated solvents used for thinning during manufacture were removed by rotary evaporation there will probably be a high protonated solvent content. This thus complicates the spectra and render quantitative comparison by peak integration inaccurate. Although not comparable the integrals showed the same degree of relative similarity between spectra within approximately 10%.

The group assignment of the  $^{13}\text{C}$  and DEPT 135 spectra has been combined giving

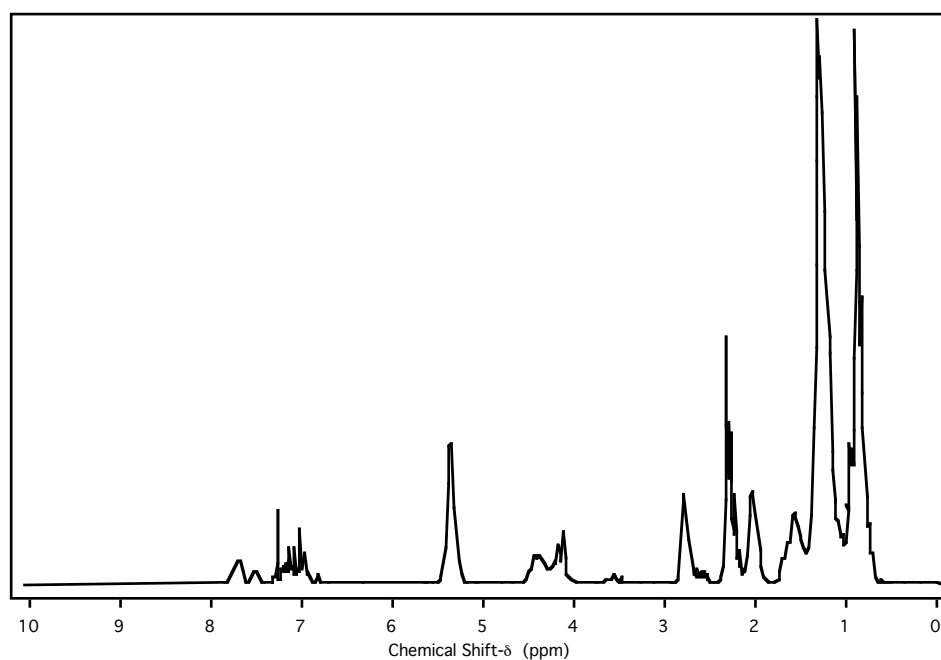


Figure 5.2:  $^1\text{H}$  NMR spectra of neat resin 826-00

Table 5.2: Assignment of  $^1\text{H}$  NMR spectra of neat resins.

| SBB-00 | S28-00 | S60-00 | CA2-00 | 444-00 | 826-00 | 850-00 | LOA-00 | THX-00 | ML7-00 | 211-00 | 270-00 | Assignment              |
|--------|--------|--------|--------|--------|--------|--------|--------|--------|--------|--------|--------|-------------------------|
| 9.15   | -      | -      | -      | -      | -      | -      | -      | -      | -      | 9.15   | -      | C(O)H                   |
| 8.75   | -      | -      | -      | -      | -      | -      | -      | -      | -      | 8.75   | -      | Ph-EWG                  |
| 7.65   | 7.65   | 7.65   | 7.7    | 7.65   | 7.7    | 7.65   | 7.65   | 7.65   | 7.65   | 7.7    | 7.65   | H-Ph (Phthalic)         |
| 7.5    | 7.45   | 7.45   | 7.45   | 7.45   | 7.5    | 7.5    | 7.5    | 7.5    | 7.45   | 7.5    | 7.5    | H-Ph (Phthalic)         |
| 7.25   | 7.25   | 7.25   | 7.25   | 7.25   | 7.25   | 7.25   | 7.25   | 7.25   | 7.25   | 7.25   | 7.25   | Ph-H                    |
| 7.1    | 7.1    | 7.1    | 7.1    | 7.1    | 7.1    | 7.1    | 7.1    | 7.1    | 7.1    | 7.1    | 7.1    | Ph-H                    |
| 6.95   | 6.95   | 6.95   | 7      | 6.95   | 7      | 6.95   | 6.95   | 7      | 6.95   | 6.95   | 7      | Ph-H                    |
| -      | -      | -      | -      | -      | -      | -      | -      | -      | 6.8    | -      | -      | Ph-H                    |
| 5.3    | 5.3    | 5.35   | 5.35   | 5.3    | 5.35   | 5.35   | 5.35   | 5.35   | 5.3    | 5.35   | 5.3    | HC=CH                   |
| 5      | -      | -      | -      | -      | -      | -      | -      | -      | -      | 5      | -      | CH-OH                   |
| 4.35   | 4.35   | 4.35   | -      | 4.35   | 4.4    | 4.4    | 4.4    | 4.35   | 4.35   | 4.35   | 4.35   | CH <sub>2</sub> -OH     |
| 4.1    | 4.15   | 4.15   | -      | -      | 4.15   | 4.1    | 4.1    | 4.15   | 4.15   | 4.15   | 4.1    | CH <sub>2</sub> -OH     |
| -      | -      | -      | -      | -      | 3.6    | -      | -      | 3.65   | -      | -      | 3.65   | CH <sub>2</sub> -OC(O)R |
| -      | 3.55   | 3.55   | -      | -      | 3.55   | -      | 3.55   | 3.55   | 3.55   | 3.55   | 3.55   | CH <sub>2</sub> -OC(O)R |
| -      | -      | -      | -      | -      | -      | -      | -      | -      | -      | 3.5    | -      | CH <sub>2</sub> -OC(O)R |
| 2.75   | 2.75   | 2.75   | 2.75   | 2.75   | 2.75   | 2.75   | 2.75   | 2.75   | 2.75   | 2.75   | 2.75   | CH <sub>2</sub> -R      |
| -      | -      | -      | -      | 2.6    | 2.6    | -      | -      | -      | -      | -      | 2.6    | CH <sub>2</sub> -R      |
| 2.3    | 2.25   | 2.25   | 2.3    | 2.25   | 2.25   | 2.25   | 2.25   | 2.3    | 2.25   | 2.25   | 2.25   | CH <sub>2</sub> -Et     |
| 1.95   | 2      | 2      | 2      | 2      | 2      | 2      | 2      | 2      | 2      | 2      | 2      | CH <sub>2</sub> -Et     |
| 1.55   | 1.55   | 1.55   | 1.55   | 1.55   | 1.55   | 1.55   | 1.55   | 1.6    | 1.55   | 1.55   | 1.6    | CH <sub>2</sub> -Me     |
| 1.25   | 1.25   | 1.25   | 1.25   | 1.25   | 1.25   | 1.25   | 1.25   | 1.25   | 1.25   | 1.25   | 1.25   | CH <sub>2</sub> -Me     |
| -      | -      | -      | -      | -      | 0.95   | -      | -      | -      | -      | -      | -      | CH <sub>3</sub>         |
| 0.9    | 0.9    | 0.9    | 0.9    | 0.9    | 0.9    | 0.9    | 0.9    | 0.9    | 0.9    | 0.9    | 0.9    | CH <sub>3</sub>         |

parity from the DEPT spectra, and shift from the standard  $^{13}\text{C}$  spectra (Table 5.3. The  $^{13}\text{C}$  and DEPT 135 spectra of 826-00 is shown below for reference Figures 5.3 and 5.4 respectively. A comprehensive set of spectra can be seen in the appendix.

As with the  $^1\text{H}$  spectra the spectral assignment of the  $^{13}\text{C}$  spectra is consistent with a system of phthalate esters, fatty acid esters, alcohols and long chain non conjugated

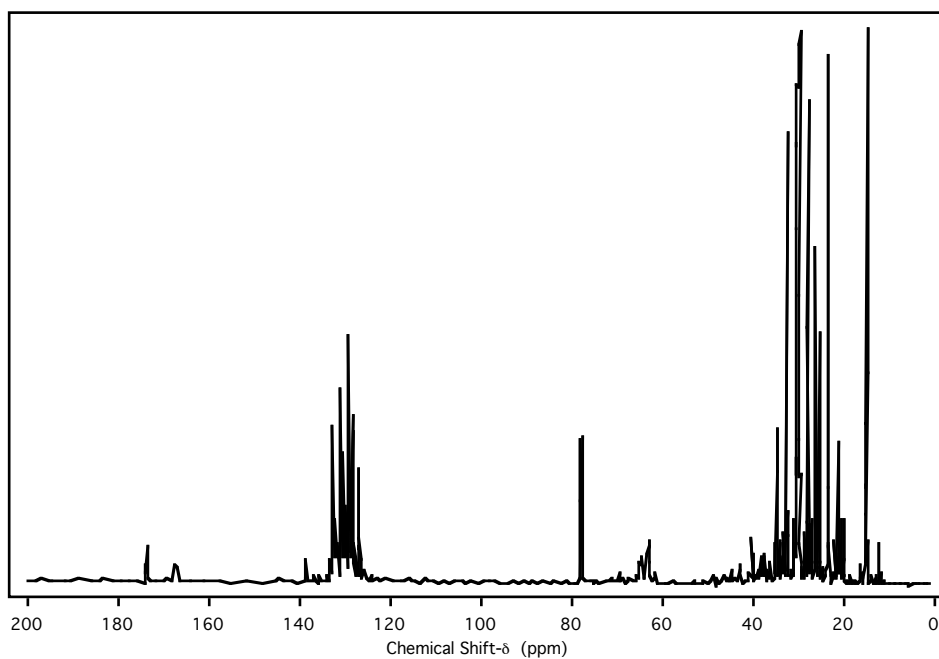


Figure 5.3: Typical  $^{13}\text{C}$  NMR spectrum of the neat resin 826-00.

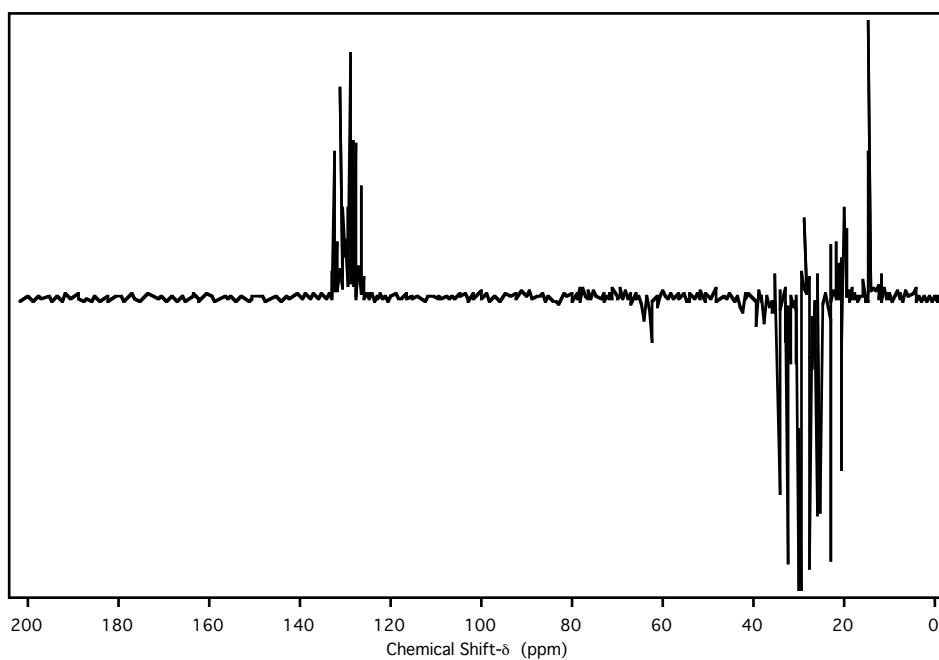


Figure 5.4: Typical  $^{13}\text{C}$  DEPT 135 NMR spectrum of the neat resin 826-00.

fatty acids. Resolution of the secondary hydroxyl carbon of the glyceride is observed in the DEPT spectra as a positive peak due to only the one proton being attached. This is not observed in all spectra and thus suggests that the  $^1J_{\text{CH}}$  value used to determine parity in DEPT experiments has just crept over the threshold value.

Table 5.3: Assignment of  $^{13}\text{C}$  and DEPT 135 NMR spectra of neat resins.

| SBB-00  | S28-00  | S60-00  | CA2-00  | 444-00  | 826-00  | 850-00  | LOA-00  | THX-00   | ML7-00   | 211-00  | 270-00  | Assignment                              |
|---------|---------|---------|---------|---------|---------|---------|---------|----------|----------|---------|---------|-----------------------------------------|
| 173.7   | 173.67  | 173.6   | -       | -       | 173.635 | 173.667 | 173.663 | 173.669  | 173.666  | 173.66  | 173.666 | OC(O)-R                                 |
| 173.1   | 173.109 | 173.05  | -       | -       | 173.1   | 173.134 | 173.107 | 173.093  | -        | -       | -       | OC(O)-R                                 |
| 176.2   | 167.223 | -       | 167.249 | 167.23  | 167.17  | 167.186 | -       | 167.309  | 167.266  | -       | -       | OC(O)-Ph                                |
| -       | 166.955 | -       | 166.952 | -       | -       | 167.013 | 166.998 | -        | 167.003  | 166.999 | -       | OC(O)-Ph                                |
| -       | 137.663 | -       | 137.645 | 137.68  | 137.633 | 137.636 | 137.635 | 137.648  | 137.3632 | 137.63  | -       | C=C-Et                                  |
| -       | -       | -       | -       | -       | -       | -       | -       | -        | 137.094  | 137.108 | -       | C=C-Et                                  |
| -       | -       | -       | 131.87  | -       | 131.857 | -       | -       | -        | -        | -       | -       | Aromatic                                |
| 131.5   | 131.485 | 131.44  | 131.365 | 131.38  | 131.454 | 131.477 | 131.468 | 131.482  | 131.467  | 131.63  | 131.496 | Aromatic                                |
| -       | -       | 130.38  | -       | 130.41  | -       | -       | 130.396 | 130.408  | 130.396  | 130.393 | 130.416 | Aromatic                                |
| -       | 130.157 | 130.19  | -       | 130.16  | -       | -       | -       | -        | 130.213  | -       | -       | Aromatic                                |
| 130.1   | 129.961 | 130.1   | 130.149 | 129.96  | 130.144 | 130.128 | 130.125 | 130.139  | 130.125  | 130.123 | 130.14  | Aromatic                                |
| 129.95  | 129.869 | 129.91  | 129.942 | 129.869 | 129.938 | 129.937 | 129.933 | 129.9414 | 129.931  | 129.931 | 129.943 | Aromatic                                |
| -       | -       | -       | -       | -       | -       | 129.849 | -       | -        | -        | 129.84  | -       | Aromatic                                |
| 129.68  | 129.697 | 129.66  | -       | 129.697 | 129.677 | 129.674 | 129.667 | 129.676  | 129.663  | 129.665 | 129.679 | Aromatic                                |
| 129.546 | 129.561 | -       | -       | 129.481 | -       | 129.538 | 129.533 | 129.473  | 129.455  | 129.456 | 129.48  | Aromatic                                |
| 129.237 | 129.184 | 129.21  | 129.193 | 129.191 | -       | 129.225 | 129.226 | 129.236  | 129.148  | 129.22  | 129.247 | Aromatic                                |
| 129.08  | 128.974 | 129.144 | -       | 128.973 | -       | 129.066 | -       | 128.959  | -        | 129.058 | 128.962 | Aromatic                                |
| 128.95  | 128.89  | 128.93  | 128.874 | -       | 128.872 | 128.948 | 128.943 | 128.873  | 128.943  | 128.943 | 128.875 | Aromatic                                |
| 128.25  | 128.276 | -       | 128.263 | 128.274 | 128.255 | 128.254 | 128.252 | -        | -        | 128.249 | 128.19  | Aromatic                                |
| -       | 128.114 | 128.04  | 128.101 | 128.116 | 128.099 | 128.096 | -       | 128.064  | 128.25   | -       | 128.074 | Aromatic                                |
| 128.04  | -       | -       | 128.021 | -       | 127.961 | 128.042 | 128.041 | -        | 128.041  | 128.044 | -       | Aromatic                                |
| -       | 127.93  | 127.89  | 127.913 | 127.911 | 127.913 | 127.898 | 127.897 | 127.913  | 27.895   | 127.897 | 127.927 | C=C                                     |
| 127.8   | 127.811 | 127.77  | 127.746 | -       | 127.746 | 127.795 | 127.798 | 127.793  | 127.773  | 127.799 | -       | C=C                                     |
| -       | -       | -       | -       | 126.903 | -       | -       | -       | -        | -        | -       | 126.903 | C=C                                     |
| 126     | 126.029 | 125.994 | 126.012 | -       | -       | 125.999 | 125.995 | 126.011  | 125.995  | 125.995 | 126.371 | C=C                                     |
| -       | -       | -       | -       | 126.016 | 126.011 | -       | -       | -        | -        | -       | 126.022 | C=C                                     |
| -       | 125.788 | -       | -       | -       | -       | -       | 125.755 | 125.771  | -        | -       | -       | C=C                                     |
| 77.36   | -77.437 | -77.43  | -77.392 | -77.376 | -77.429 | -77.435 | -77.42  | -77.39   | -77.416  | -77.419 | -77.378 | CH <sub>2</sub> -OR                     |
| 77.04   | -77.12  | -77.121 | -77.071 | -77.056 | -77.109 | -77.119 | -77.104 | -77.07   | -77.101  | -77.102 | -77.06  | CH <sub>2</sub> -OR                     |
| 76.727  | -76.8   | -76.801 | -76.756 | -76.741 | -76.793 | -76.798 | -76.784 | -76.753  | -76.78   | -76.782 | -76.753 | CH <sub>2</sub> -OR                     |
| -       | -       | -       | 66.452  | 66.451  | -       | -       | -       | -        | -        | -       | -       | CH-OR                                   |
| -       | -64.02  | -63.996 | -       | -       | -       | -64.047 | -64.045 | -64.029  | -63.965  | -64.046 | -64.063 | CH <sub>2</sub> -OR                     |
| -63.79  | -       | -       | -       | -       | -63.925 | -       | -       | -        | -        | -       | -       | CH <sub>2</sub> -OR                     |
| -       | -       | -       | -63.588 | -63.583 | -63.657 | -       | -       | -        | -        | -       | -       | CH <sub>2</sub> -OR                     |
| -62.3   | -62.32  | -62.288 | -       | -       | -62.448 | -62.288 | -62.287 | -62.364  | -62.337  | -62.292 | -62.37  | CH <sub>2</sub> -OR                     |
| -62.1   | -62.11  | -62.082 | -       | -62.092 | -62.096 | -62.096 | -62.092 | -62.104  | -62.094  | -62.094 | -62.101 | CH <sub>2</sub> -OR                     |
| -61.97  | -62.01  | -62.008 | -       | -       | -61.989 | -61.993 | -61.988 | -62      | -61.981  | -61.997 | -62.003 | CH <sub>2</sub> -OR                     |
| -       | -60.69  | -60.668 | -       | -       | -       | -       | -       | -        | -60.588  | -       | -       | CH <sub>2</sub> -OR                     |
| -       | -43.92  | -43.882 | -       | -       | -       | -43.875 | -       | -        | -43.888  | -       | -       | C-(CHOR) <sub>4</sub>                   |
| -       | -       | -       | -       | -       | -42.021 | -       | -41.992 | -        | -        | -41.995 | -       | C-(CHOR) <sub>4</sub>                   |
| -39.44  | -39.477 | -39.452 | -39.474 | -39.471 | -39.466 | -39.44  | -39.443 | -39.474  | -39.442  | -39.442 | -39.494 | CH <sub>2</sub> -C(O)R                  |
| -39.079 | -39.113 | -39.387 | -39.114 | -39.112 | -       | -39.079 | -39.082 | -        | -39.08   | -39.081 | -       | CH <sub>2</sub> -C(O)R                  |
| -34.04  | -34.053 | -34.019 | -       | -       | -34.033 | -34.033 | -34.032 | -        | -34.034  | -34.032 | -       | CH <sub>2</sub> -C(O)R                  |
| -31.94  | -31.98  | -31.95  | -31.984 | -31.983 | -31.968 | -31.948 | -31.95  | -31.981  | -31.948  | -31.949 | -32     | CH <sub>2</sub> -Et                     |
| -31.52  | -31.559 | -31.533 | -       | -       | -       | -31.533 | -31.535 | -31.554  | -31.531  | -31.534 | -31.572 | CH <sub>2</sub> -Et                     |
| -       | -29.8   | -29.786 | -29.767 | -29.755 | -29.754 | -       | -       | -29.801  | -29.784  | -       | -29.819 | R-CH <sub>2</sub> -R                    |
| -29.72  | -29.724 | -29.732 | -29.724 | -29.723 | -29.718 | -29.735 | -29.736 | -29.749  | -29.692  | -29.735 | -29.741 | R-CH <sub>2</sub> -R                    |
| -29.64  | -29.58  | -29.632 | -29.627 | -29.584 | -29.625 | -29.634 | -29.637 | -29.585  | -29.628  | -29.637 | -29.607 | R-CH <sub>2</sub> -R                    |
| -       | -       | -       | -29.533 | -29.532 | -29.535 | -       | -29.52  | -        | -        | -29.519 | -29.548 | R-CH <sub>2</sub> -R                    |
| -29.39  | -29.426 | -29.393 | -29.43  | -29.428 | -29.414 | -29.394 | -29.394 | -29.424  | -29.394  | -29.394 | -29.446 | R-CH <sub>2</sub> -R                    |
| -       | -29.223 | -29.19  | -29.226 | -29.227 | -29.205 | -29.186 | -       | -29.221  | -29.191  | -29.185 | -29.24  | R-CH <sub>2</sub> -R                    |
| -29.135 | -       | -29.134 | -29.136 | -29.142 | -29.146 | -29.131 | -29.135 | -        | -29.132  | -29.132 | -       | R-CH <sub>2</sub> -R                    |
| -27.197 | -27.226 | -27.199 | -27.215 | -27.215 | -27.218 | -27.199 | -27.2   | -27.218  | -27.198  | -27.198 | -27.234 | R-CH <sub>2</sub> -C=C                  |
| -25.62  | -25.659 | -25.627 | -25.628 | -25.642 | -25.628 | -25.625 | -25.626 | -25.643  | -25.626  | -25.626 | -25.658 | C=C-CH <sub>2</sub> -C=C                |
| -       | -       | -       | -25.538 | -       | -25.537 | -       | -       | -        | -        | -       | -       | C=C-CH <sub>2</sub> -C=C                |
| -24.835 | -24.86  | -24.827 | -24.852 | -24.854 | -24.844 | -24.834 | -24.833 | -24.843  | -24.842  | -24.836 | -24.861 | CH <sub>2</sub> -CH <sub>2</sub> -C(O)R |
| -22.707 | -22.73  | -22.709 | -22.73  | -22.731 | -22.728 | -22.71  | -22.711 | -22.73   | -22.708  | -22.709 | -22.747 | CH <sub>2</sub> -Me                     |
| -22.649 | -22.61  | -22.621 | -22.633 | -22.645 | -22.61  | -22.646 | -22.644 | -22.641  | -22.64   | -22.59  | -22.633 | CH <sub>2</sub> -Me                     |
| -19.193 | -       | -       | -19.184 | -19.198 | -20.554 | -21.288 | -       | -        | -        | -       | -       | C=C-CH <sub>2</sub> -Me                 |
| 14.388  | -       | -       | 14.384  | -       | 14.269  | -       | -       | 14.396   | -        | -       | 14.399  | CH <sub>3</sub>                         |
| 14.096  | 14.12   | 14.092  | 14.093  | 14.101  | 14.111  | 14.109  | 14.105  | 14.099   | 14.095   | 14.094  | 14.107  | CH <sub>3</sub>                         |

### 5.1.1 2D NMR analysis of 826-00

Due to the relatively long time needed to carry out two dimension NMR experiments homonuclear and heteronuclear correlation were only obtained for 826-00. The two experiments carried out were  $^1\text{H}$ - $^1\text{H}$  COSY and  $^1\text{H}$ - $^{13}\text{C}$  HMQC, these can be seen in Figure 5.5 and Figure 5.6 respectively. Assignment has been made in Table 5.4 and Table 5.5 respectively. A fully expanded set of spectra can be seen in the appendix.

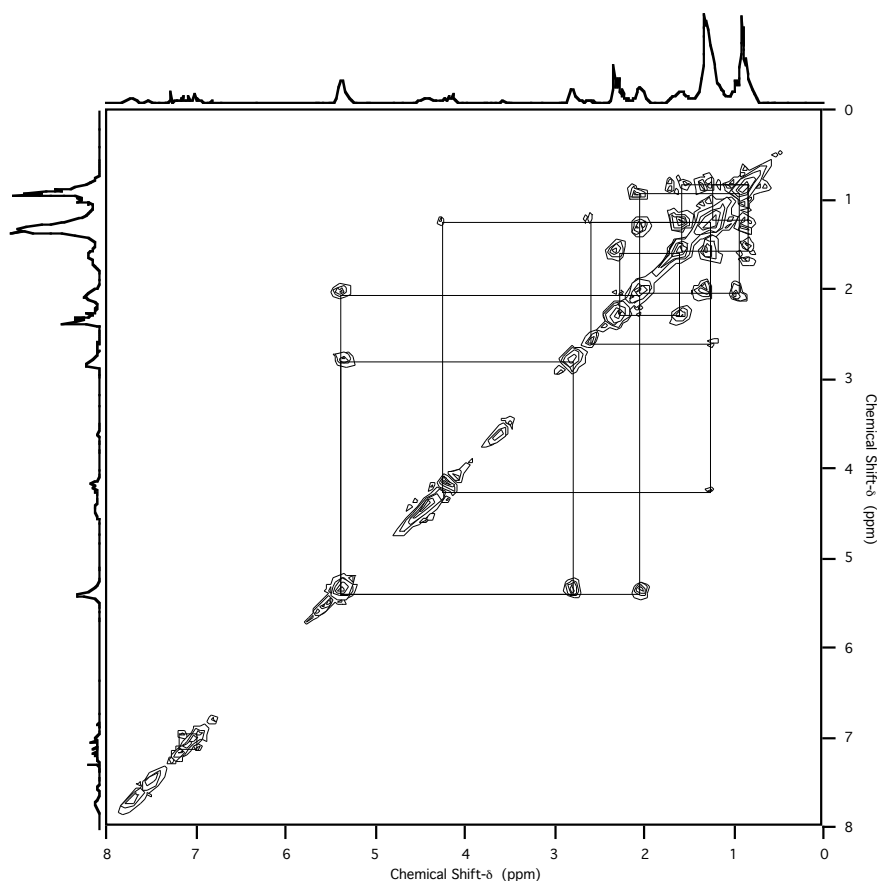


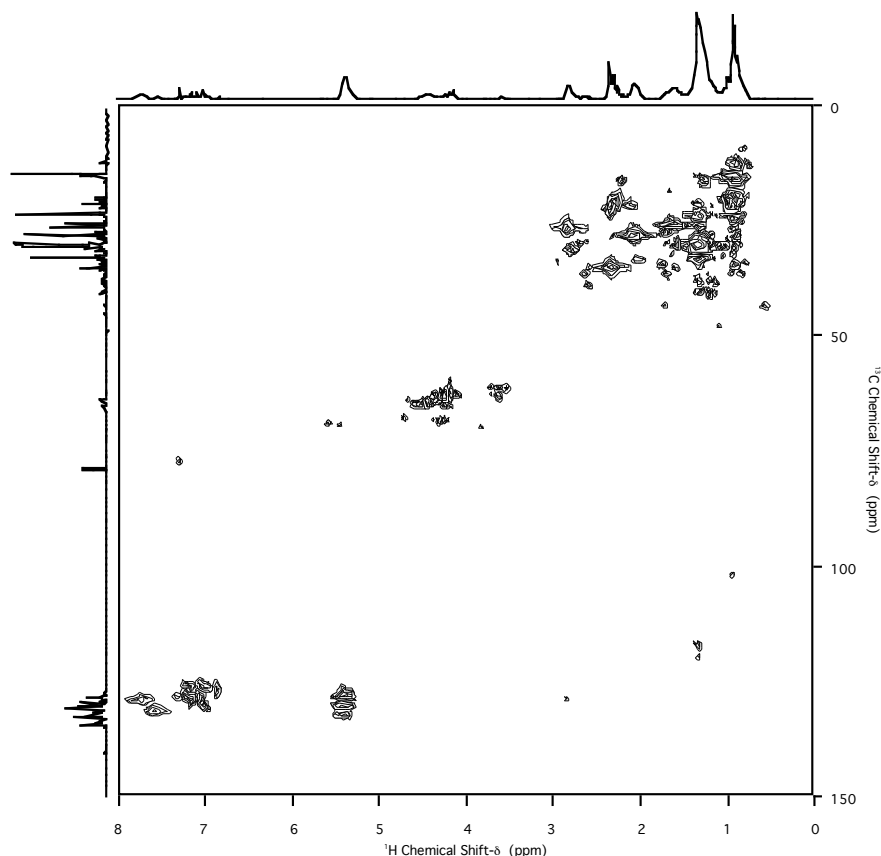
Figure 5.5:  $^1\text{H}$ - $^1\text{H}$  COSY NMR spectra of 826-00.

Although complicated by residual protonated solvent the COSY spectrum shows the unsaturated fatty acid side chains of the oil, A-C-E-M-H, and the adjacent nature of the aromatic protons on phthalic anhydride, O-N. Analysis is further complicated by the distribution of different fatty acids present in vegetable oils.

Conformation that the protons of a particular functional group are associated with the carbons of the same group are shown here. Again complication by residual protonated solvent is seen.

Table 5.4: Assignment of  $^1\text{H}$ - $^1\text{H}$  COSY NMR spectra of 826-00 (Figure 5.5).

| Shift | ID | X Peaks | Assignment                     | Implications                           |
|-------|----|---------|--------------------------------|----------------------------------------|
| 0.90  | A  | C(D)    | Methyl F-ACID                  | Adjacent to methylene C (D)            |
| 0.95  | B  | E       | Methyl F-ACID                  | Adjacent to methylene E                |
| 1.25  | C  | ADE(K)  | Methalene F-ACID               | Adjacent to methyl A and methalene D/E |
| 1.55  | D  | CF(A)   | Methalene F-ACID               | Adjacent to methalene C and F          |
| 2.00  | E  | CAM     | Methalene F-ACID               | Adjacent to methyl A and methalene M   |
| 2.25  | F  | D       | Methalene F-ACID               | Adjacent to methylene D                |
| 2.60  | G  | (C)     | Methalene F-ACID               | Adjacent to methylene (C)              |
| 2.75  | H  | M       | Methalene F-ACID               | Adjacent to methylene M                |
| 3.55  | I  | -       | $\text{CH}_2\text{-OC(O)R}$    | No correlation or residual reagent     |
| 3.60  | J  | -       | $\text{CH}_2\text{-OC(O)R}$    | No correlation or residual reagent     |
| 4.15  | K  | (C)     | $\text{CH}_2\text{-OH PENT-E}$ | Adjacent to methylene (C)              |
| 4.40  | L  | -       | $\text{CH}_2\text{-OH PENT-E}$ | No correlation or residual reagent     |
| 5.35  | M  | EH      | Non-conjugated C=C             | Adjacent to Methalene E and H          |
| 7.00  | N  | O       | Aromatic                       | Adjacent to aromatic O                 |
| 7.10  | O  | N       | Aromatic                       | Adjacent to aromatic N                 |
| 7.25  | P  | -       | Aromatic                       | No correlation or residual solvent     |
| 7.50  | Q  | -       | Aromatic-Phthalic              | No correlation or residual reagent     |
| 7.70  | R  | -       | Aromatic-Phthalic              | No correlation or residual reagent     |

Figure 5.6:  $^1\text{H}$ - $^{13}\text{C}$  HMQC NMR spectra of 826-00.

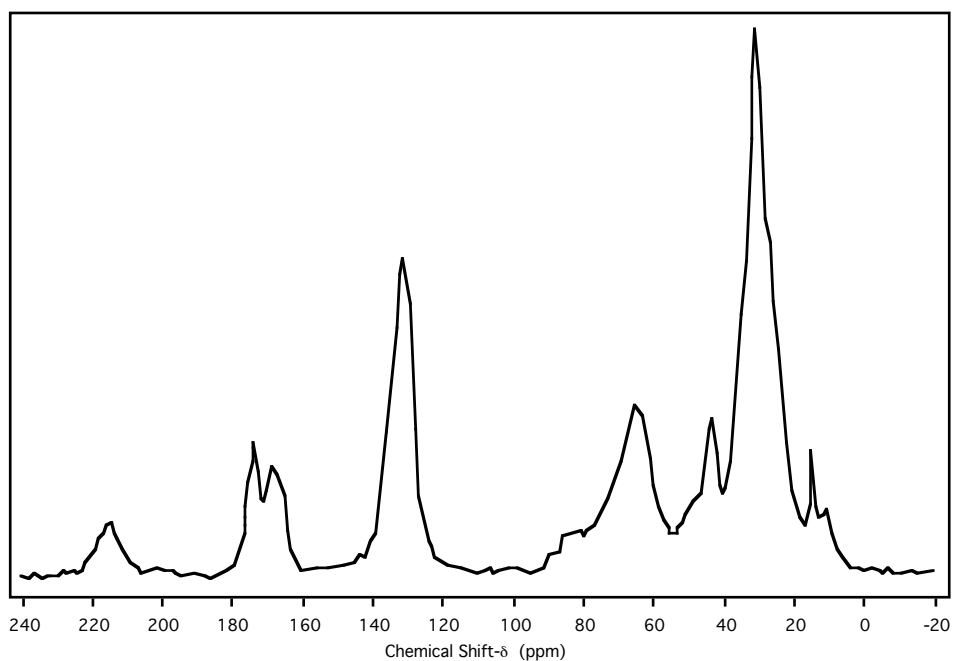
## 5.2 Solid state spectral analysis of cured resin

As with the neat spectra high similarity in cured resin spectra was observed, group assignment of spectra can be seen in Table 5.6. The solid state CPMAS spectrum of

**Table 5.5:** Assignment of  $^1\text{H}$ - $^{13}\text{C}$  HMQC NMR spectra of 826-00 (Figure 5.6).

| $^1\text{H}$ | Assignment                  | $\Leftrightarrow$ | Assignment                   | $^{13}\text{C}$ |
|--------------|-----------------------------|-------------------|------------------------------|-----------------|
| 0.9          | $\text{CH}_3$               | $\Leftrightarrow$ | $\text{CH}_3$                | 14              |
| 0.9          | $\text{CH}_3$               | $\Leftrightarrow$ | $\text{CH}_2\text{-Me}$      | 23              |
| 1.3          | $\text{CH}_2\text{-Me}$     | $\Leftrightarrow$ | $\text{CH}_2\text{-Me}$      | 23              |
| 1.3          | $\text{CH}_2\text{-Me}$     | $\Leftrightarrow$ | $\text{R-CH}_2\text{-R}$     | 29              |
| 1.6          | $\text{CH}_2\text{-Me}$     | $\Leftrightarrow$ | $\text{C=C-CH}_2\text{-C=C}$ | 25              |
| 2.2          | $\text{CH}_2\text{-Et}$     | $\Leftrightarrow$ | $\text{R-CH}_2\text{-C=C}$   | 27              |
| 2.3          | $\text{CH}_2\text{-Et}$     | $\Leftrightarrow$ | $\text{CH}_2\text{-Me}$      | 22              |
| 2.3          | $\text{CH}_2\text{-Et}$     | $\Leftrightarrow$ | $\text{CH}_2\text{-Et}$      | 33              |
| 2.8          | $\text{-CH}_2\text{-R}$     | $\Leftrightarrow$ | $\text{CH}_2\text{-Et}$      | 31              |
| 2.9          | $\text{-CH}_2\text{-R}$     | $\Leftrightarrow$ | $\text{C=C-CH}_2\text{-C=C}$ | 25              |
| 3.5          | $\text{CH}_2\text{-OC(O)R}$ | $\Leftrightarrow$ | $\text{CH}_2\text{-OR}$      | 61              |
| 3.6          | $\text{CH}_2\text{-OC(O)R}$ | $\Leftrightarrow$ | $\text{CH}_2\text{-OR}$      | 61              |
| 3.6          | $\text{CH}_2\text{-OC(O)R}$ | $\Leftrightarrow$ | $\text{CH}_2\text{-OR}$      | 62              |
| 4.1          | $\text{CH}_2\text{-OH}$     | $\Leftrightarrow$ | $\text{CH}_2\text{-OR}$      | 62              |
| 4.2          | $\text{CH}_2\text{-OH}$     | $\Leftrightarrow$ | $\text{CH}_2\text{-OR}$      | 62              |
| 4.3          | $\text{CH}_2\text{-OH}$     | $\Leftrightarrow$ | $\text{CH}_2\text{-OR}$      | 62              |
| 4.4          | $\text{CH}_2\text{-OH}$     | $\Leftrightarrow$ | $\text{CH}_2\text{-OR}$      | 64              |
| 4.5          | $\text{CH}_2\text{-OH}$     | $\Leftrightarrow$ | $\text{CH}_2\text{-OR}$      | 64              |
| 5.2          | $\text{HC=CH}$              | $\Leftrightarrow$ | Aromatic                     | 128             |
| 7.2          | Ph-H                        | $\Leftrightarrow$ | Aromatic                     | 127             |
| 7.7          | H-Ph-(Phthalic)             | $\Leftrightarrow$ | Aromatic                     | 131             |
| 7.9          | H-Ph-(Phthalic)             | $\Leftrightarrow$ | Aromatic                     | 129             |

cured 826-00 is shown in Figure 5.6. A comprehensive set of spectra can be seen in the appendix.

**Figure 5.7:** Typical CPMAS NMR spectra of the cured resin 826-00.

Spinning side bands are seen for spectra taken with the 7 mm rotors spun at 4 kHz  $\approx$  80 ppm, these are manifestations of the partial removal of the CSA of the aromatic peak at 130 ppm. Confirmation of two types of ester carbonyls, glyceride carbons and a quaternary centre very similar to that of pentaerythritol is seen. Methylene

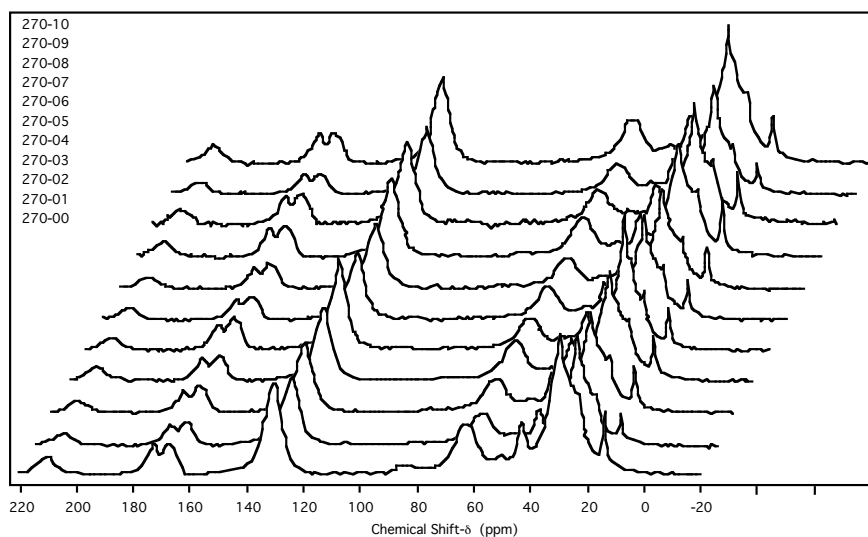
**Table 5.6:** Assignment of CPMAS NMR spectra of cured resins.

| SBB-00 | S28-00 | S60-00 | CA2-00 | 444-00 | 826-00 | 850-00 | LOA-00 | THX-00 | ML7-00 | 211-00 | 270-00 | Assignment            |
|--------|--------|--------|--------|--------|--------|--------|--------|--------|--------|--------|--------|-----------------------|
| -      | -      | 210.9  | -      | -      | 215.3  | -      | 209.7  | -      | 210.2  | 209.5  | 210.4  | SSB                   |
| 174.2  | 174.2  | 173    | 174.1  | 174.4  | 173.6  | 173.9  | 173.2  | 174.2  | 173.2  | 173.4  | 173    | OC(O)-R               |
| 168.3  | 168.3  | 167.5  | 168.1  | 167.9  | 168.8  | 167.9  | 167.1  | 168.8  | 167.8  | 167    | 167.7  | OC(O)-Ph              |
| 131.1  | 131.2  | 130.5  | 131.2  | 131.8  | 131    | 131    | 130.3  | 131.3  | 130.4  | 130.2  | 130.1  | Aromatic              |
| 87.2   | 86.1   | 82.6   | 85.2   | 85.6   | 83     | 83.2   | 83.1   | 85     | 81.7   | 82.5   | 85     | SSB                   |
| 65.1   | 65.6   | 64.1   | 67.9   | 66.6   | 64.7   | 64.9   | 64.1   | 65.6   | 63.2   | 63.5   | 63.8   | CH <sub>2</sub> -OR   |
| -      | -      | 50.5   | -      | -      | -      | -      | 51.4   | -      | 50.1   | -      | 50.6   | SSB                   |
| 43.7   | 43.8   | 42.4   | -      | -      | 43.2   | 43.4   | 42.3   | 43.9   | 42.5   | 42.3   | 43.1   | C-(CHOR) <sub>4</sub> |
| 30.8   | 30.8   | 29.5   | 30.7   | 31     | 30.4   | 30.6   | 29.6   | 30.9   | 29.5   | 29.6   | 29.5   | CH <sub>2</sub> -R    |
| 28.1   | 27.2   | -      | 28     | 28.5   | -      | 28     | 26.1   | 28.3   | -      | -      | -      | CH <sub>2</sub> -Et   |
| 24     | 24.3   | 24     | 26.9   | 24     | -      | 24     | 22.3   | 24.2   | 22.1   | 23.4   | 22.1   | CH <sub>2</sub> -Me   |
| 15.4   | 15.4   | 14.1   | 15.4   | 15.4   | 15     | 15.1   | 14.1   | 15.5   | 14.1   | 14.1   | 14.1   | CH <sub>3</sub>       |
| -      | -      | -      | -      | -      | 11     | -      | -      | -      | -      | -      | -      | CH <sub>3</sub>       |

carbons show shoulders possibly due to proximity to chain terminus. Sharp methyl resonance are also seen.

### 5.3 Solid state spectral analysis of aged resin

The three resins chosen to be exposed to controlled amounts of light at the National Gallery were 270-00, 444-00 and 826-00. Each sample taken on a fortnightly basis was analysed by CPMAS solid state NMR, creating an eleven sample set of XXX-00 to XXX-10. All the data accumulated can be seen in the stacked plots in Figures 5.8–5.10 respectively.

**Figure 5.8:** CPMAS spectra of 270-00 to 270-10.

It can be seen from the stacked plots that little change in the CPMAS spectra has occurred on aging. Only slight differences in intensity and can be seen. In order to quantify these small changes comparison between XXX-00, XXX-10 and XXX-UV has been employed.

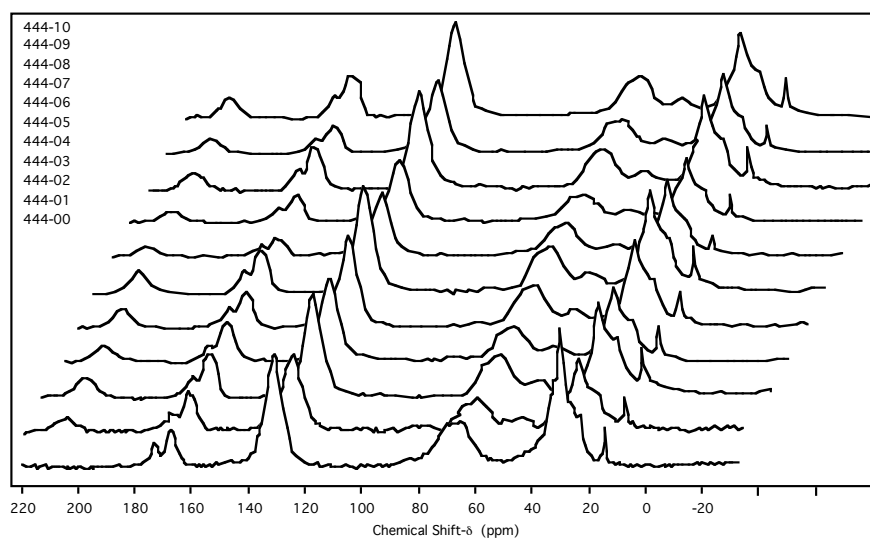


Figure 5.9: CPMAS spectra of 444-00 to 444-10.

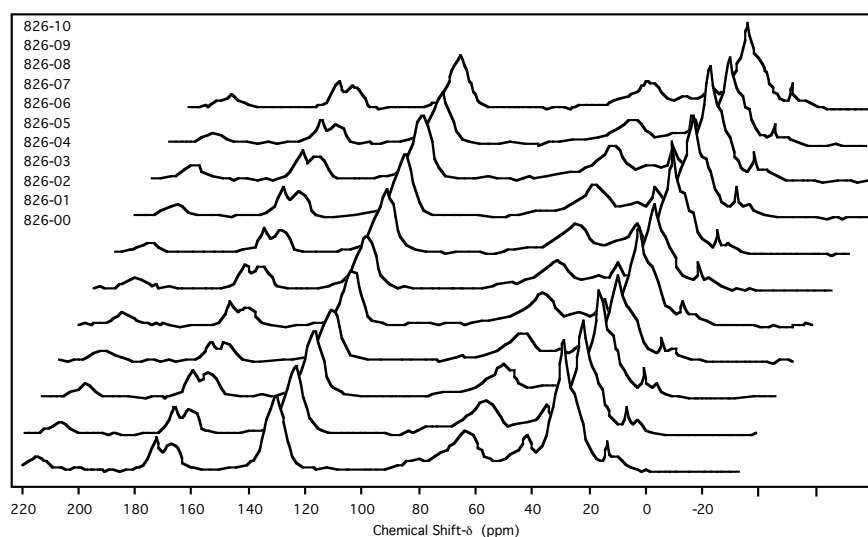


Figure 5.10: CPMAS spectra of 826-00 to 826-10.

## 5.4 Solid state spectral analysis of UV irradiated resin

Comparison between the unaged, aged and the UV aged resins can be seen in the following section. Stacked plots for 270-XX, 444-XX and 826-XX can be seen in Figures 5.11–5.13. Spectra have been normalised to the largest peak at 30 ppm. Assignment and changes occurring can be seen in Tables 5.7–5.9 respectively.

Through direct comparison it can be seen that reaction still takes place during aging suggesting a continuation of the curing process. The main similarity between the three systems is the marked reduction in intensity at 88 ppm this seems to entirely disappear between the unaged sample and the first aged sample XXX-01. Further

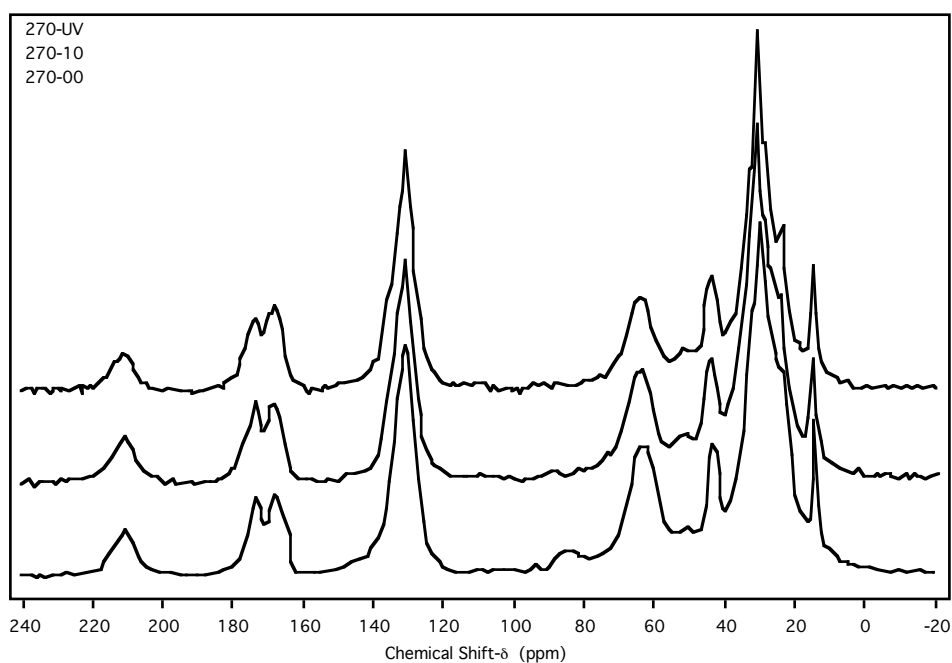


Figure 5.11: CPMAS spectra of 270-00, 270-10 and 270-UV.

Table 5.7: Assignment and change of 270-XX CPMAS spectra.

| 270-XX | Assignment            | Change                                                   |
|--------|-----------------------|----------------------------------------------------------|
| 210.4  | SSB                   | No change                                                |
| 173.0  | OC(O)-R               | Slight decrease in intensity                             |
| 167.7  | OC(O)-Ph              | Slight increase in intensity                             |
| 130.1  | Aromatic              | No change                                                |
| 85.0   | SSB                   | Decrease in intensity                                    |
| 63.8   | CH <sub>2</sub> -OR   | Decrease in intensity                                    |
| 50.6   | SSB                   | No change                                                |
| 43.1   | C-(CHOR) <sub>4</sub> | Decrease in intensity                                    |
| 29.5   | CH <sub>2</sub> -R    | No change                                                |
| 22.1   | CH <sub>2</sub> -Et   | Shoulder becomes more prominent                          |
| 14.1   | CH <sub>2</sub> -Me   | Slight decrease in intensity and slight shift down field |

Table 5.8: Assignment and change of 444-XX CPMAS spectra.

| 444-XX | Assignment          | Change                                          |
|--------|---------------------|-------------------------------------------------|
| -      | SSB                 | No change                                       |
| 174.4  | OC(O)-R             | No change                                       |
| 167.9  | OC(O)-Ph            | Slight increase in intensity                    |
| 131.8  | Aromatic            | No change                                       |
| 85.6   | SSB                 | No change                                       |
| 66.6   | CH <sub>2</sub> -OR | Increase in intensity                           |
| -      | SSB                 | No change                                       |
| 31.0   | CH <sub>2</sub> -R  | No change                                       |
| 28.5   | CH <sub>2</sub> -Et | No change                                       |
| 24.0   | CH <sub>2</sub> -Me | Shoulder becomes more prominent                 |
| 15.4   | CH <sub>3</sub>     | Increase in intensity and slight shift up field |

information on assignment of the peak at 88 ppm can be seen in the discussion.

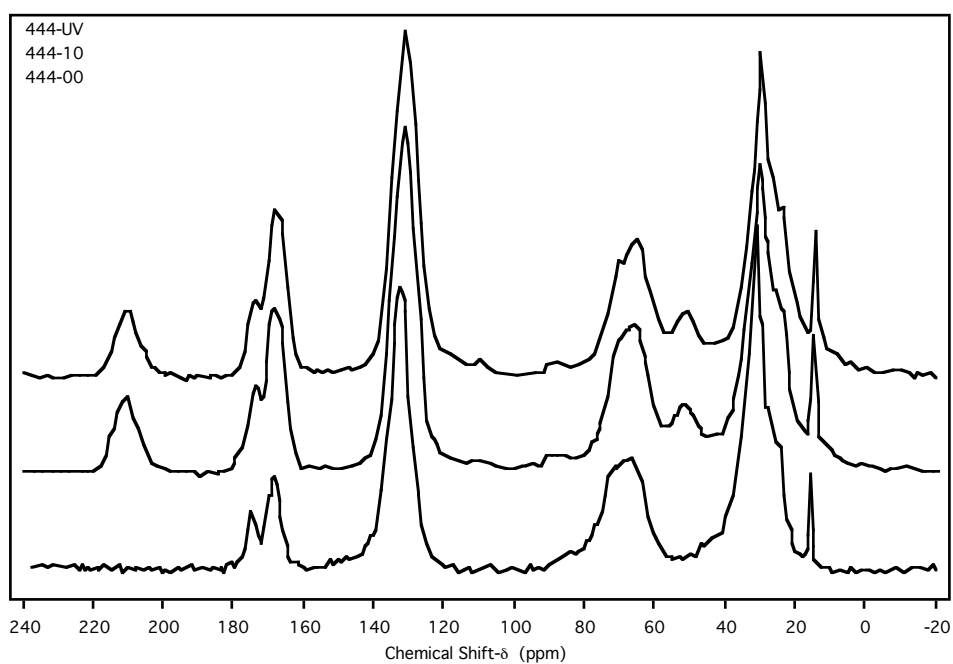


Figure 5.12: CPMAS spectra of 444-00, 444-10 and 444-UV.

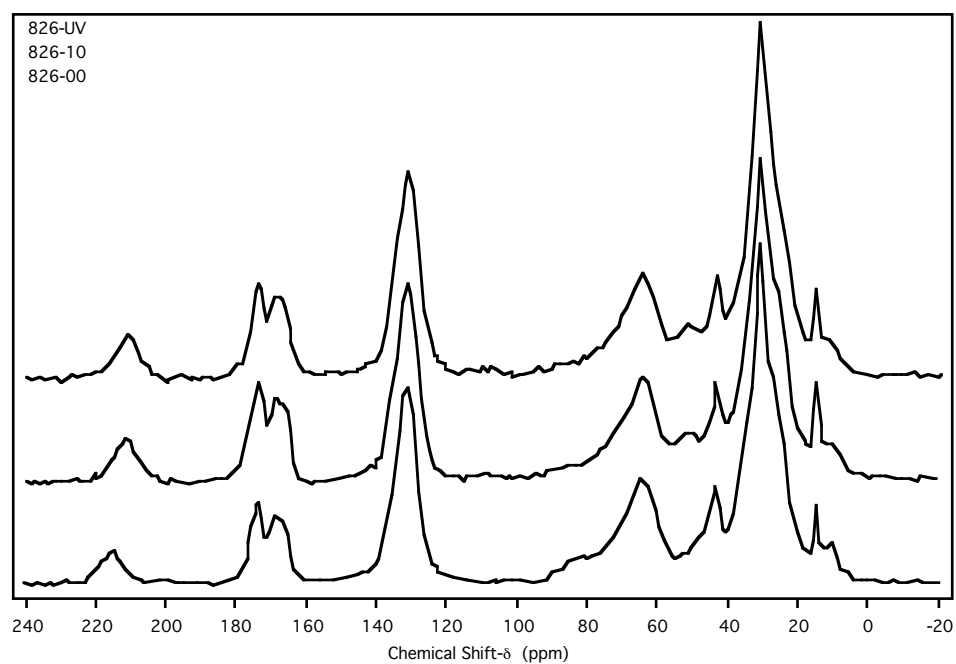


Figure 5.13: CPMAS spectra of 826-00, 826-10 and 826-UV.

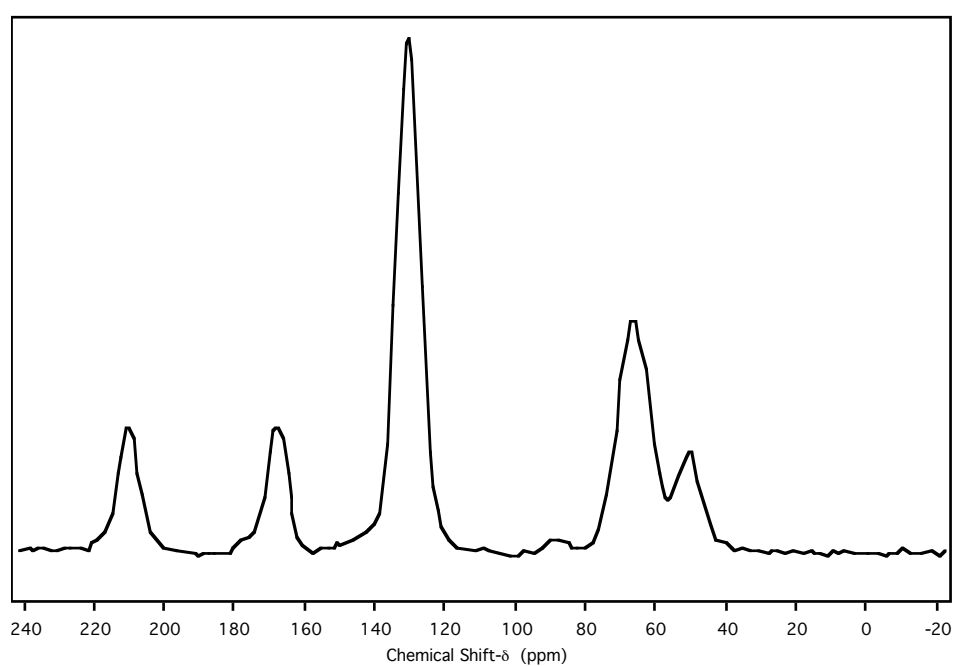
## 5.5 Solid state spectral analysis of glyptalic resin

The crosslinked glyptalic resins TG-21D and TP-21D were characterised using solid state CPMAS NMR, the spectra can be seen in Figure 5.14 and Figure 5.15 respec-

**Table 5.9:** Assignment and change of 826-XX CPMAS spectra.

| 826-XX | Assignment            | Change                          |
|--------|-----------------------|---------------------------------|
| 215.3  | SSB                   | No change                       |
| 173.6  | OC(O)-R               | Slight increase in intensity    |
| 168.8  | OC(O)-Ph              | Slight increase in intensity    |
| 131.0  | Aromatic              | No change                       |
| 83.0   | SSB                   | Decrease in intensity           |
| 64.7   | CH <sub>2</sub> -OR   | No change                       |
| 51.0   | SSB                   | No change                       |
| 43.2   | C-(CHOR) <sub>4</sub> | No change                       |
| 30.4   | CH <sub>2</sub> -R    | Shoulder becomes more prominent |
| 15.0   | Me                    | Slight increase in intensity    |
| 11.0   | Me                    | Decrease in intensity           |

tively. Both spectra have been assigned in Table 5.10.

**Figure 5.14:** CPMAS spectra of TG-21D.**Table 5.10:** Assignment of CPMAS spectra of neat glyptalic resins.

| TG-21D | TP-21D | Assignment            |
|--------|--------|-----------------------|
| 210.3  | 209.6  | SSB                   |
| 167.6  | 168.1  | OC(O)-Ph              |
| 130.2  | 130.1  | Aromatic              |
| 89.7   | 88.6   | SSB                   |
| 65.9   | 64.3   | CH <sub>2</sub> -OR   |
| 50.4   | 50.9   | SSB                   |
| -      | 43.9   | C-(CHOR) <sub>4</sub> |

Both resins show similar characteristics with the peak at 88 ppm present in both. The quaternary carbon of pentaerythritol can be seen in TP-21D.

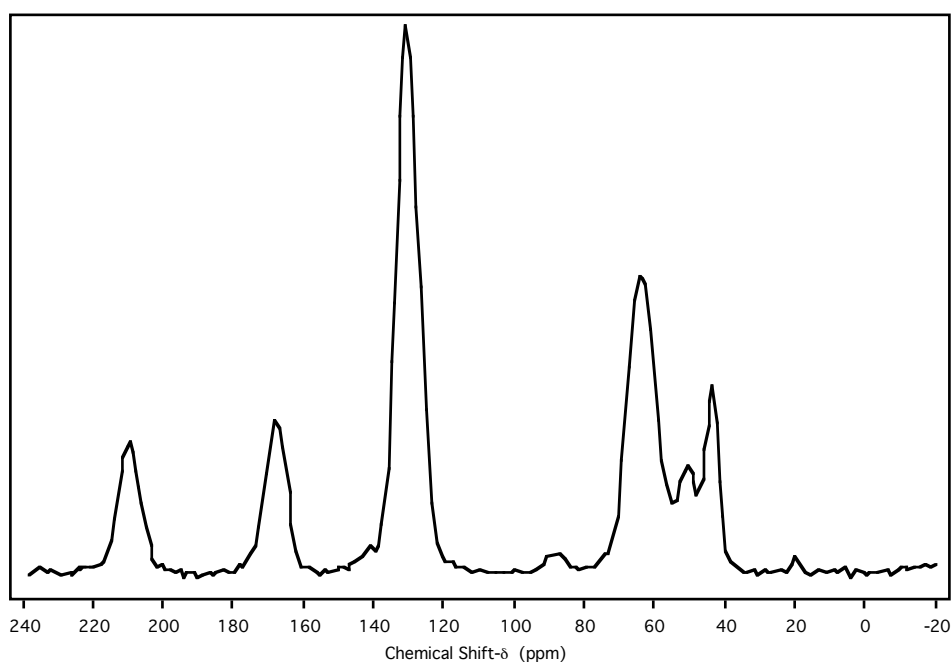


Figure 5.15: CPMAS spectra of TP-21D.

## 5.6 Spectral analysis of control resin

The neat IR spectra of ALK-00 is shown in Figure 5.16. As this synthetic resin was based on linseed oil comparison to the neat IR spectra of 826-00 has also been assigned in Table 5.11.

Table 5.11: Assignment of IR spectra of neat ALK-00.

| ALK-00 | 826-00 | Assignment  |
|--------|--------|-------------|
| 3466.0 | 3538.4 | O-H stretch |
| 3012.8 | 3009.8 | C-H stretch |
| 2926.1 | 2923.5 | C-H stretch |
| 2853.9 | 2853.7 | C-H stretch |
| 1737.8 | 1738.2 | C=O stretch |
| 1598.2 | 1599.6 | Aromatic    |
| 1581.2 | 1580.0 | Aromatic    |
| 1456.3 | 1463.8 | C-O stretch |
| 1371.0 | 1378.1 | C-O stretch |
| 1268.6 | 1272.8 | C-O stretch |
| 1122.7 | 1122.2 | C-O stretch |
| 1070.3 | 1072.3 | C-H stretch |
| 1041.6 | 1040.6 | C-H stretch |
| 967.2  | 968.4  | C-H stretch |
| 741.3  | 741.5  | Aromatic    |
| 705.6  | 705.6  | Aromatic    |

Good correlation between spectra is seen even in the longer wavelength fingerprint region implying a close match of the resin was synthesised. The solution state proton NMR spectra of neat ALK-00 is shown in Figure 5.17. Again comparison to the neat proton spectra of 826-00 has also been assigned in Table 5.12.

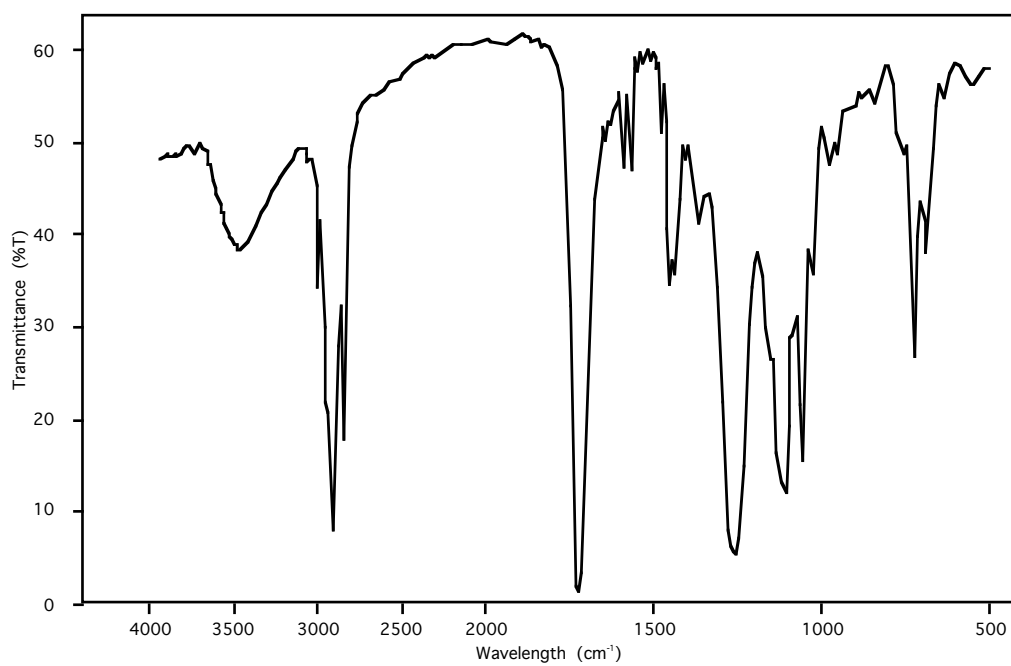


Figure 5.16: IR spectra of neat ALK-00.

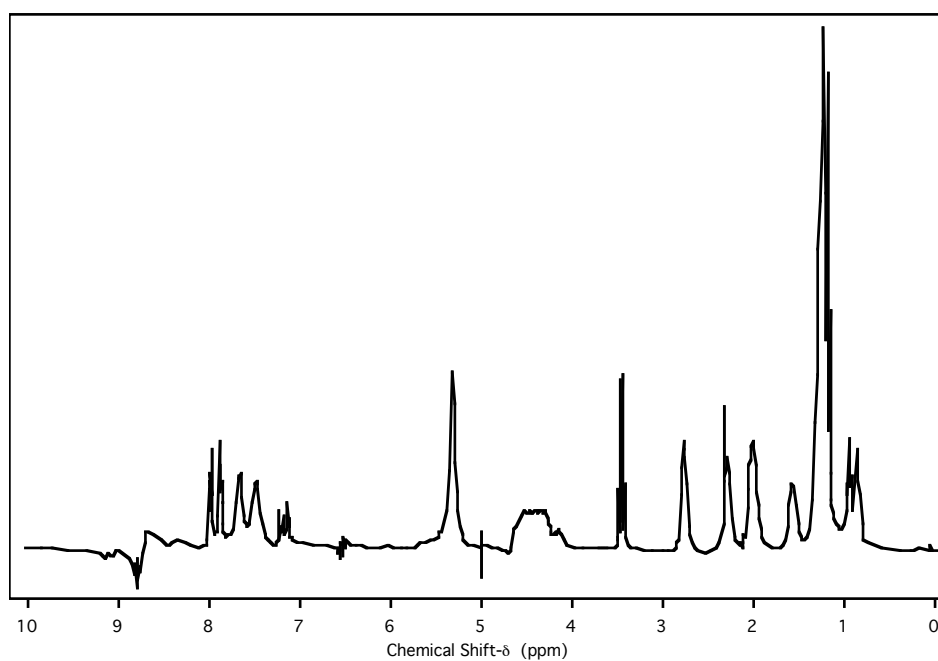


Figure 5.17: <sup>1</sup>H NMR spectra of neat ALK-00.

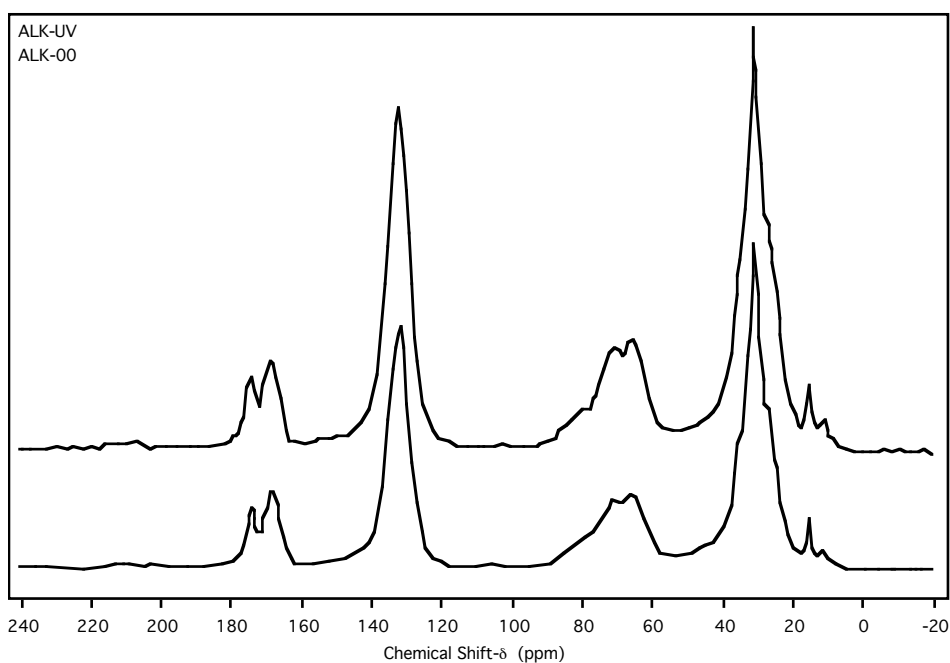
Again a good overall correlation is seen between 826-00 and ALK-00. The presence of aldehydes in the synthetic resin is a possible byproduct of the reaction, as these have also been seen in the other <sup>1</sup>H spectra of neat resin, SBB-00 and 211-00.

**Table 5.12:** Assignment of  $^1\text{H}$  NMR spectra of neat ALK-00.

| ALK-00 | 826-00 | Assignment              |
|--------|--------|-------------------------|
| 8.80   | -      | C(O)H                   |
| 8.00   | -      | C(O)H                   |
| 7.70   | 7.70   | H-Ph-(Phthalic)         |
| 7.50   | 7.50   | H-Ph-(Phthalic)         |
| 7.25   | 7.25   | Ph-H                    |
| 7.10   | 7.10   | Ph-H                    |
| -      | 7.00   | Ph-H                    |
| 6.50   | -      | Ph-H                    |
| 5.35   | 5.35   | HC=CH                   |
| 5.00   | -      | SFO1 Pulse              |
| 4.40   | 4.40   | CH <sub>2</sub> -OH     |
| 4.15   | 4.15   | CH <sub>2</sub> -OH     |
| -      | 3.60   | CH <sub>2</sub> -OC(O)R |
| 3.55   | 3.55   | CH <sub>2</sub> -OC(O)R |
| 2.75   | 2.75   | CH <sub>2</sub> -R      |
| -      | 2.60   | CH <sub>2</sub> -R      |
| 2.25   | 2.25   | CH <sub>2</sub> -Et     |
| 2.00   | 2.00   | CH <sub>2</sub> -Et     |
| 1.55   | 1.55   | CH <sub>2</sub> -Me     |
| 1.25   | 1.25   | CH <sub>2</sub> -Me     |
| 0.95   | 0.95   | CH <sub>3</sub>         |
| 0.90   | 0.90   | CH <sub>3</sub>         |

## 5.7 Solid state spectral analysis of control resin.

The CPMAS spectra of cured ALK-00 and UV irradiated ALK-UV can be seen in Figure 5.18. Assignment and change with irradiation can be seen in Table 5.13, along with comparison to the CPMAS of 826-00.

**Figure 5.18:** CPMAS spectra of ALK-00 and ALK-UV.

A correlation can be seen between the spectra. The presence of a peak at 70 ppm is

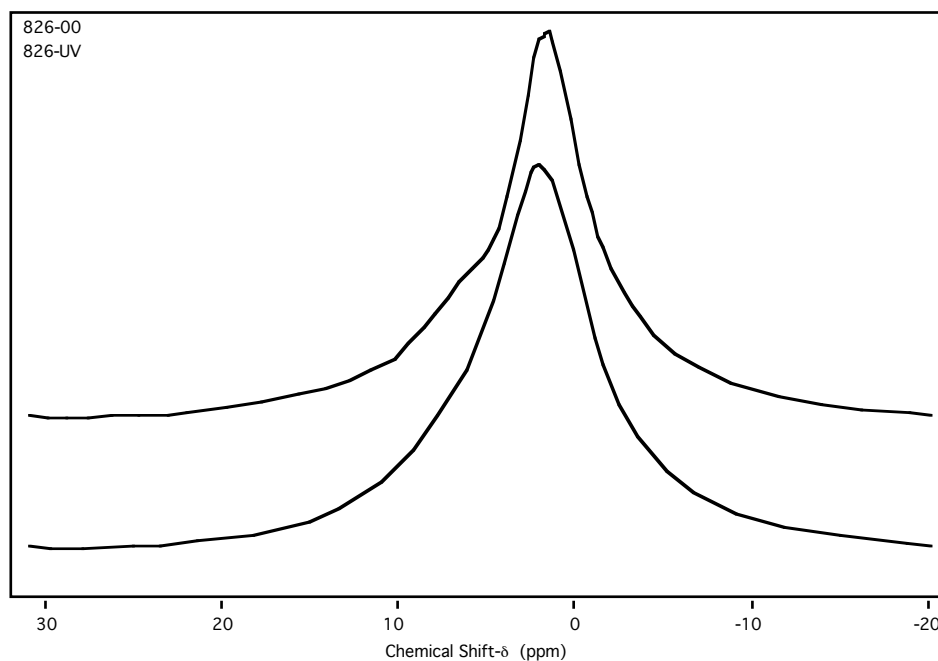
**Table 5.13:** Assignment of CPMAS spectra of ALK-00 and ALK-UV.

| ALK-00 | ALK-UV | 826-00 | Assignment            | Comment                         |
|--------|--------|--------|-----------------------|---------------------------------|
| -      | -      | 215.3  | SSB                   | Not present                     |
| 173.8  | 173.9  | 173.6  | OC(O)-R               | Slight decrease in intensity    |
| 168.2  | 168.6  | 168.8  | OC(O)-Ph              | Slight decrease in intensity    |
| 131.2  | 131.4  | 131.0  | Aromatic              | Slight increase in intensity    |
| 83.2   | 83.2   | 83.0   | SSB                   | No change                       |
| 70.8   | 70.7   | -      | CH <sub>2</sub> -OR   | Slight increase in intensity    |
| 65.2   | 65.2   | 64.7   | CH <sub>2</sub> -OR   | Slight increase in intensity    |
| -      | -      | 51.0   | SSB                   | Not present                     |
| -      | -      | 43.2   | C-(CHOR) <sub>4</sub> | Not present                     |
| 30.5   | 30.5   | 30.4   | CH <sub>2</sub> -R    | Shoulder becomes more prominent |
| 15.1   | 15.1   | 15.0   | CH <sub>3</sub>       | No change                       |
| 10.9   | 10.9   | 11.0   | CH <sub>3</sub>       | Slight increase in intensity    |

interesting possibly due to a different CH<sub>2</sub>-OR environment. The quaternary carbon, typified by pentaerythritol, is not seen either as pentaerythritol was not used or cross linking to form now quaternary centres has not taken place.

## 5.8 Solid state proton spectral analysis

Although high resolution spectra cannot be obtained a valuable insight into the degree of motion within the solid can be gained with <sup>1</sup>H single pulse excitement. Samples of 826-00 and 826-UV were analysed both static and with MAS at 10 kHz, comparison spectra can be seen for SPE static and SPEMAS in Figure 5.19 and Figure 5.20 respectively.

**Figure 5.19:** <sup>1</sup>H SPE Static spectra of 826-00 and 826-UV.

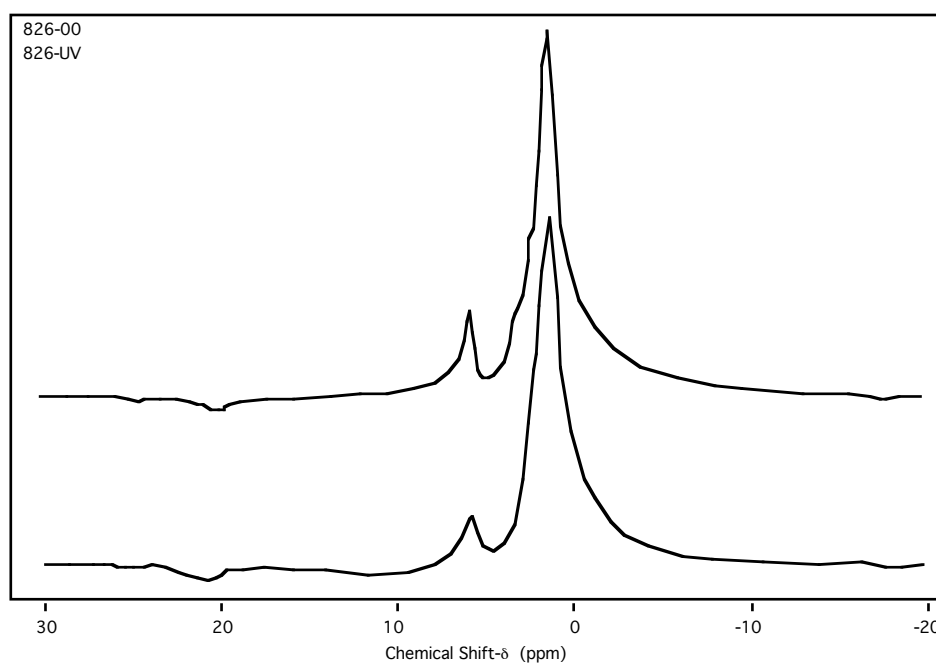


Figure 5.20:  $^1\text{H}$  SPE MAS spectra of 826-00 and 826-UV.

The static SPE experiment show broad peaks of approximately 3 kHz. The SPEMAS spectra show unusually high resolution implying a high degree of molecular motion within the resin. Two clear peaks can be seen at 6.1 and 1.6 ppm due to aromatic and methylene protons respectively.

The spin-lattice relaxation time constants ( $T_1$ ) of 826-00, 826-UV and ALK-UV were also measured using the inverse recovery technique. These can be seen in Table 5.14.

Table 5.14: Spin-lattice relaxation times of 826-00, 826-UV and ALK-00.

| XXX-XX | $T_1$ [s] |
|--------|-----------|
| 826-00 | 0.495     |
| 826-UV | 0.534     |
| ALK-00 | 0.349     |

These are of the magnitude expected for such a cross linked system.

## 5.9 Calorimetric analysis of resin

Differential scanning calorimetry was used to analysis various resins. The DSC traces for, 826-00, 826-10 and 826-UV are shown in Figure 5.21. All scans were repeated but due to decomposition showed little or no information and so are not shown.

Similar traces can be seen for the resins of different degrees of artificial aging. Slight baseline shift indicative of a glass transition could possibly be interpreted from the 10–50°C region but a lower start temperature and slower temperature ramp were

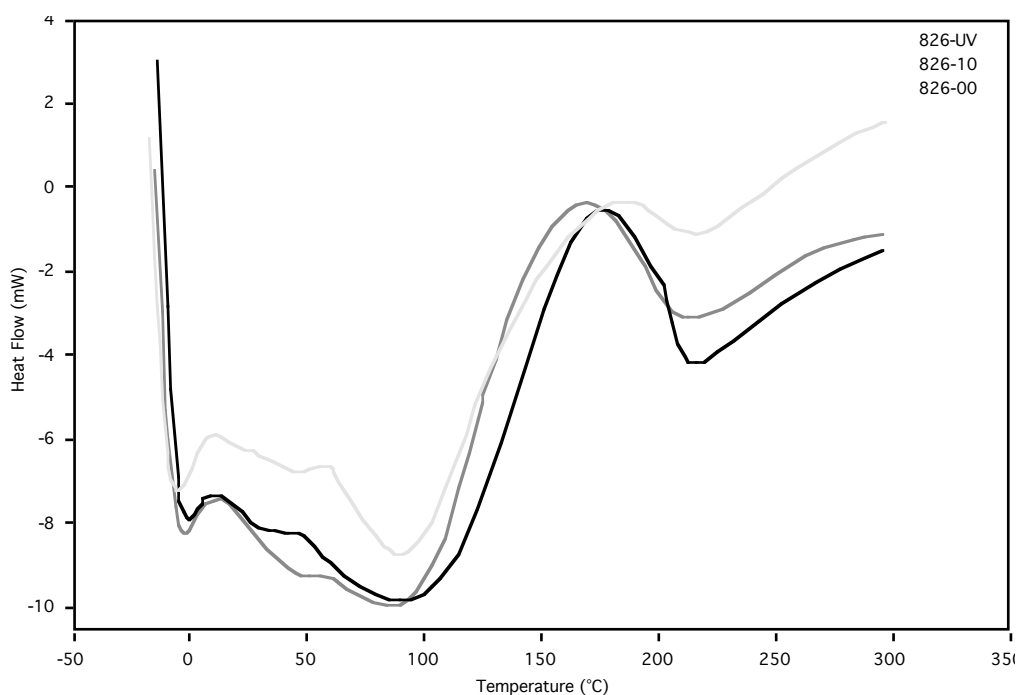


Figure 5.21: DSC trace of 826-00, 826-10 and 826-UV.

needed. Decomposition is seen to take place at approximately the same place.

The control alkyd, ALK-00, and the UV aged version, ALK-UV, were also examined, their DSC traces can be seen in Figure 5.22.

Similarity with that of 826-XX is seen with ALK-XX. Again a slight change of baseline is observed at  $\approx 50^\circ\text{C}$ . The glyptalic resins TG-21D and TP-21D were also probed for heat flow changes by DSC, the results can be seen in Figure 5.23. As the base line shift was more pronounced in the repeat run this has also been shown (Figure 5.24).

In the first heating run a more pronounced endotherm at  $\approx 80^\circ\text{C}$  is seen for TG-21D than for TP-21D but the implication of this are undetermined. A slight change in base line is also seen at  $\approx 150^\circ\text{C}$ , this more clearly observed in the repeat run. If the change in baseline is interpreted as a  $T_g$ , TG-21D has a lower  $T_g$  than TP-21D. Due to the similar nature of information gained from DSC analysis, assignment of all DSC traces has been approached as group, this can be seen in Table 5.15.

Table 5.15: Assignment of DSC analysis.

| 826-00 | 826-10 | 826-UV | ALK-00 | ALK-UV | TP-21D | TG-21D | Assignment     |
|--------|--------|--------|--------|--------|--------|--------|----------------|
| 35.1   | 42.5   | 43.0   | 34.9   | 28.1   | -      | -      | Baseline shift |
| 89.2   | 83.3   | 89.5   | -      | -      | -      | -      | Endotherm      |
| -      | -      | -      | -      | -      | 71.1   | 71.0   | Endotherm      |
| -      | -      | -      | -      | -      | 115.0  | 119.7  | Endotherm      |
| -      | -      | -      | -      | -      | 135.9  | 117.4  | Further RXN    |

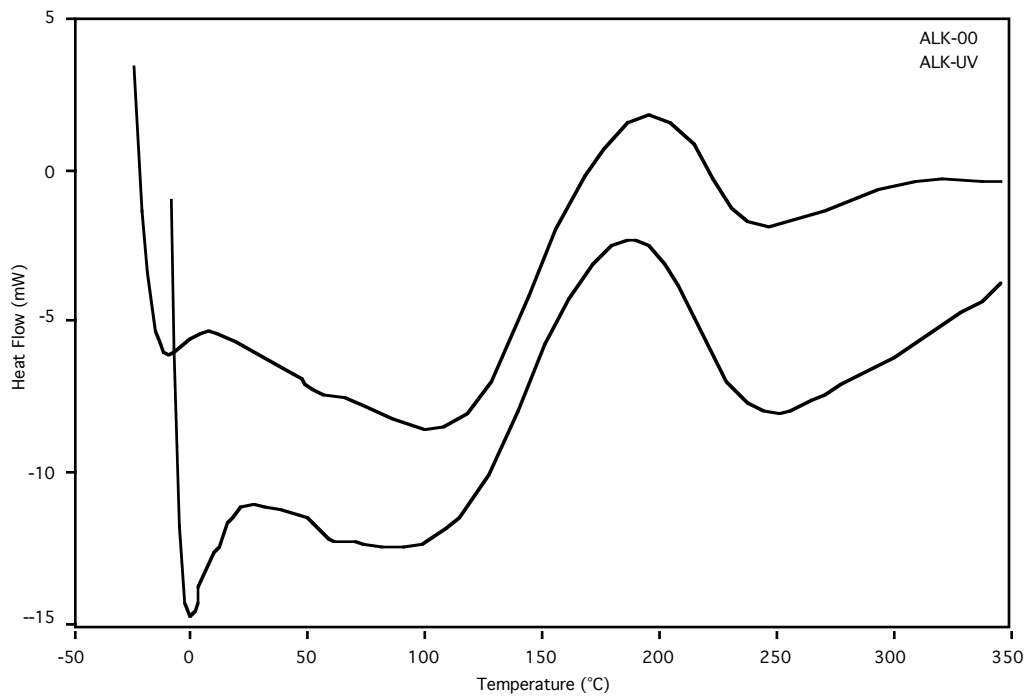


Figure 5.22: DSC traces of ALK-00 and ALK-UV.

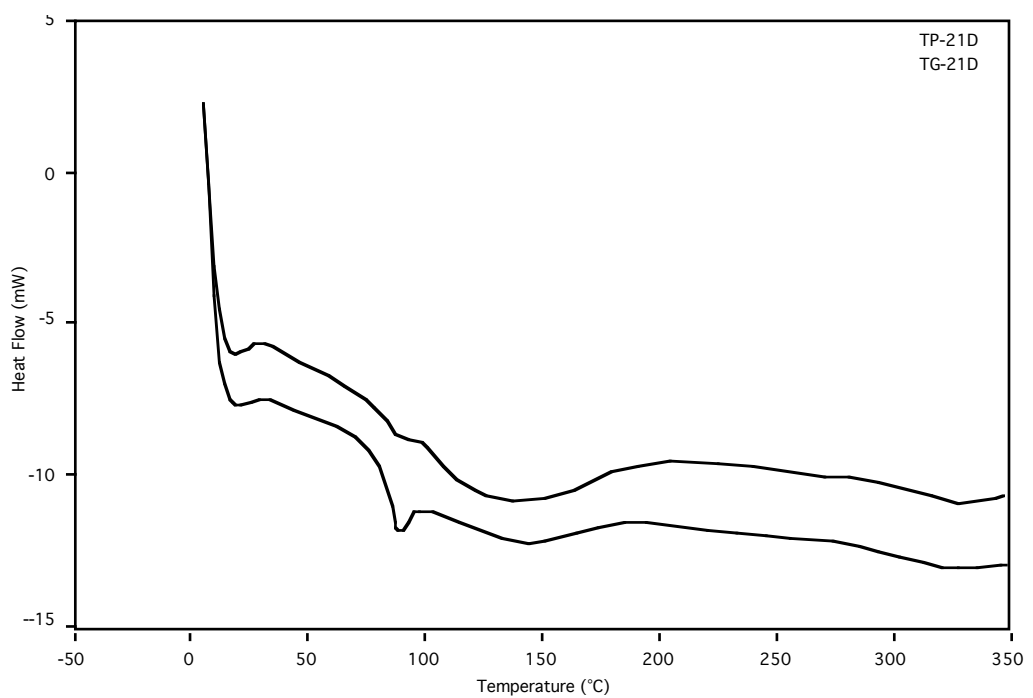
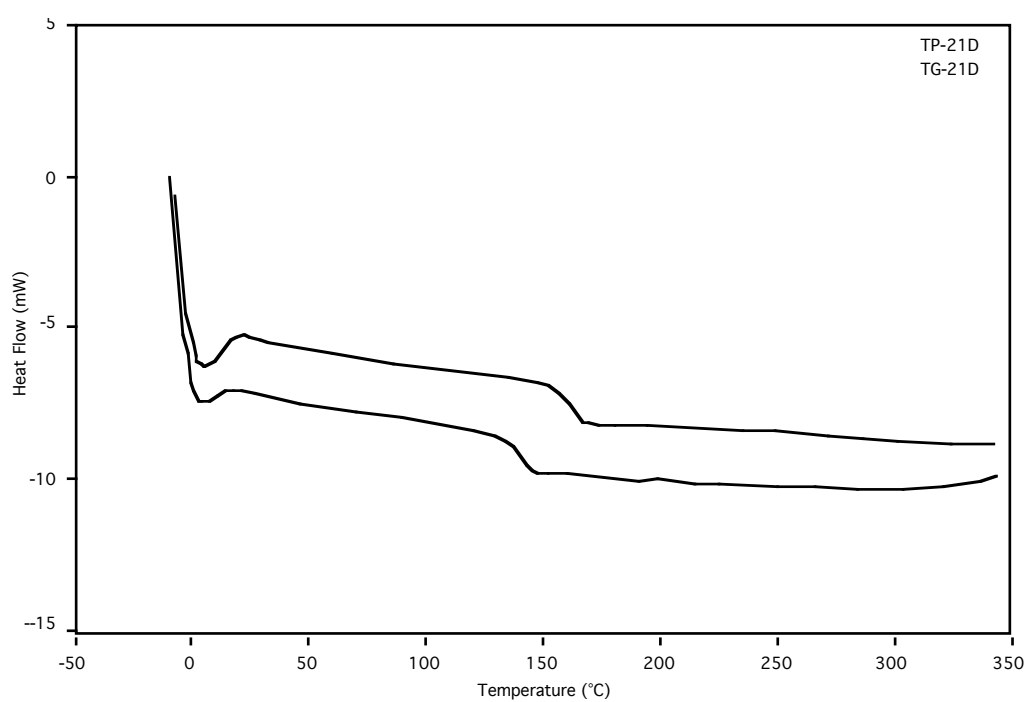


Figure 5.23: DSC traces of TG-21D and TP-21D.



*Figure 5.24: Repeat DSC traces of TG-21D and TP-21D.*

## Chapter 6

# Discussion

The research that has been undertaken in the past has concentrated on the crosslinking process of oil modified alkyd resins. During this project the glyceride phthalate, or glyptalic, backbone has been concentrated on. By synthesis of model compounds conformation widely accepted glyptalic backbone structural model has been achieved.

### 6.1 Model resin synthesis

Although only a small number of synthetic model resins were produced the difficulty in finding reliable protocols lead to a large amount of time being spent on this section of the project. Of particular importance was the esterification catalyst. After a number of acidic catalyst being tried with no success basic catalyst was investigated. Eventually  $\text{Ca}(\text{OH})_2$  was found to work at 1 mol% and so synthesis proceeded. Crosslinked glycerol phthalate and pentaerythritol phthalate were synthesised along with their linear equivalents. An ethylene glycol phthalate was also synthesised. Sorbitol phthalate was found to undergo dehydration at the elevated temperatures required for esterification esterification and so this material was not pursued any further.

The protocol used for production of ALK-00 took approximately two months to perfect. The problem was when to quenching the esterification reaction, judged by the acid number. If quenching was undertaken too soon curing did not readily take place. If reaction was allowed to carry on, the gel point would be exceeded and a heterogeneous system was formed that was not comparable to the neat commercial resins. With repetition, and tuning of conditions, the acid value at which to quench the reaction was found and a resin of desired viscosity formed. When ALK-00 was analysed it was found to be surprisingly similar to the linseed based resin 826. Although only a small number of model resins were synthesised and characterised the

glyptalic resins TG-21D and TP-21D have proven indispensable in aiding solid state assignment and structural determination. The synthesis of ALK-00 was intended to lead to the synthesis of alkyds of defined functionality by controlled esterification of glycerol with pure fatty acids. Unfortunately due to time constraints this was not possible. Although a reliable method has been determined for lab scale production of alkyd resins comparable to industrial resins.

## 6.2 Alkyd structural assignment

Infrared analysis of the neat resins has shown the expected functionality present. Surprisingly little difference was seen between the resins, even in the low frequency fingerprint region of the spectrum. This suggests that the neat resin structures are very similar, no matter from which manufacturer they originate, or the method of synthesis. The high degree of similarity between commercial and ALK-00 shows the components react in the same fashion producing approximately the same polymeric material. This is most likely due to the limited modes of esterification reaction that can take place.

### 6.2.1 Solution-state NMR

The  $^1\text{H}$  NMR spectra also confirms the similarity in structure seen in the IR spectra. Aldehyde byproducts are responsible for the distinctive odour of alkyds and their existence in SBB-000 and 211-00 is implied by the chemical shift at 9.1 ppm. The complex nature the aromatic signals suggests residual aromatic protonated solvent, probably toluene used to azeotrope off water during manufacture. The addition of other protonated solvents as thinners, and to quench the esterification reaction before gelation occurs, are also present. The methylene protons adjacent to hydroxyl groups on pentaerythritol are seen at 4.3 ppm and those adjacent to hydroxyls in glycerol at 3.6 ppm. The shift down field is probably due to reaction of the hydroxyl with phthalic anhydride causing the more electron withdrawing group of the ester to be present. From 2.2–1.2 ppm the methylene protons of the fatty acid are observed higher shifts are noted for those close to the ester linkage and double bonds. Finally the methyl protons of the fatty acid are seen at 0.9 ppm.

Although structural assignment is implied with the IR and  $^1\text{H}$  NMR spectra full characterisation of each carbon environment is achieved with the  $^{13}\text{C}$  NMR spectra. By reference to previous research and the linear model resins synthesised the full assignment of the solution state  $^{13}\text{C}$  spectra of alkyds has been achieved. Assignment of the glyptal backbone can be seen in Figure 6.1. Assignment of the four main fatty acids, stearic, oleic, linoleic and linolenic, has also been achieved (Figure 6.2).

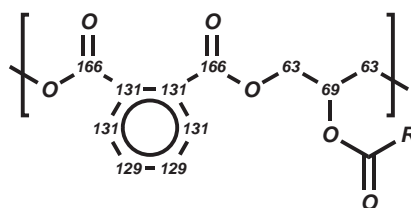


Figure 6.1: Structural assignment of glyptalic backbone of alkyd resins.

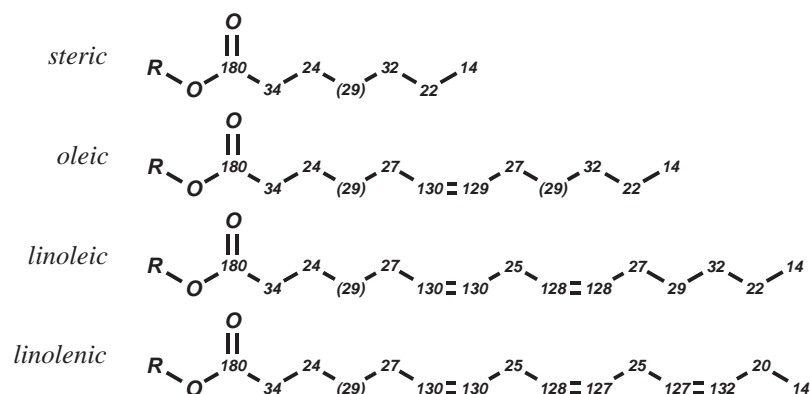


Figure 6.2: Structural assignment of the four main fatty acids

## 6.2.2 Solid-state NMR

With the full  $^{13}\text{C}$  solution state assignment CPMAS chemical shifts can easily be transposed for the cured resins. As the methylene carbons are not so resolved in the solid state only the proximity to the fatty acid ester and methyl group can be distinguished (Figure 6.3).

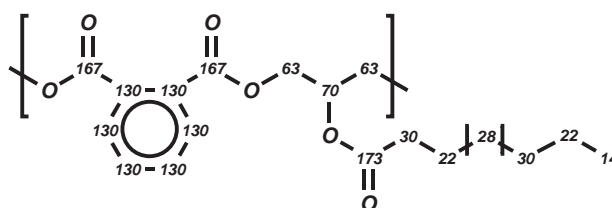


Figure 6.3: Structural assignment of cured oil modified alkyd resin

A pronounced difference between the carbonyls of the fatty acid and phthalate esters can be seen at 173 and 167 ppm respectively, possibly due to shielding effects of the phenyl ring system. The methylene of the glyceride can be seen at 63 ppm and the central glyceride carbon at 70 ppm. Due to the glyceride nature of the oils these two peaks will be observed in all alkyd resins. In peak at 43 ppm is indicative of the quaternary centre of pentaerythritol seen at 45 ppm. In previous research it has been suggested that quaternary centres are formed by the crosslinking process between

the fatty acid side chains. As these will probably be formed in a lower concentration than quaternary centres in a pentaerythritol based alkyd the presence of a strong peak is indicative of a pentaerythritol based resin. This is proven by the existence of the peak in 270-XX, known to be pentaerythritol based, and not in, 444-XX, known to be glycerol based. This indicates that 826-XX is a pentaerythritol based resin, information previously unknown. Between 30–22 ppm the methylene protons of the fatty acids are seen, shoulders show the existence of three distinct environment possibly due to proximity to ester linkage, carbon-carbon double bond, or the methyl group. The terminal methyl carbons are seen at 14 ppm. In 826-XX a second methyl group is seen at 10 ppm. This might be due to reaction of the double bond closes to the chain terminus leading to a change in environment and thus chemical shift.

### Chronological CPMAS analysis

The minor changes in the CPMAS spectra with artificial aging imply little structural change occurs with aging. Due to the unresolved nature of the methylene region this conclusion is only really applicable to the glyptalic backbone. The changes in the carbonyl signal are probably due to further esterification taking place as part of the continued curing process of the resins. The only major change observed is loss of intensity of the peak at 88 ppm. Although assigned as a spinning side band, of the phthalate carbonyl at 167 ppm, the uneven intensity relative to the corresponding peak at 246 ppm implies an overlapping signal. This is also confirmed by a 4 mm 10 kHz CPMAS spectra. The next obvious question is what causes this signal? A chemical shift of 88 ppm is unusual as few examples of resonance in this region are known. It has been known for a methylene group with two adjacent ethers to have shifts in the region of 90 ppm (Figure 6.4).

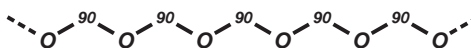


Figure 6.4: Polyether with unusually high methylene chemical shift.

Also, as this peak reduces in intensity rapidly on exposure to light aging, seen in the XXX-01 CPMAS spectra. This implies the loss of such structural moiety is occurring. One sensible possibility is the possibility that this is due to a peroxy crosslink between chains, due to the high electronegativity this might pull the chemical shift up to 88 ppm (Figure 6.5). The possible reactions leading to this structure being formed are discussed later.

It is also interesting to note that the peak is not seen in ALK-00 or ALK-UV. A peak is present in TG-21D and TP-21D but this is assigned as a spinning side band due to the similar intensity to the other side band at 248 ppm. Unfortunately further investigation into the origin of this peak was able to be determined during this project.

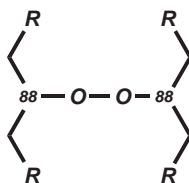


Figure 6.5: Possible peroxy crosslink between fatty acid side chains.

### UV irradiation analysis

The irradiation of resin samples with high intensity light has shown little change in the CPMAS spectra, not previously observed in the light box aged samples. This suggests that the UV light does not effect the glyptalic backbone to a sufficient degree, and only effects the fatty acid side chain. As only a finite amount of reaction can take place, due to the limited number of fatty acids, once this has taken place little interaction with UV light is probable. This implies that once full crosslinked a high tolerance to UV degradation is possibly achieved. The problems with material breakdown are not due to to UV light breaking down the polymer network but as an implication of the increase in crosslinking and thus rigidity and stress in the network.

### Solid state proton spectra

Although solid state proton work produces very broad peaks, valuable information on the mobility of the polymer can be gain. As the dipole-dipole interaction of the protons is reduced by molecular motion, in a similar way seen with tumbling in solution, line widths are reduced with high degrees of molecular motion. The static spectra show narrower lines than expected for a crosslinked resin. Even with moderate MAS of 4 kHz in the 7 mm probe three distinct peak are seen implying a high degree of molecular motion. It can also be seen that the intensity of the peak at 6.1 ppm reduces with artificial aging, from 826-00 to 826-UV. This can also be seen in the static SPE spectra as a loss of shoulder on the low field side of the peak. If this peak is attributed to olafinic protons then this correlates with crosslinking via reaction of the double bonds. Unfortunately the use of the 4 mm probe with MAS > 10 kHz was not employed, due to time constraints. Possible examination of the resin with CRAMPS would also have shed more light on the unusual phenomena observed in the SPEMAS experiments.

### Spin-lattice relaxation of phthalic anhydride

The pyrolysis GCMS research, being carried out at the Tate Gallery, has show significant amounts of unreacted phthalic anhydride being driven off the cured resins

when heated. It was hoped that by fully characterising phthalic anhydride the degree of unreacted phthalic anhydride could be determined. This would enable an idea of the extent of reaction to be gauged. Solution state  $^1\text{H}$  NMR showed a strong multiple for aromatic protons as expected but the  $^{13}\text{C}$  spectra was more more informative. The proximity of the aromatics to the electron withdrawing anhydride group could be seen with the subtle differences in aromatic chemical shift and the anhydride carbonyl carbon can clearly be distinguished (Figure 6.6).

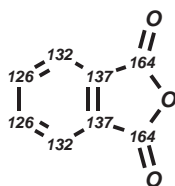


Figure 6.6: Assignment solution state  $^{13}\text{C}$  NMR of pure phthalic anhydride.

In order for phthalic anhydride content to be judged in the cured resin the CP-MAS spectra of pure phthalic anhydride would be needed for comparison. When attempted this was not successful with no FID produced indicating no relaxation decay. This implied that some of the acquisition parameters, needed for spectra acquisition, were not optimised for phthalic anhydride. These were then changed to optimise acquisition for a crystalline material but still no signal was obtained. A SPEMAS experiment was then carried out to determine whether a signal could be obtained from the protons in the sample. This was unsuccessful with only a background proton spectra obtained for the probe. The implications of this is that phthalic anhydride has a long spin-lattice relaxation time,  $T_1$ . As pulse NMR measures the decay from a saturated spin system back to the equilibrium the time between pulses has to be significantly longer than  $T_1$ . If insufficient time is left between pulses the equilibrium state will not be reached before the next pulse resaturated the spin system, thus no decay process will take place. The delay time used for the resins during the CPMAS experiment was 2 s, thus 2000 scans took just over an hour to complete. Using SPE the delay time was extended to 100 s and the experiment left to run overnight. This still produced no signal. The conclusion that is drawn from this is that phthalic anhydride has an extremely high spin-lattice relaxation time. This phenomena is not unique, and extremely large  $T_1$  values are known for other compounds, but they are rare. Unfortunately due to time constraints this phenomena could not be further investigated.

If however the  $T_1$  of phthalic anhydride could be measured the CPMAS acquisition parameters could be adjusted to allow spectral information to be obtained. It is possible that this could be used as manor of detecting the degree of phthalic anhydride present by running two experiments on the same sample. One with a short delay, thus screening out unreacted reagent, and one with a long delay, showing unreacted reagent. By comparison these spectra could determine the extent of reaction.

### 6.3 Thermal Analysis

From the differential scanning calorimetry carried out it can be seen that many thermal changes occur within the resin system before final decomposition takes place. The existence of a glass transition temperature in crosslinked resins is debatable. Previous research has reported a  $T_g$  in the region of  $5^\circ\text{C}$  unfortunately accurate sub ambient analysis was not achieved to confirm this. The best evidence for existence of a glass transition in alkyds is the application of cryomilling during solid state NMR sample preparation. It was noticed that the glassy state could be induced by immersion of the resin in liquid nitrogen thus facilitating crushing into a powder, or returning to ambient temperature the brittle property of the glassy state was lost and the flexible property of the rubbery state regained. A another important observation was also made, although overlooked at the time. It was found that the most aged samples, XXX-10 and XXX-UV, did not crush into a powder. Instead the sample fragmented into small pieces. This possibly implies that the transition into the glassy state had not been achieved by application of liquid nitrogen. Alternatively the transition had broadened allowing only partial rigidity to be induced by application of liquid nitrogen. To investigate this phenomena DSC from liquid nitrogen temperatures is desired, but unfortunately this was not achieved during this project.

### 6.4 Polymerisation and cross-linking

There are two distinct types of reaction that are possible in the oil modified alkyd resin system. Those involved with the glycerol phthalate backbone, and those involved with the unsaturated of the fatty acids. The current model for alkyd structure has a glycerol phthalate backbone with fatty acid side chains attached to the secondary alcohols (Figure 6.7).

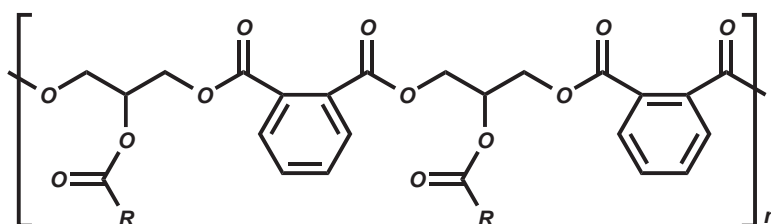


Figure 6.7: Alkyd resin phthalate backbone.

If synthesis is carried out by the fatty acid or monoglyceride process the coupling of the phthalic anhydride and glyceride will form phthalate esters. Whether further reaction takes place is dependent on the structure of the glyceride. As the glyceride can be any isomer of the mono, bi or tri glyceride many possibilities are possible. Possible glycerides are shown in Figure 6.8. These will all compete for the phthalic

anhydride in the system.

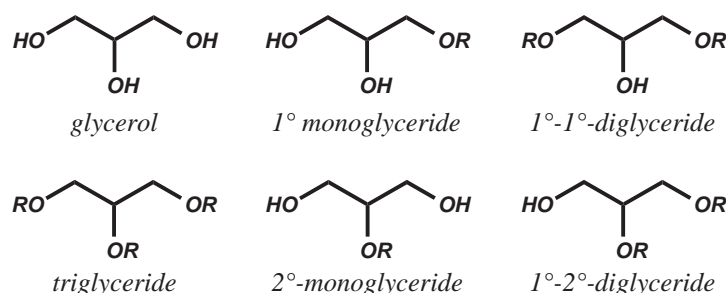


Figure 6.8: Possible glycerides competing for phthalic anhydride.

If we assume the phthalate esters are formed from condensation between hydroxyl and the anhydride there is a limited number of products formed with the glyceride present. Using the possible glycerides in Figure 6.8 six possible products are formed. Out of these six only four can further react to continue the polymer chain. Due to the higher reactivity of the primary hydroxyls over the secondary the production of phthalates with primary hydroxyls is low. Thus producing less reactive products. Because of this it is proposed that the polymer chains will not be very long as soon only unreactive secondary hydroxyls will be present. It should also be noted that only the reaction of glycerol introduces the possibility of branching into the system and even then the secondary hydroxyl will be less active. From this analysis it is proposed that the majority of polymer chains produced will be linear with little degree of branching. However this is not the only way the reaction possible, transesterification is also possible. This could explain the possibility of formation of more phthalate ester linkages to primary hydroxyls and fatty acid ester linkages to secondary hydroxyls.

### 6.4.1 Cross-linking

If the glyptalic backbone is not the source of cross linking in alkyds the unsaturation in the fatty acids must fulfil this role. Due to the unconjugated nature of the double bonds the Diels-Alder reaction is highly unlikely. Even Diels-Alder reaction with one of the possible conjugated systems is highly unlikely due structural alignment requirements. The possibility of cyclic addition of oxygen to the olefin via the ene reaction is one of the more promising reaction for crosslink formation, producing a hydroperoxide (Figure 6.9).

The reaction introduces a trans double bond into the system, and is promoted by the formation of a conjugated system when occurring in linoleic or linolenic acid. The next stage of the reaction is the breakdown of the hydroperoxide to form  $\text{RO}\cdot$  and  $\text{HO}\cdot$  free radicals. These radicals can then propagate and finally terminate producing C-C single bond crosslinks, C-O-C ether crosslinks, or C-O-O-C peroxide crosslinks (Figure 6.10)

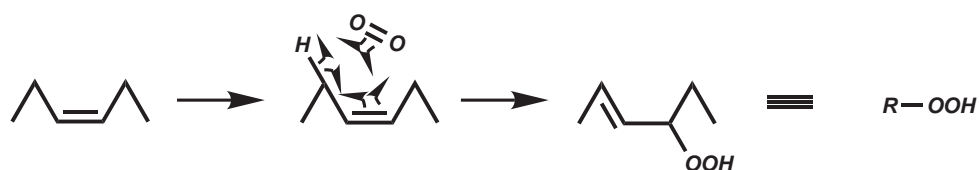


Figure 6.9: The ene reaction

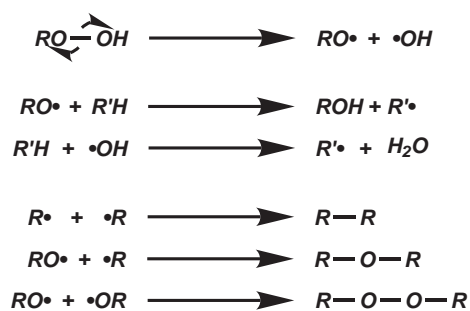


Figure 6.10: Radical and crosslink formation.

The decomposition of the hydroperoxide is catalysed by cobalt salts known as driers. These salts undergo single electron transfer (SET) reactions producing  $\text{RO}\cdot$  and  $\text{ROO}\cdot$  radicals (Figure 6.11). Again recombine will form crosslinks.

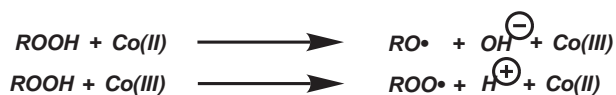


Figure 6.11: Action of cobalt salt driers on hydroperoxides.

The propagation step of radical addition to a carbon-carbon double bond would also produce crosslinking.

## 6.5 Implication for conservation

### 6.5.1 Aging of alkyd resins

Previous research into the durability of alkyds has concentrated on their colour retention and film forming properties. This has been investigated to the relevant level of detail needed for the average lifespan of a painted surface. Each surface will have a desired lifespan that the paint will have to perform for. When compared to the use in alkyds in art, the commercial lifespan of alkyds, before repainting is required, is relatively short. The long term effects of aging are not of importance to the manufacturers, and so research has not been carried out. Generally when your alkyd finish

starts to age after a time you repaint it. Unfortunately stripping and repainting is not an option in conservation of modern art of historical importance! This means that the alkyd resin will exceed the lifespan expected by the manufacturers and nobody really knows what will happen. So the big question to the conservator becomes: what happens when alkyd resins age? An insight into this has been started to be achieved by current research but a lot of work still needs to be carried out for a full understanding to be achieved. To begin to start to answer this question another question is raised that needs to be answered first. What is the neat resin? At first this seems a simple question but on examination this is crucial to the understanding of alkyd aging.

### 6.5.2 Neat resin composition

It has been shown that significant amount of the starting materials are present in the commercial resins both when in their neat solvated forms and their cured films. It has also been shown, through analysis of the neat resin during this project, that there is a surprising degree of similarity between the neat resin in the liquid state and the cured resin in the solid state. This means that the neat resin is neither pure starting material that react in situ or a monomer that polymerises in situ. Another alternative would be a dissolved form of the cured resin but this unlikely due to the cross linked nature of the cured state. The conclusion is a partially polymerised system with properties as such. That is some properties of the reagents and some of the cured resin. This hypothesis is further justified by the synthesis of ALK-00. This was a simple shake and bake reaction with an end point chosen to allow the product to be easily handled, all be it as a highly viscous liquid. SEC work has shown the neat resin to have a distribution of molecular weight as seen in polymers. On addition of a drier or exposure to air and light further polymerisation takes place producing a solid cross linked material with similar spectroscopic properties.

### 6.5.3 Structural deterioration of alkyds

As curing takes place more and more crosslinks are formed forming a more rigid system. This will introduce tension into the system which, when large enough, might disrupt the continuity of the surface. Combined with a non rigid support the development of fractures within the resin matrix will proliferate. This will cause the crazing and lifting sometimes noticed in the worst cases of alkyd deterioration. This is similar to the deterioration of oil paints but due to the lack of a varnish layer intervention may be needed sooner due to the deterioration of the pigmented alkyd surface.

### 6.5.4 Yellowing

It has been known for a long time that oxidising oil and alkyd based paints yellow with age. This is indicative of the generation of conjugated systems being formed within the fatty acid side chains of the material. These systems absorb light of particular wavelength thus leading to the generation of a yellow appearance. Due to the sensitivity of spectroscopic effects the concentration of conjugated systems does not need to that high before a noticeable change in absorption is detected. The production of conjugated system, however, is not substantiated with the NMR analysis. As only a low concentration of these unsaturated systems is needed for a colour change it is possible that both conjugated and unconjugated systems are present. This could be confirmed by UV/VIS spectroscopy which would give an indication of the degree of conjugation by the characteristic absorbance.

### 6.5.5 Alkyd identification

Other than studying the changes upon aging, the other major reason for studying alkyds is for identification purposes. In this respect all the techniques used have shown great potential. The high degree of similarity between CPMAS spectra has shown that conformation of a suspected alkyd could be achieved. The main characteristic features, that would set the resin apart from linseed based media, would be the phthalate ester and fatty acid ester carbonyl chemical shifts observed at  $\approx 172$  and  $168$  ppm respectively. The existence of aromatic carbons at  $130$  ppm would confirm alkyd media is present. Due to later alkyds, post 1960, being mostly based on pentaerythritol and not glycerol, possible classification before and after this time might also be possible. The observation of a resonance at  $\approx 44$  ppm would suggest the quaternary carbon of pentaerythritol was present and thus post 1960. This however is open to much interpretation as it has been seen that sometimes these signals can form from crosslinks. For NMR to be of characterisation interest a library of spectra of as many different types and examples of paint media would need to be compiled and thus allow accurate characterisation.

### 6.5.6 Future use of NMR in conservation

Although solid state NMR has provided valuable insight into the cured structure of alkyd resins it is not a technique that will become highly used by the world of conservation for measuring degradation. The probing of deterioration, and surface effect, is particularly difficult due to the dilution of effected surface by unaffected bulk. The inherent insensitivity of the technique also puts detection of low concentration changes, such as colour and finish, into question. Another drawback is the relatively large sample quantities required for analysis, commonly not available to the conservator. Even though not distractive in itself, sample preparation renders samples into

small particles which could be unacceptable.

The main strengths of NMR are in identification of unknown sample, or particularly conformation of a suspected identity. In this aspect NMR can be employed as a quick easy method of compound identification from a range of possible materials. Although this is applicable to all aspects of conservation, one area stands out prominently, with respects to potential use of NMR techniques. This is the field of polymeric synthetic materials. As a high degree of research has been carried out regarding synthetic polymers, and their characterisation by NMR, much information can be obtained from a single sample. As a growing number of artifacts of historical importance are made of plastics, of one kind or another, characterisation of the material will be paramount. With modern plastic artifacts generally being relatively large in size, samples providing 20 mg, for a solution state analysis, or 100 mg, for solid state analysis, might be available.

# Chapter 7

## Conclusions

### 7.1 Main conclusions

1. Alkyd resins are a complex, multi component system
2. CPMAS spectra characteristic of alkyd and therefore allow identification
3. CPMAS spectra allow identification of polyol

### 7.2 Other conclusions

1. Glyptalic backbone model holds for alkyd structure
2. Curing process continue after initial 'drying
3. Cross linking caused by unsaturated fatty acids
4. Possible increased tension within material causes degradation
5. CPMAS spectra shown minor changed with artificial aging
6.  $^1\text{H}$  SPE MAS spectra imply unusually high degree of molecular motion

# Appendix A

## Research proposal

Initial November 1999 research proposal.

### A.1 Aim & Background

The aim of this research is to investigate the structure of alkyd resins, before and after artificial aging, by probing their structure by nuclear magnetic resonance (NMR) spectroscopy. It is hoped that this research will complement the work currently being undertaken at the Tate and be of further use to conservators working in this field. The long term aim of this research is to try and gain an understanding of the aging processes of alkyd resins so to help safeguard our artistic heritage for future generations.

#### A.1.1 Natural to Synthetic Media

In the past fine art media has been confined to a small verity of natural materials, e.g. linseed oil, the decomposition pathways of which are known [Horie 88]. This enables safe interventive conservation to be carried out successfully. Research into paint media used in works of fine art this century has shown an increasing move to modern synthetic and semi-synthetic materials as alternatives to the traditional oils, gums and proteinaceous glues, as they became available [Marshall 87]. Of particular interest are the alkyd resins, these first started to appear in the 30s and by the 50s was common place [Maciel 83]. This switch by artists from more traditional media to alkyd resins has prompted research into their decomposition pathways.

### A.1.2 NMR Spectroscopy

In the past NMR spectroscopy has been used to investigation the structure of organic molecules and polymers in the solution or swollen state. In more recent years the advent of more powerful spectrometers has allowed the development of solid state NMR which is more applicable to polymers due to their high molecular weight. Solid state NMR also allows for the analysis of inhomogenous samples again broadening the possibilities for polymers [Voelkel 88].

### A.1.3 Alkyd Resins

Alkyd resins are polyesters formed by step growth polymerisation. They can be formed by direct esterification of the carbonyl group by a hydroxyl group, transesterification, or by esterification of polyfunctional alcohols with an anhydrides. As each of these possible methods of synthesis is reversible an equilibrium is set up which determines the molecular weight of the final polymeric product [English 83]. The esterification of polyfunctional alcohols by anhydrides is the most common method of alkyd resin formation for paint media. An example of an alkyd resin is glyptal, this is formed form glycerol and phthalic anhydride (Figure A.1).

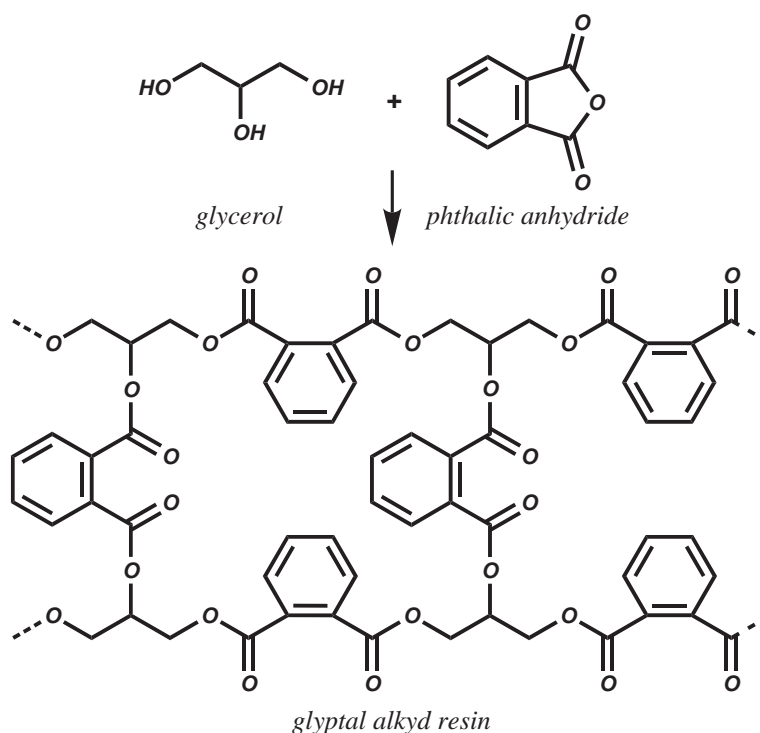


Figure A.1: The formation of glyptal, an alkyd resin [Chatfield 62].

Other common anhydrides and polyfunctional alcohols used in alkyd resins include succinic anhydride, maleic anhydride, pyromellitic anhydride, pentaerythritol,

propylene glycol and ethylene glycol (Figure A.2).

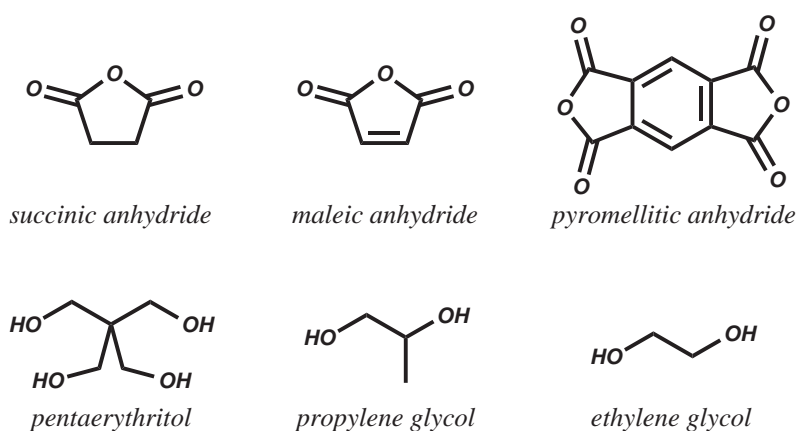


Figure A.2: Other common alkyd resin constituents [Chatfield 62].

A three dimensional polymer network forms cross links between polymer chains forming a macromolecule of high molecular weight, this tends not to occur at synthesis stage but as a polymer modification reaction either initiated by light or the addition of a highly unsaturated molecule, such as natural or dehydrated vegetable oils such as castor, soya, and coconut<sup>2</sup>. These oils, contain glycerides of fatty acids that vary in degree of unsaturation and chain length. When the oils are added to the polymer the fatty acids are incorporated into the polymer changing its properties [Marshall 87].

#### A.1.4 Present Work in this Field

At present research is being carried out at the Tate Gallery <sup>†</sup> into developing an analytical methodology for the identification and characterisation of binding materials used in fine art this century. At present this research is based around, pyrolysis gas chromatography mass spectrometry (PY-GCMS). The aim of this research is to identify the presence of alkyd resins in aged paint films, specifically characterise the alkyd and determine its present state of oxidation/degradation.

<sup>†</sup>Francesca Cappitelli, RCA/V&A Conversation Course (M.Phil.), supervised by Dr Tom Learner, Tate Gallery, London, UK.

## **A.2 Program and Methodology**

### **A.2.1 Training**

In order to carry out research in this field accurately and safely training is required on the relevant apparatus and equipment. Of main importance are the relevant solution and solid state NMR spectrometers that might be needed, and artificial aging apparatus. Revision of the various safety protocols for the different aspects of the research will also be needed.

### **A.2.2 Neat Analysis**

Samples of the neat liquid resin, pre-drying, will be analysed by solution state NMR spectroscopy. This will allow characterisation of the resin before it dries and crosslinks hopefully allowing an understanding of the drying process. Both  $^1\text{H}$  and  $^{13}\text{C}$  nuclei will be probed and various editing techniques will be employed to gain insight into the structure of the polymer. Experiments which will be undertaken for solution state samples will include;  $^1\text{H}$ ,  $^{13}\text{C}$ , DEPT 135, 2D correlation spectroscopy (COSY) and 2D nuclear Overhauser spectroscopy (NOESY).

### **A.2.3 Film Preparation**

To allow the drying of the resins to take place in a standard controlled method of film preparation is required. This will increase both the accuracy and the reproducibility of the data. The resins will be dried on a surface of polytetrafluoroethylene (PTFE), polyethylene (PE) or silicon paper, depending on which surface gives the best results, in a vacuum oven for a period of 24 hours [Marshall 88]. These surfaces will allow the easy removal of the dried crosslinked resins for analysis.

### **A.2.4 Artificial Aging**

To accurately investigate the chemical processes of aging and degradation a standard method will be used to create artificial aged resin. This will be achieved by controlled exposure to light for a known duration of time. Studies have shown that at 15,000 lux a period of irradiation 1 day is equivalent to 0.6 years in the museum environment [Learner 99]. Samples will be taken throughout the aging process at 2 week intervals, equivalent to 8.4 years, to allow the degradation process to be monitored against time.

### A.2.5 Solid State NMR Analysis

Due to the high degree of cross linking expected in the resin system the main method of analysis of solid state products will be solid state NMR spectroscopy. Again both  $^1\text{H}$  and  $^{13}\text{C}$  nuclei will be probed and various editing techniques will be employed. Experiments which will be undertaken will include;  $^1\text{H}$ - $^{13}\text{C}$  cross polarisation magic angle spinning (CP/MAS),  $^{13}\text{C}$  CP/MAS non quaternary carbon suppression (CP/MAS NQS),  $^1\text{H}$  combined rotational and multi pulse spectroscopy (CRAMPS) and nuclear overhouse effect enhancement spectroscopy.

### A.2.6 Solid State DSC Analysis

The possible existence of phase transitions in the resin will be investigated using differential scanning calorimetry (DSC). This will provide information of whether the resin has a glass transition temperature ( $T_g$ ) and the associated thermodynamic properties which this imparts.

### A.2.7 Solid State Swelling

A brief investigation into the swelling properties of the resin will be carried out to determine the degree of cross linking that has taken place. If swelling occurs to a desirable extent solution state NMR experiments will be performed include;  $^1\text{H}$ ,  $^{13}\text{C}$ , DEPT 135, 2D COSY and 2D NOSY.

### A.2.8 Polymer Digestion

The digestion or breaking down of the polymer into smaller, low molecular weight, components will be carried out as an indirect investigation of the polymer structure. The digestion will be carried out using reagents such as; concentrated potassium hydroxide (KOH)/ concentrated sulphuric acid ( $\text{H}_2\text{SO}_4$ )/lithium aluminium hydride ( $\text{LiAlH}_4$ ) with methyl iodide (MeI), or boron trifluoride ( $\text{BF}_3$ ) with trimethyl silyl chloride (TMSCl). Chromatographic separation of the digest products will allow the analysis of the major components by solution state NMR spectroscopy include;  $^1\text{H}$ ,  $^{13}\text{C}$ , DEPT 135, 2D COSY and 2D NOSY. Investigation into the digestion time and conditions of digestion will also be investigated. This work will complement current work being carried out jointly at the Tate and Imperial College (IC) <sup>†</sup>.

<sup>†</sup>Chemistry with conservation science masters research project of Matthew Hindley supervised by Dr David Widdowson at Imperial College, London.

### **A.2.9 Interpretation**

Through interpretation of the spectral data obtained it is hoped that the structure of the polymer network can be deduced and the aging process understood. This may be confirmed by modelling and simulation of the various spectra.

## **A.3 Relevance to Beneficiaries**

### **A.3.1 Potential Impact of Proposed Work**

By understanding the degradation pathways in modern synthetic paint media it is hoped that the methods of conservation of fine art containing this media will be improved. This will lead to fine art being conserved for future generations.

### **A.3.2 Beneficiaries**

The main beneficiaries of this work will be paintings conservators. Their work, based on this research, will lead to more fine art going back on display leading to greater public accessibility to fine art. In the long term this will benefit the nation.

### **A.3.3 Collaboration**

Through this project collaboration will take place with the conservation community at the Victoria and Albert Museum (V&A), the Tate Gallery, and IC. This is needed due to the relative lack of expertise of each party in the others field. This process has already begun with the setting up of the Chemistry with Conservation Science MSci course at IC. This will hopefully lead to the better understanding of the chemistry for the conservators and the chemistry of the conservation process for the chemists.

## **A.4 Dissemination and Exploitation**

### **A.4.1 Transfer of Knowledge to Beneficiaries**

Most conservators have basic science knowledge with the possibility of an A level or science degree. Paintings conservation in general seems to have more chemistry graduates than other areas due to the complex chemical nature of pigments, media, and the process of diagnostics and cleaning. Also within the profession of conservation there is a steady drive to become more rigorous with the scientific content, as this allows more specific communication, especially with the science community. For these reasons it is thought that the transfer of information from the report to the main beneficiaries, paintings conservators, will be acceptable.

### **A.4.2 Communication of Findings**

The final project report will be submitted to IC for assessment as part of the undergraduate degree in Chemistry with Conservation Science. The report will also be assessed by a representative of the joint V&A/Royal College of Art (RCA), Conservation Course. If the report is deemed of high enough standard, and relevant to others, a copy will be made available to conservators at the V&A. Through the well established links with other conservation departments access to this work will be possible for others working in this field.

## Appendix B

# Data gathered from commercial resin manufacturers data sheets

The resin manufacturers produced data sheets to accompany each resin sold, these provide compositional data and physical properties of that particular resin. These are intended to allow educated selection of resin for the intended task by the client. A table comparing the compositions and properties of the 12 resins obtained can be seen in Table B.1.

*Table B.1: Manufacturers data for supplied resins.*

| Supplier     | Code   | Description             | Oil       | Oil % | Solv. % | PA % | polyol   |
|--------------|--------|-------------------------|-----------|-------|---------|------|----------|
| Attiva       | SBB-00 | Smalto Brillante Bianco | -         | -     | -       | -    | -        |
| Cray Valley  | S28-00 | Synolac 28w             | soya      | 60    | 65      | -    | pent-E   |
|              | S60-00 | Synolac 60w             | soya      | 62    | 70      | -    | pent-E   |
| Croda Resins | CA2-00 | Crodakys a2/1028        | -         | -     | -       | -    | -        |
|              | 444-00 | Crodakyd 444w           | soya      | 47    | 50      | -    | glycerol |
|              | 826-00 | Crodakyd 826w           | linseed   | 64    | 65      | -    | -        |
|              | 850-00 | Crodakyd 850w           | vegetable | 65    | 65      | -    | -        |
| Kalon        | LOA-00 | Long Oil Alkyd          | -         | -     | -       | -    | -        |
|              | THX-00 | Thixotropic Alkyd       | -         | -     | -       | -    | -        |
| Scott Bader  | 124-00 | Sobral 1241 ML 70       | soya      | 63    | 70      | -    | pent-E   |
| Vil          | 211-00 | Vilkyd 211              | soya      | 64    | 55-70   | 26   | pent-E   |
|              | 270-00 | Vilkyd 270w65           | soya      | 64    | 65      | 26   | pent-E   |

# Appendix C

## Abbreviations

|        |                                                      |
|--------|------------------------------------------------------|
| CI-MS  | Chemical Ionisation Mass Spectrometry                |
| COSY   | Correlation Spectroscopy                             |
| CP     | Cross Polarisation                                   |
| CPMAS  | Cross Polarisation Magic Angle Spinning              |
| CRAPMS | Combined Rotation and Multi Pulse Spectroscopy       |
| CSA    | Chemical Shift Anisotropy                            |
| DEPT   | Distortionless Enhancement by Polarisation Transfer  |
| DSC    | Differential Scanning Calorimetry                    |
| FAB-MS | Fast Atom Bombardment Mass Spectrometry              |
| FID    | Free Induction Decay                                 |
| FT     | Fourier Transform                                    |
| FTIR   | Fourier Transform InfraRed                           |
| FTNMR  | Fourier Transform Nuclear Magnetic Resonance         |
| GCMS   | Gas Chromatography Mass Spectrometry                 |
| HMQC   | Heteronuclear Multiple Quantum Coherence             |
| HPLC   | High Performance Liquid Chromatography               |
| ICSTM  | Imperial College of Science, Technology and Medicine |
| IR     | InfraRed                                             |
| LCMS   | Liquid Chromatography Mass Spectrometry              |
| MAS    | Magic Angle Spinning                                 |
| MS     | Mass Spectrometry                                    |
| NMR    | Nuclear Magnetic Resonance                           |
| NOEMAS | Nuclear Overhauser Enhancement Magic Angle Spinning  |
| NQS    | Non Quaternary Suppression                           |
| PPM    | Parts Per Million                                    |
| RCA    | Royal College of Art                                 |

---

|        |                                              |
|--------|----------------------------------------------|
| RF     | Radio Frequency                              |
| SEC    | Size Exclusion Chromatography                |
| SET    | Single Electron Transfer                     |
| SIMS   | Secondary Ion Mass Spectroscopy              |
| SPE    | Single Pulse Excitement                      |
| SPEMAS | Single Pulse Excitement Magic Angle Spinning |
| SSB    | Spinning Side Band                           |
| TMA    | ThermoMechanical Analysis                    |
| TMS    | Tetra Methyl Silane                          |
| UV     | UltraViolet                                  |
| V&A    | Victoria and Albert Museum                   |

# Bibliography

- [Atkins 95] P.W. Atkins. Physical Chemistry. Oxford University Press, Oxford (1995). [Cited on: p28]
- [Bovey 96] F.A Bovey, P. A. Mirau. NMR of Polymers. Academic Press, London (1996). [Cited on: p26, 28]
- [Chang 98] J.C.S. Chang. Emissions of odorous aldehydes from alkyd paint. *Atmospheric Environment* **32**(20), 3581–3586 (1998). [Cited on: p23]
- [Chapman 83] C. Chapman. Surface Coatings, Kap. Raw materials and their uses. Chapman and Hill, London (1983). [Cited on: p12, 15, 17, 19, 20]
- [Chatfield 62] H. W. Chatfield (Hrsg.). The Science of Surface Coatings. Ernest Benn Limited (1962). [Cited on: p10, 12, 15, 17, 19, 20, 74, 75]
- [Delahay 95] N. Delahay. Alkyd based thermosetting resins: influence of temperature and UV radiation on curing kinetics. *J. Coatings Tech.* **67**(844), 67–70 (1995). [Cited on: p23]
- [English 83] A. D. English, D. B. Chase. Structure and Degradation of an Intractable polymeric System; Melamine Formaldehyde Cross-Linked Acrylic Coatings. *Macromolecules* **16**, 1422–1427 (1983). [Cited on: p74]
- [Falla 92] N.A.R. Falla. Linoleic based coatings: a study of the dry film structure. *J. Coatings Tech.* **64**(815), 55–60 (1992). [Cited on: p23]
- [Holmberg 87] K. Holmberg. High Solid Alkyd Resins. Marcel Dekker Inc., New York (1987). [Cited on: p28]
- [Horie 88] C. V. Horie (Hrsg.). Materials in Conservation, Organic Consolidants, Adhesives and Coatings. Butterworths (1988). [Cited on: p12, 17, 19, 20, 73]
- [Hubert 97a] J.C. Hubert. Mechanistic study of drying of alkyd resins using (Z,Z)- and (E,E)-3,6-nonadiene as model substances. *Prog. Org. Coatings* **31**, 331–340 (1997). [Cited on: p22]
- [Hubert 97b] J.C. Hubert. Singlet oxygen drying of alkyd resins and model compounds. *J. Coatings Tech.* **69**(869), 59–64 (1997). [Cited on: p23]
- [Ibbett 93] R.N. Ibbett (Hrsg.). NMR Spectroscopy of Polymers. Blackie Academic and Professional (1993). [Cited on: p26, 28, 30]
- [Learner 99] T. Learner, F. Cappitelli. Personal communication. Basic reciprocal nature of artificial ageing. (1999). [Cited on: p25, 76]

- [Maciel 83] G.E. Maciel, N. M. Szeverenyi, T. A. Early, G. E. Mayers.  $^{13}\text{C}$  NMR Studies of Solid Urea-Formaldehyde Resins Using Cross Polarisation and Magic Angle Spinning. *Macromolecules* **16**, 598–604 (1983). [Cited on: p73]
- [Marshal 85a] G.L. Marshal. The characterisation of alkyd paint binders using  $^{13}\text{C}$  NMR spectroscopy. *Eur. Polym. J.* **21**(11), 949–958 (1985). [Cited on: p24]
- [Marshal 85b] G.L. Marshal. Characterisation of cured alkyd paint binders using swollen state  $^{13}\text{C}$  NMR. *Eur. Polym. J.* **21**(11), 959–966 (1985). [Cited on: p24]
- [Marshal 86] G.L. Marshal. The analysis of cured drying oils by swollen state  $^{13}\text{C}$  NMR spectroscopy. *Eur. Polym. J.* **22**(3), 231–241 (1986). [Cited on: p23]
- [Marshall 87] G. L. Marshall.  $^{13}\text{C}$  Solid State Nuclear Magnetic Resonance Spectra of Some Air Cured Alkyd Polyester Paints. *Polymer* **28**, 1093–1097 (1987). [Cited on: p24, 73, 75]
- [Marshall 88] G. L. Marshall.  $^{13}\text{C}$  CP-MAS Solid State NMR Spectra of Stoved Alkyd Paints. *Polymer* **29**, 1501–1506 (1988). [Cited on: p76]
- [Morgans 90] W.M. Morgans. *Outline of Paint Technology*. Edward Arnold, London (1990). [Cited on: p12, 15, 17, 19, 20]
- [Muizebelt 94] W.J. Muizebelt. Mechanistic study of drying of alkyd resins using ethyl lanoleate as a model substance. *Prog. Org. Coatings* **24**, 263–279 (1994). [Cited on: p15, 17, 19, 20, 22]
- [Paul 85] S Paul. *Surface Coating: Science and Technology*. John Wiley and Sons, New York (1985). [Cited on: p12, 17, 19, 20, 21]
- [Rauve 95] A. Rauve. *Principles of Polymer Chemistry*. Plenum Press, New York (1995). [Cited on: p12, 17, 19, 20]
- [Rodriguez 96] Rodriguez. *Principles of Polymer systems*. Taylor and Francis, London (1996). [Cited on: p12, 15, 17, 19, 20]
- [Schmidt-Rohr 94] K. Schmidt-Rohr, H. W. Spiess. *Multidimensional Solid-State NMR and Polymers*. Academic Press, London (1994). [Cited on: p26, 28]
- [Seymour 97] R.B. Seymour. *Handbook of Organic Coatings*. Elsevier, London (1997). [Cited on: p12, 15, 17, 19, 20]
- [Stevens 99] M.P. Stevens. *Polymer Chemistry an Introduction*. Oxford University Press, New York (1999). [Cited on: p12, 15, 17, 19, 20]
- [Swarup 92] S. Swarup. Fourier analysis of alkyd resin using X-ray diffraction techniques. *JOCCA* **75**(7), 256–258 (1992). [Cited on: p24]
- [Turner 86] G.P. Turner. *Introduction to Paint Chemistry and Principles of Paint Technology*. Chapman and Hill, London (1986). [Cited on: p12, 15, 17, 19, 20]
- [Voelkel 88] R. Voelkel. High-Resolution Solid-State  $^{13}\text{C}$ -NMR Spectroscopy of Polymers. *Angew. Chem. Int. Ed. Engl.* **27**, 1468–1483 (1988). [Cited on: p74]

# Acknowledgements

Through out this project I have been helped and supported by a number of different people, amongst these I would specially like to thank:

- *Dr Rob Law* (ICSTM) for supervising my project and providing direction.
- *Prof. Alan Cummings* (RCA/V&A) for supervising my project.
- *Dr Tom Learner* (Tate Gallery) for collecting the resin samples, providing valuable background information and showing interest in my research.
- *Francesca Cappitelli* (Tate Gallery) for providing valuable background information.
- *Jo Kirby-Atkinson* (National Gallery) for allowing use of and access to the National Galleries light boxes on a regular basis
- *David Saunders* (National Gallery) for allowing access to National Galleries light boxes in Jos absence.